The Qubit is the Transistor:

Si-Based Transistor and Analog-Mixed-Signal Circuit Scaling and the Natural Progression of Moore's Law to Si Quantum Computing at the Atomic Scale

Sorin P. Voinigescu

U of T, December 17, 2018

QC is HOT, HEAVY and very COOL!

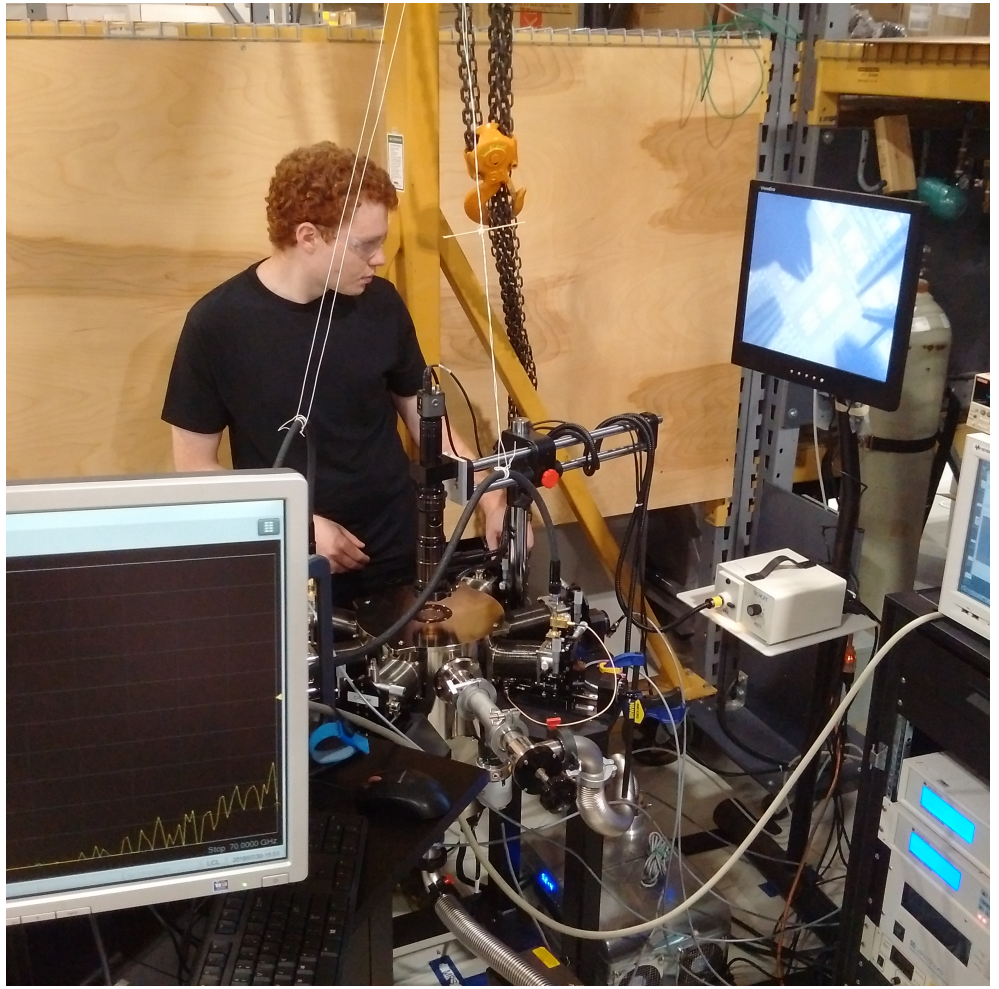

Outline

- **Quantum computing fundamentals**
- Quantum computing ICs in 22-nm FDSOI at 2 K
- Scaling for high temperature quantum computing
- Conclusions

Quantum computing basics

Information encoded in particle ***spin*** or charge location

Basis states

$|\uparrow\rangle = |0\rangle; |\downarrow\rangle = |1\rangle$

Superposition states

$|\Psi\rangle = \mathbf{a}|\uparrow\rangle + \mathbf{b}|\downarrow\rangle$

a and **b** are ***complex*** numbers

- **a** = $\cos(\theta/2)$
- **b** = $e^{i\varphi}\sin(\theta/2)$
- $|\mathbf{a}|^2 + |\mathbf{b}|^2 = 1$
- Only ***two deterministic real*** variables: φ, θ

Bloch sphere

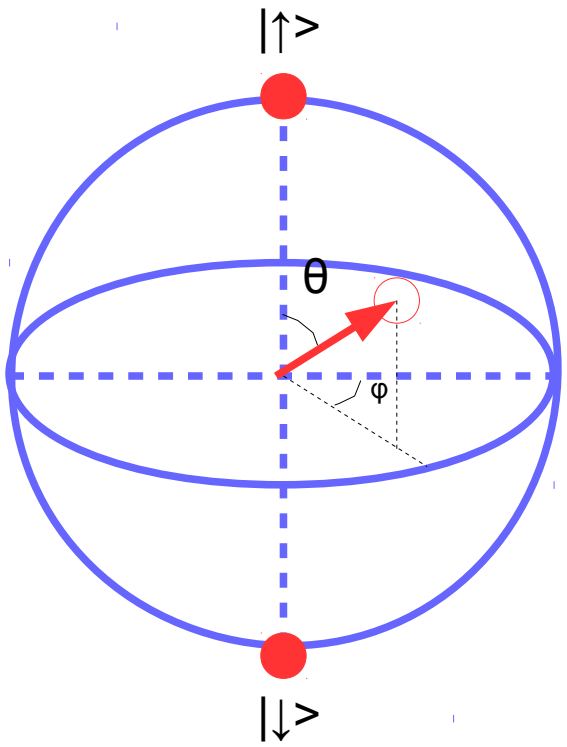

Universal single and double-spin (entangled) gates

Rotation around X, Y, Z axes

$$\sigma_X = \begin{bmatrix} 0 & 1 \\ 1 & 0 \end{bmatrix}$$

$$\sigma_Y = \begin{bmatrix} 0 & -i \\ i & 0 \end{bmatrix}$$

$$\sigma_Z = \begin{bmatrix} 1 & 0 \\ 0 & -1 \end{bmatrix}$$

$$CNOT = \begin{bmatrix} 1 & 0 & 0 & 0 \\ 0 & 1 & 0 & 0 \\ 0 & 0 & 0 & 1 \\ 0 & 0 & 1 & 0 \end{bmatrix}$$

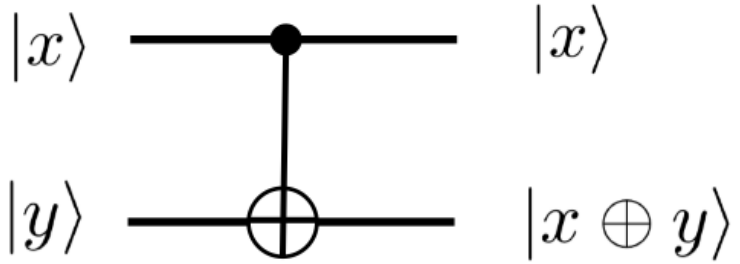

Bloch sphere

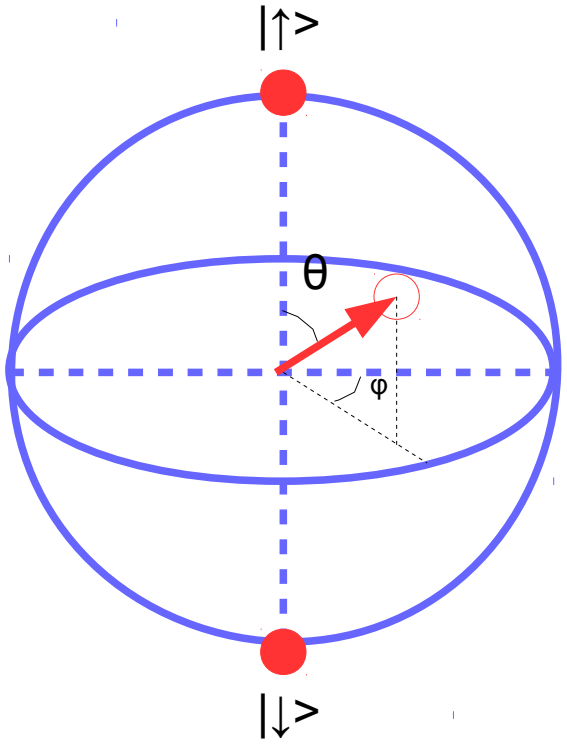

Running quantum computing algorithms

Quantum algorithm example

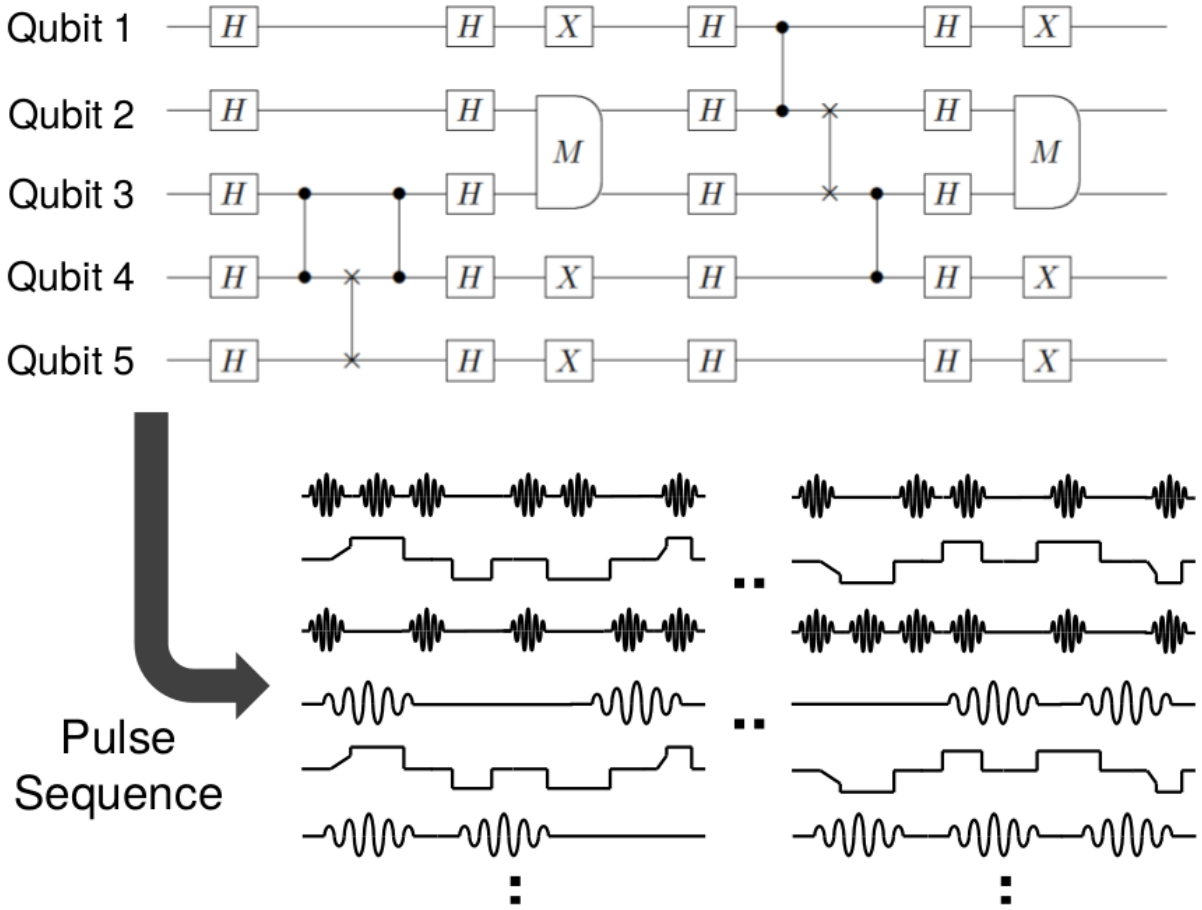

Source: Keysight

Challenging control system

- **Generation**
  - Phase-coherent uW / RF / baseband pulses
  - Excellent spectral purity
  - FDM to address several qubits simultaneously
- **Acquisition**
  - uW acquisition with real-time IQ demodulation
  - FDM to address several qubits simultaneously
  - Pulse counting and timestamping
- **Scalable to hundreds/thousands of channels: cost/channel is important**
- **Tight inter-channel synchronization and phase control**
- **Real-time feedback for Quantum Error Correction (QEC)**

QC processor: qubits+sync-ed AWGs, VSGs, PSAs, RTOs

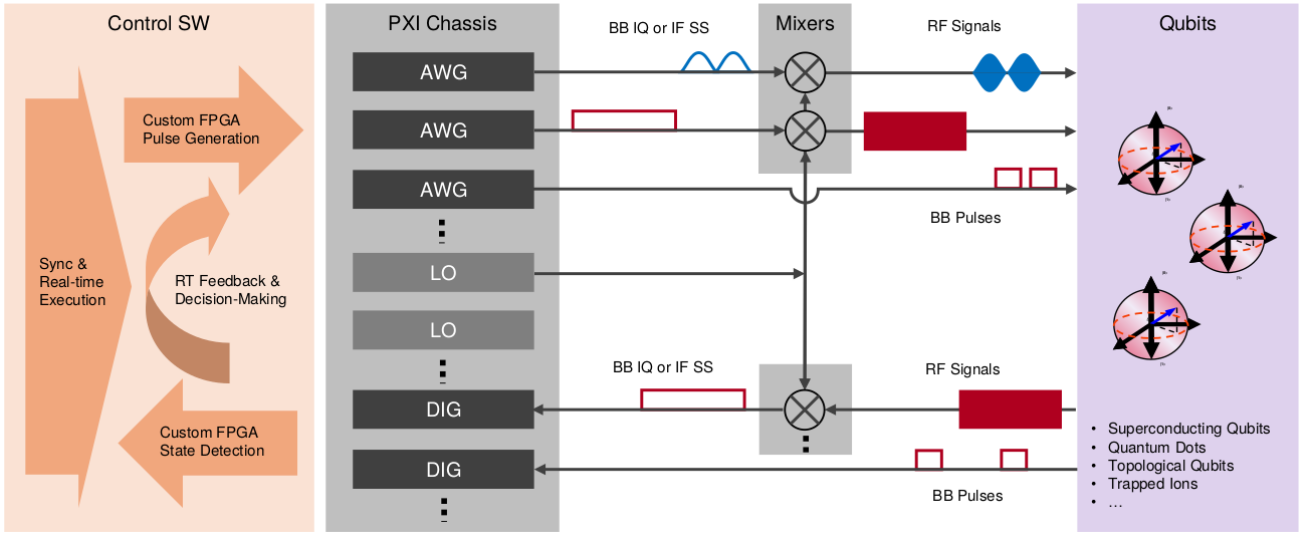

Source: Keysight

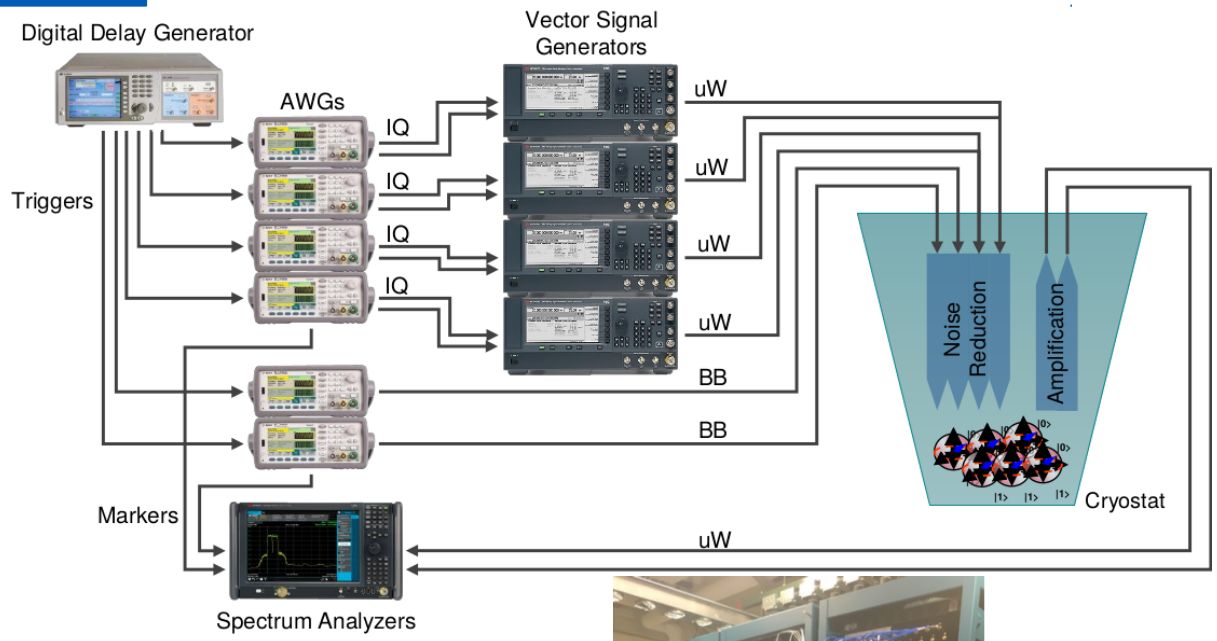

Challenges

- Scalability: footprint and cost
- Signal/phase synchronization
- SW and real-time sequencing control
- Real-time DSP (e.g. qubit state decoding)
- Real-time feedback for QEC

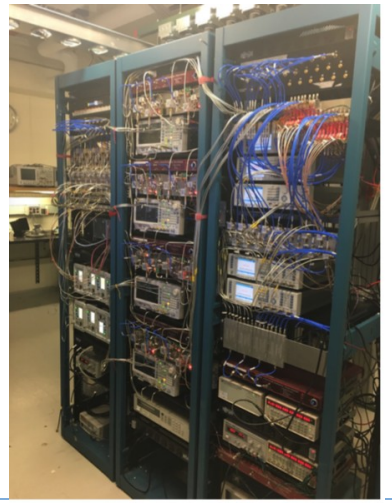

Types of qubits (gates)

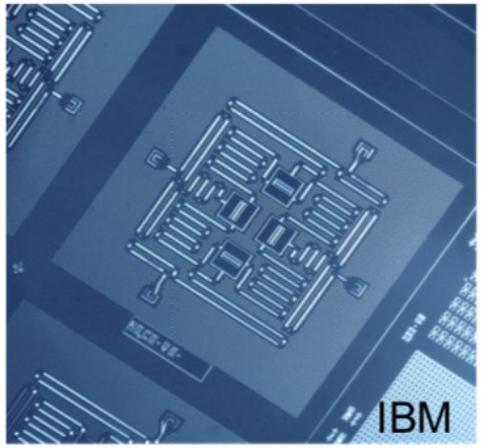

Superconducting Qubits
Transmon,
Phase, CSFQ

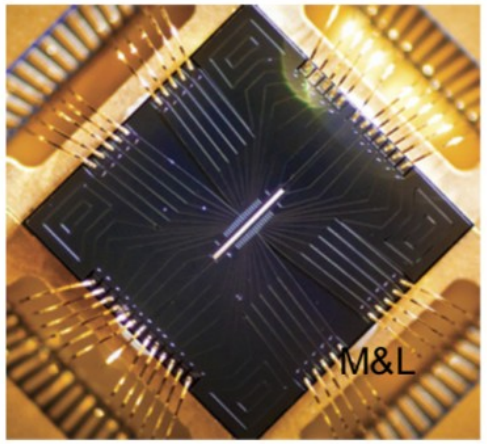

Trapped Ions
Be+, Ca+, Yb+

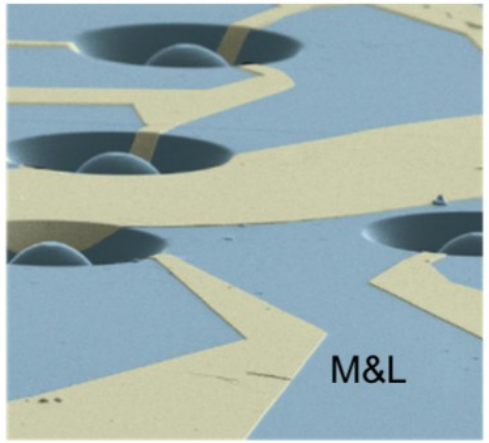

Engineered Defects
P atoms in Si,
NV Centers in Diamond, Dimers In SiC

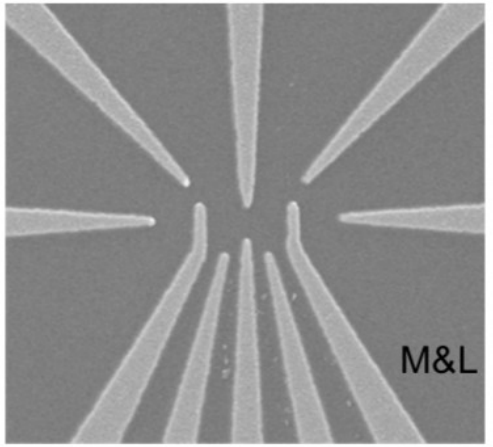

Quantum Dots
Single Electron

[M.B. Ritter, IEDM 2018 short course]

M&L: Morton and Lo, IEEE Spectrum, 8/2014

Superconducting qubits: most common today

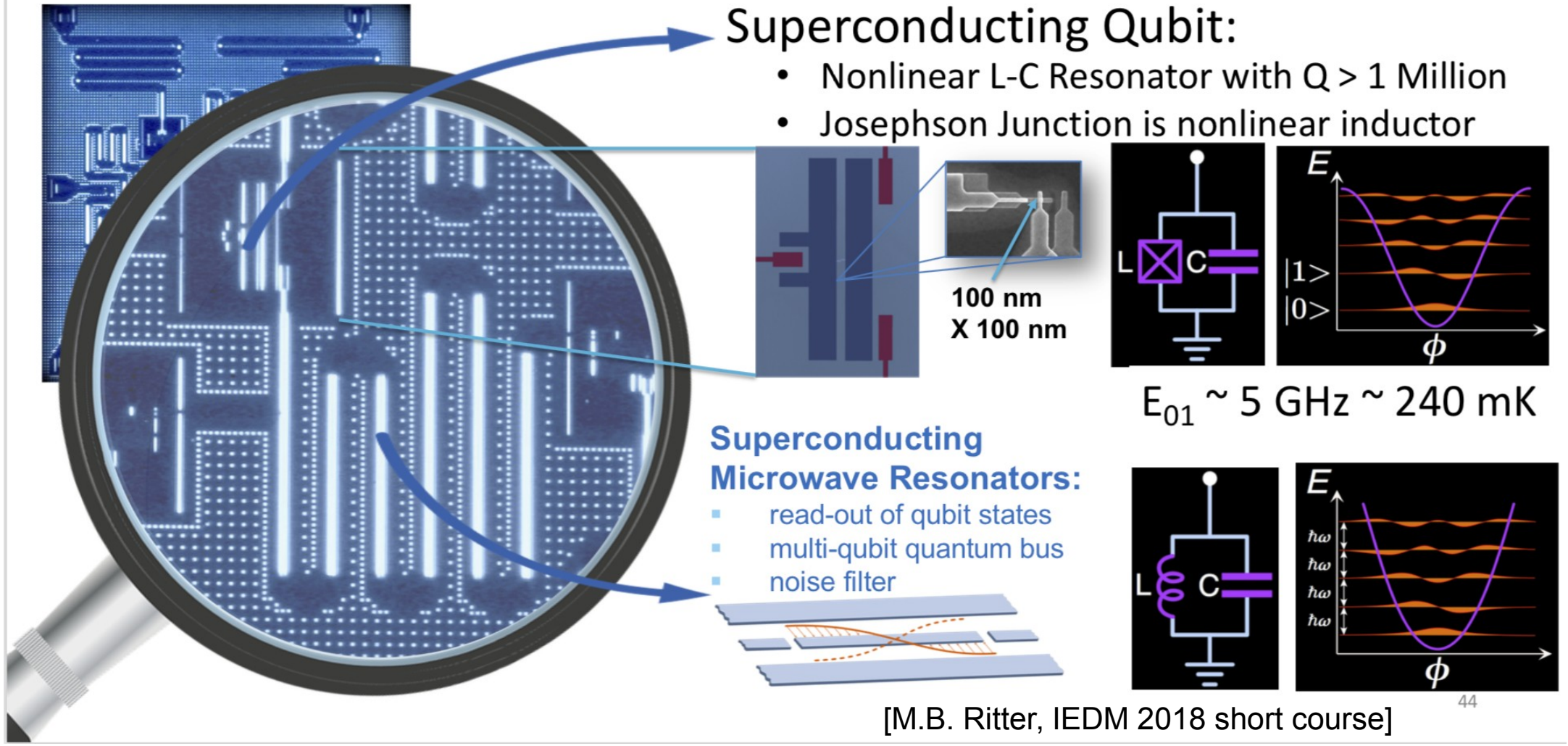

[M.B. Ritter, IEDM 2018 short course]

Superconducting qubits: coupling

SC Qubits: two-qubit gates

[M.B. Ritter, IEDM 2018 short course]

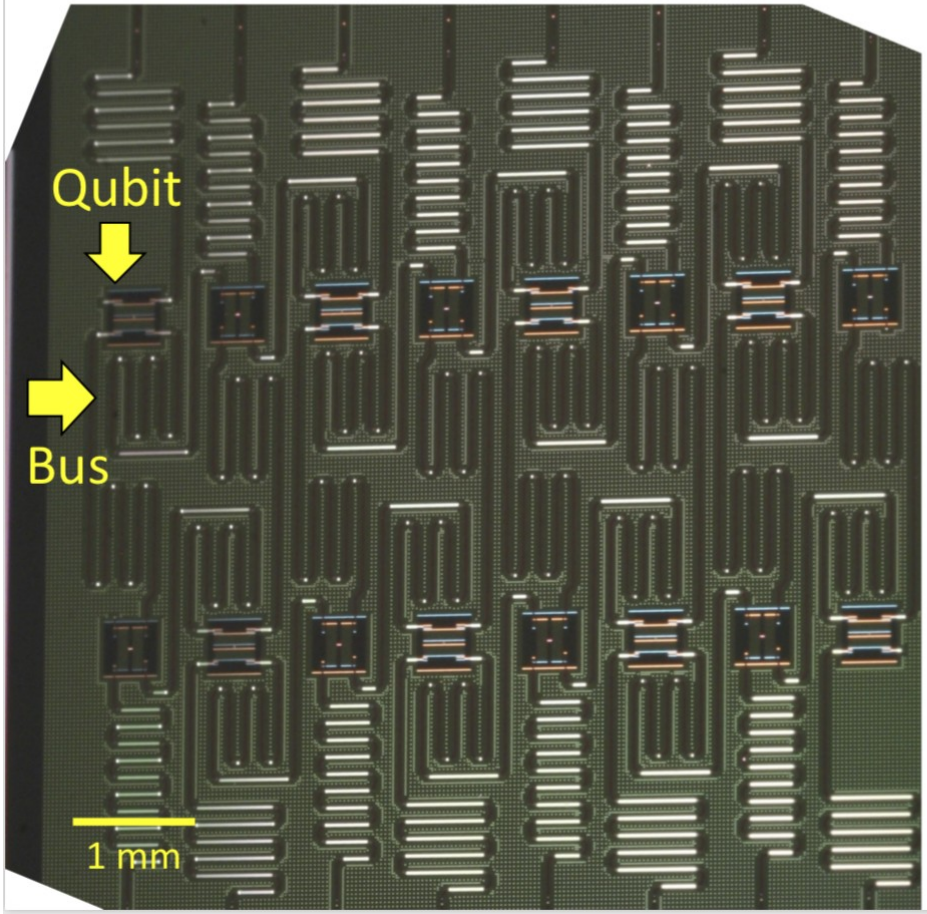

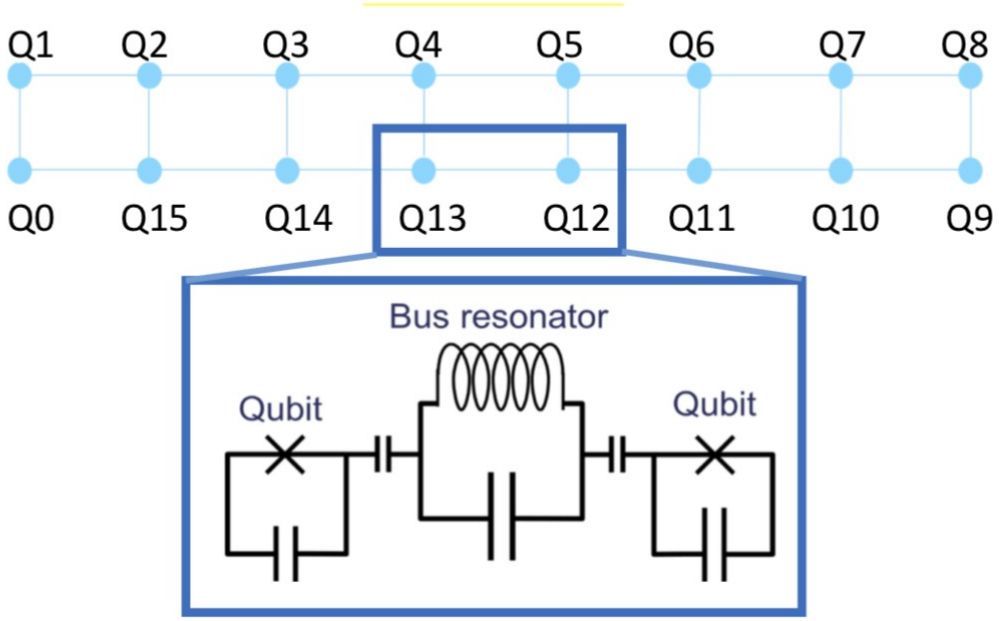

Bus frequency detuned from qubit frequencies. $|f_{qubit} - f_{bus}| >> g$

Two-qubit exchange interaction J via virtual photons is mediated by the bus resonator.

48

Superconducting qubits: spin control and readout

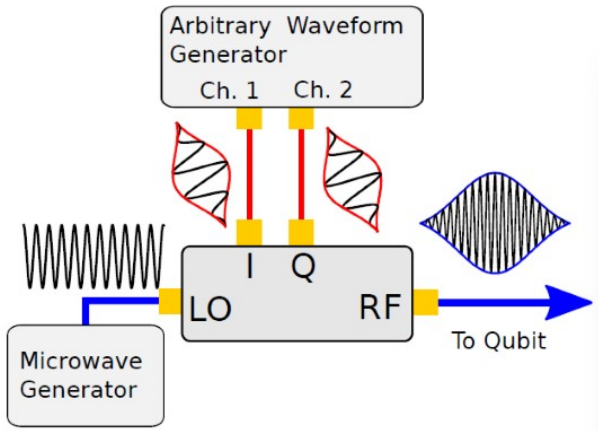

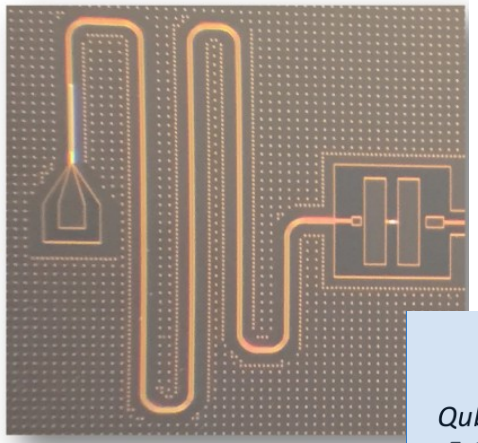

Drive around the Bloch sphere using microwave pulses (typically 10-50ns @ 5-6 GHz)

I/Q upconversion and Gaussian pulse modulation

[M.B. Ritter, IEDM 2018 short course]

"Dispersive" = direct detection of change in resonance frequency of detuned readout resonator

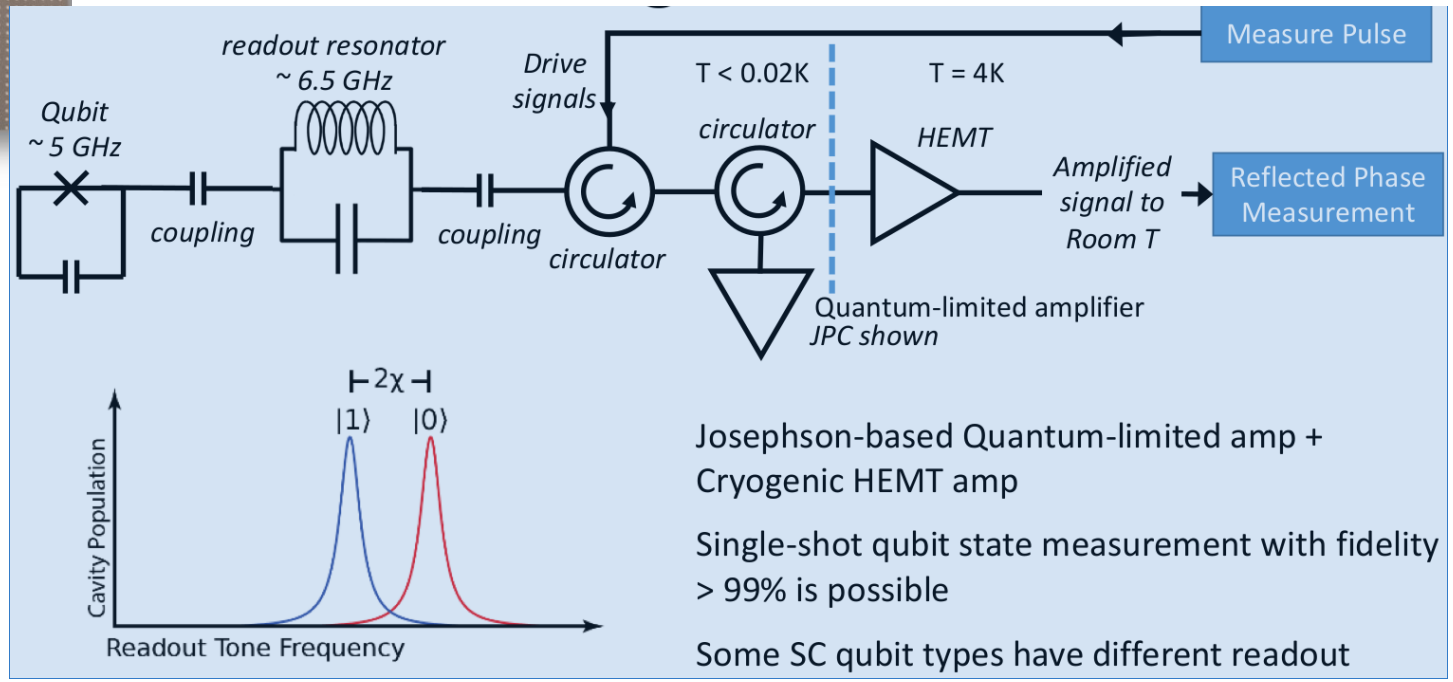

Josephson-based Quantum-limited amp + Cryogenic HEMT amp

Single-shot qubit state measurement with fidelity > 99% is possible

Some SC qubit types have different readout

SC qubits: noise, energy, frequency, temperature

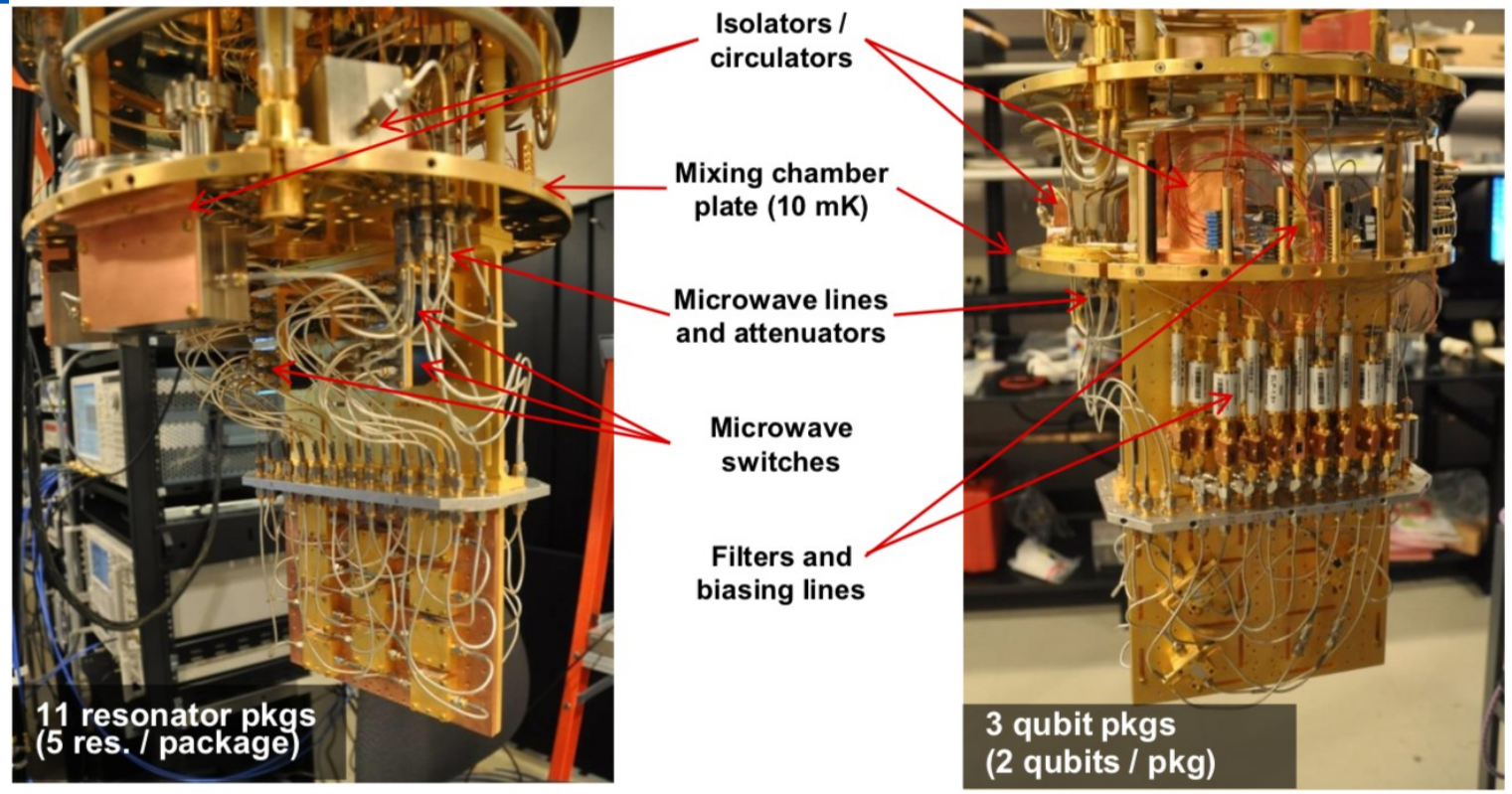

[W. Oliver, EuMW 2018 short course]

5 GHz has a thermal energy of 250 mK → operate at 20 mK.

Commercially available, turn-key dilution refrigerators.

Electron-spin coupled quantum dot (QD) concept

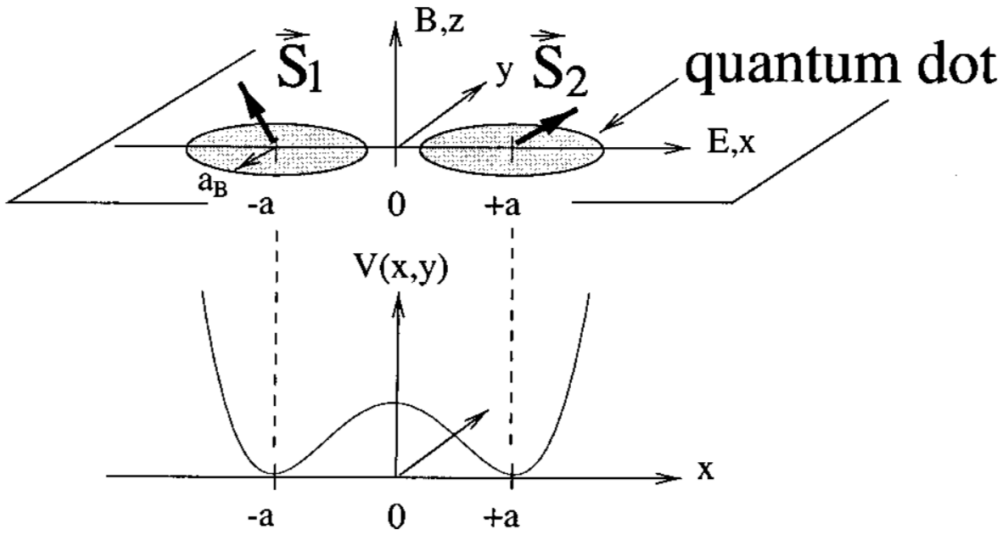

FIG. 1. Two coupled quantum dots with one valence electron per dot. Each electron is confined to the xy plane. The spins of the electrons in dots 1 and 2 are denoted by $\mathbf{S}_1$ and $\mathbf{S}_2$. The magnetic field B is perpendicular to the plane, i.e., along the z axis, and the electric field E is in plane and along the x axis. The quartic potential is given in Eq. (3) and is used to model the coupling of two harmonic wells centered at $(\pm a,0,0)$. The exchange coupling J between the spins is a function of B, E, and the interdot distance $2a$.

[Burkard, Loss and DiVincenzo Phys Rev B, 1999]

Larmor frequency $\omega_L = \gamma_e B$

γ_e is the electron gyromagnetic factor ~28 GHz/T

E-level splitting due to Zeeman effect with dc *B*

[L Hutin, Hole-spin qubit. VLSI 2016]

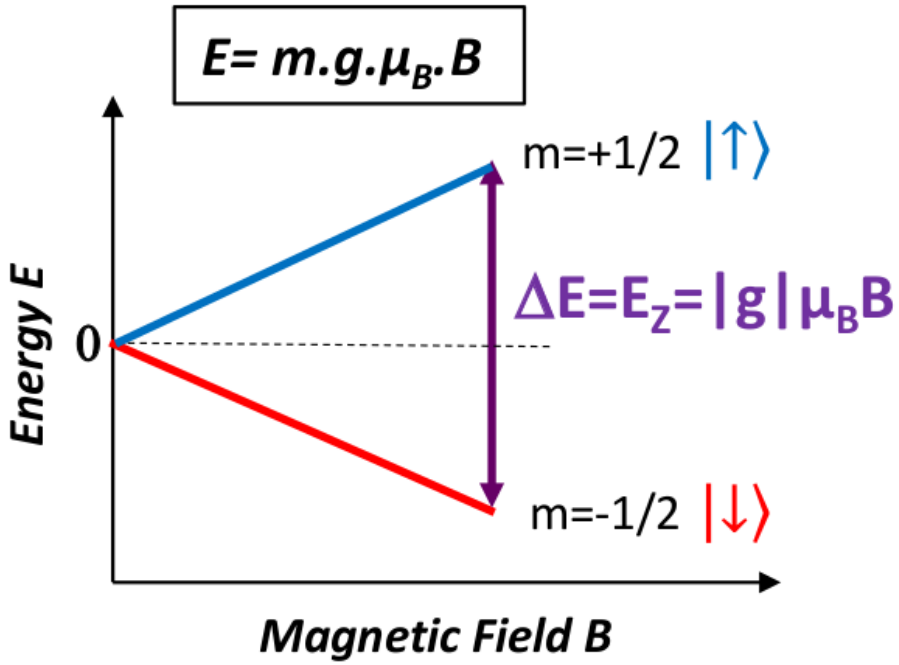

$$E_m = m\, g\, \mu_B B = 115.74\, \mu eV \cdot m \cdot B[Tesla]$$

$$f_{Larmor} = \frac{\Delta E}{2\pi\hbar} = 27.92\, GHz \cdot B[Tesla]$$

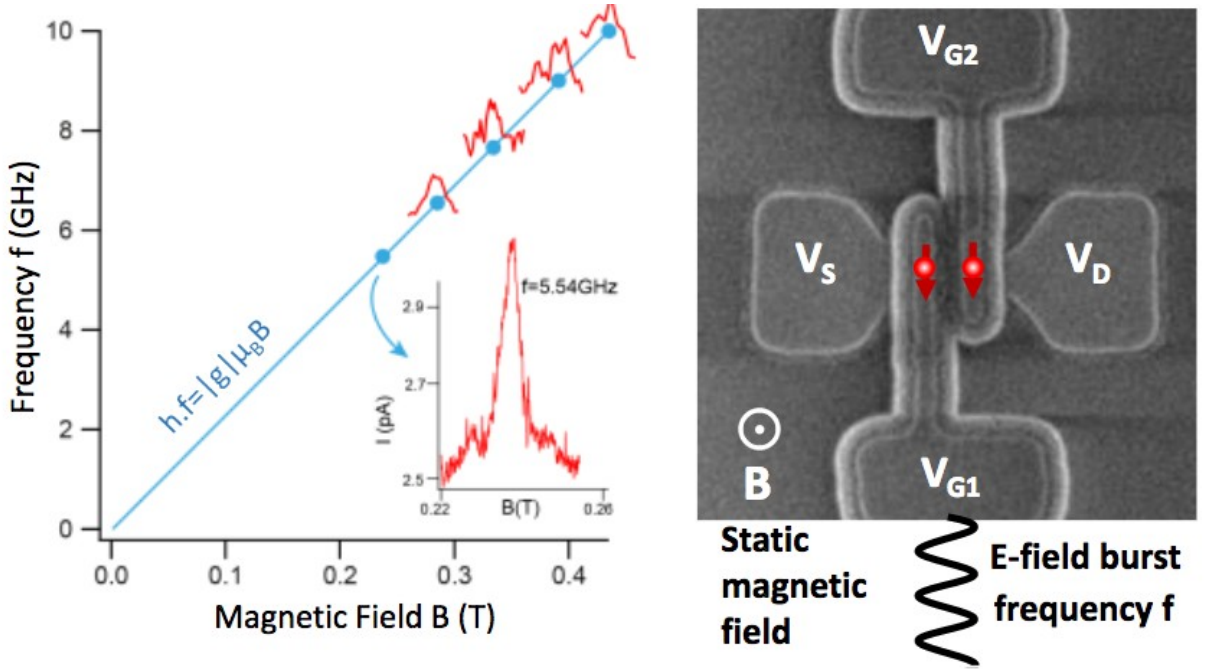

Fig.8: Measured Electrically Driven Spin Resonance (EDSR) signals. Spin transitions can occur if the energy of an EM excitation matches the Zeeman energy. Here, the Pauli Spin Blockade is lifted using only an E-field excitation on the G1 Gate. Plotting the current versus static magnetic field strength for various E-field frequencies yields spikes located along a line verifying the equation $hf=E_Z=|g|\mu_B B$.

E-level splitting due to coupling between QDs

AlGaAs/GaAs/AlGaAs double well

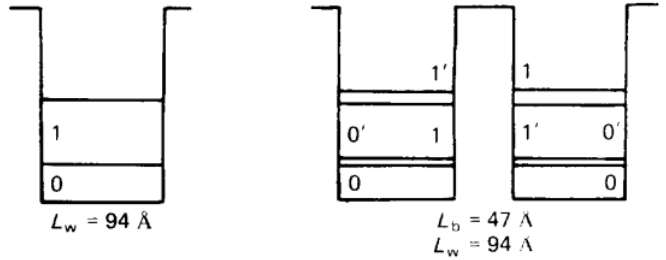

Coupling frequency $f_C = \frac{2\Delta E}{2\pi\hbar}$; $2\Delta E = 1\text{meV} \rightarrow 241.47\,GHz$

ΔE (or t or J) = coupling energy

ΔE must be > kT

Want electric control of ΔE (barrier) for Swap or C-NOT gate

$$E_{0+} = E_0 + \Delta E$$

$$E_{0-} = E_0 - \Delta E$$

[S. Voinigescu, IJE Feb. 1989]

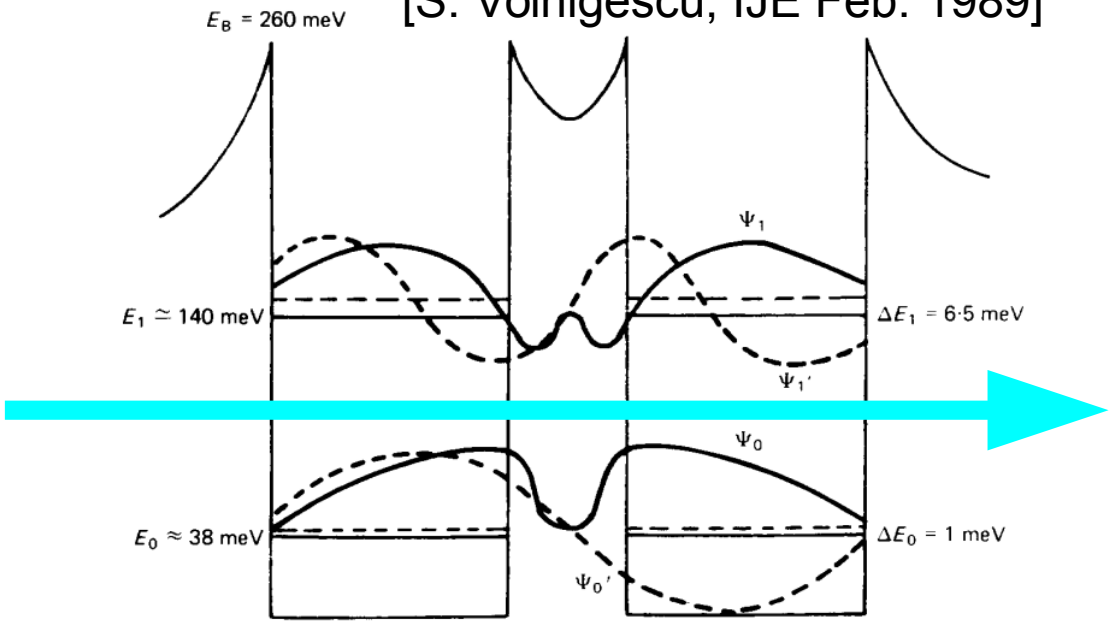

gure 6. Subbands and wave functions in an idealized quadruple heterojunction structure with quantum channel coupling.

Electron-spin coupled quantum dot gates

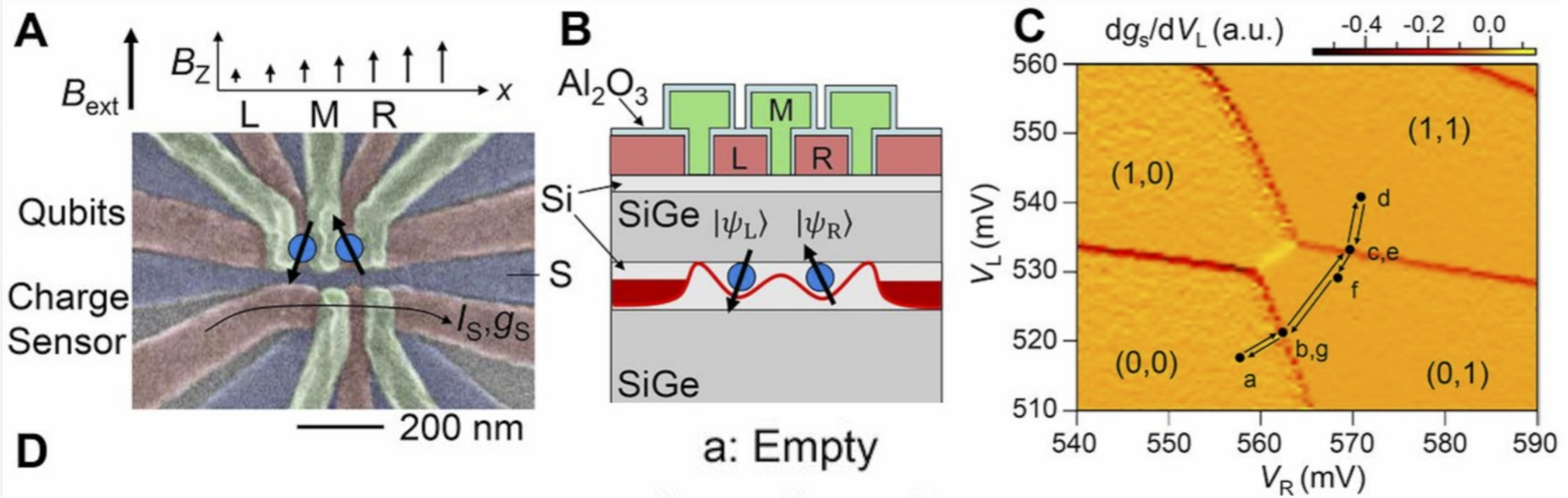

[M.B. Ritter, IEDM 2018 short course]

Resonantly driven CNOT gate for electron spins
By D. M. Zajac, A. J. Sigillito, M. Russ, F. Borjans, J. M. Taylor, G. Burkard, J. R. Petta
Published Online07 Dec 2017
DOI: 10.1126/science.aao5965

Magnetic field gradient produces different Zeman energy for two dots, hence two distinguishable qubits

Quantum computing with coupled QD

Spin **Rotations**

- Apply a mm-wave signal of amplitude V_{mmw} at $f_{Larmour}$ for pulse duration τ on QD gate

$$\theta = 2\pi f_R \tau$$

where $f_R \sim V_{mmw}$ is the **Rabi** frequency, $f_R << f_{Larmour}$

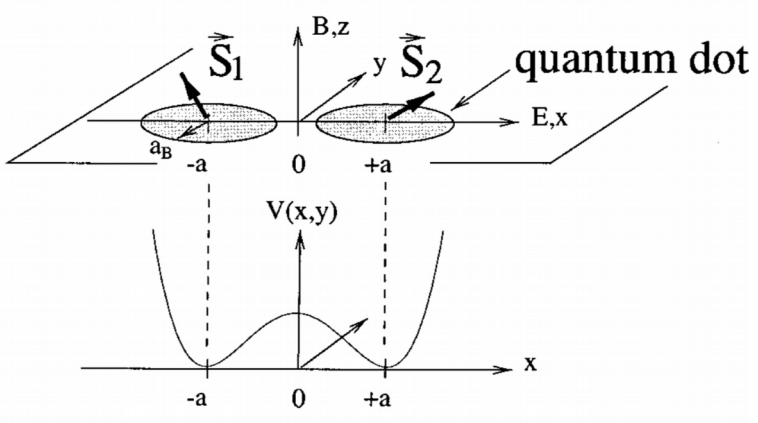

Spin **Swap or C-NOT gate**

- Apply a pulsed inter-dot voltage and/or on barrier gate

$$H_s(t) = J(t)\vec{S}_L \cdot \vec{S}_R$$

f_R determines speed of quantum gate and processor

From FDSOI MOSFET to quantum dot

- Wide spacers and small L_G lead to forming a well between two barriers
- Carriers have no thermal energy and have to tunnel through
- Energy states are quantized in the well
- Small V_{DS} to scan precisely the resolved quantum states

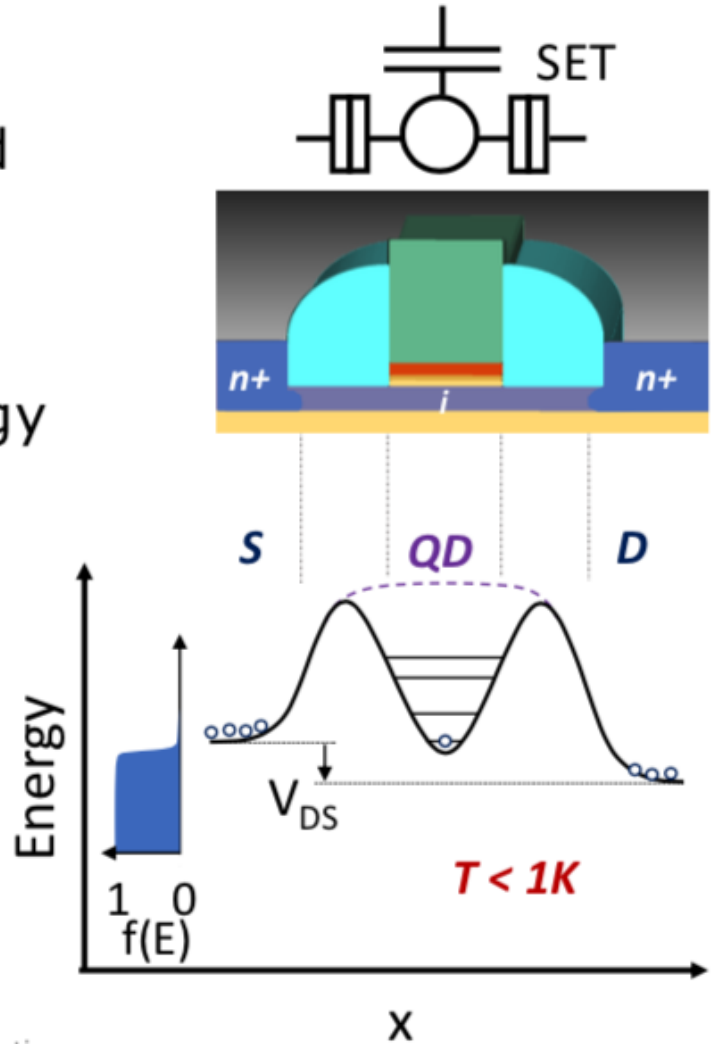

[L. Hutin, ESSDERC 2018]

From quantum dot to spin qubit

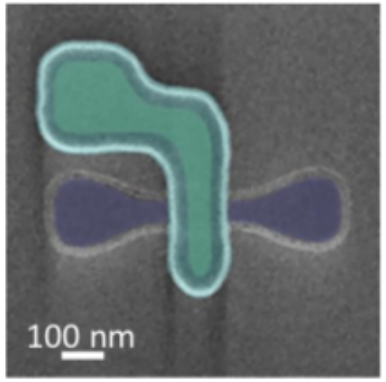

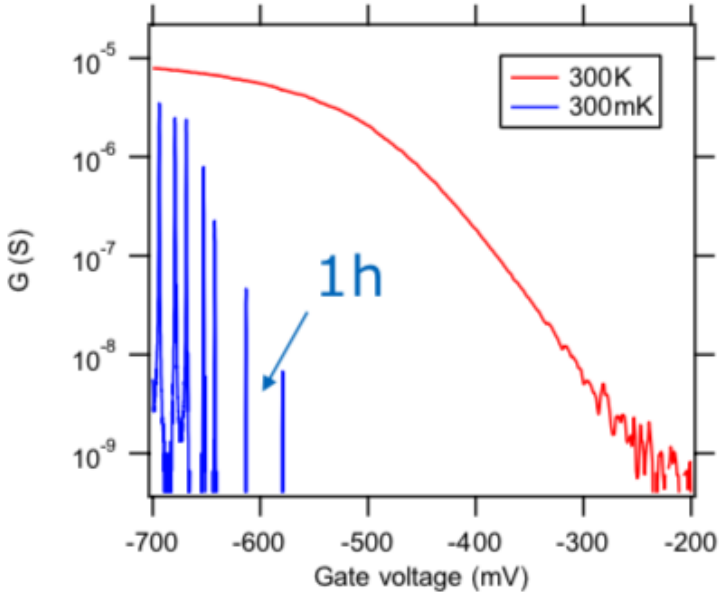

"Artificial atom"

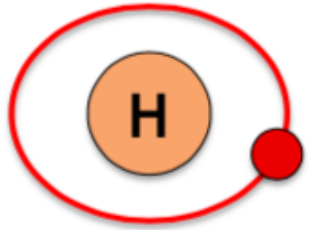

Spin S = ±1/2

Applying a static magnetic field B, two-level spin qubit:

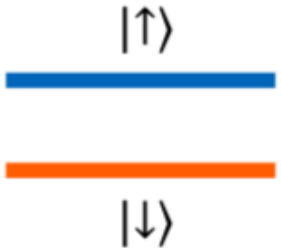

$E_Z = |g.\mu_B.B|$

[L. Hutin, ESSDERC 2018]

Hamiltonian of single-spin gates with excitation

$$H_{lab} = -\omega_L + \gamma_e B(t)\frac{\sigma_x}{2}$$

$$B(t) = \frac{2}{\gamma_e}\omega_R \cos(\omega_{mmw} t + \phi)$$

$$H = (\omega_{mmw} - \omega_L)\frac{\sigma_z}{2} + \omega_R\left[\cos(\phi)\frac{\sigma_x}{2} - \sin(\phi)\frac{\sigma_y}{2}\right]$$

$$U = e^{-iHt}$$

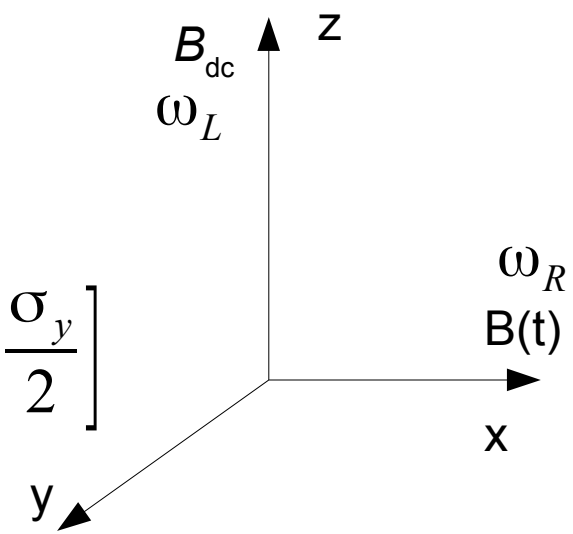

Bloch sphere

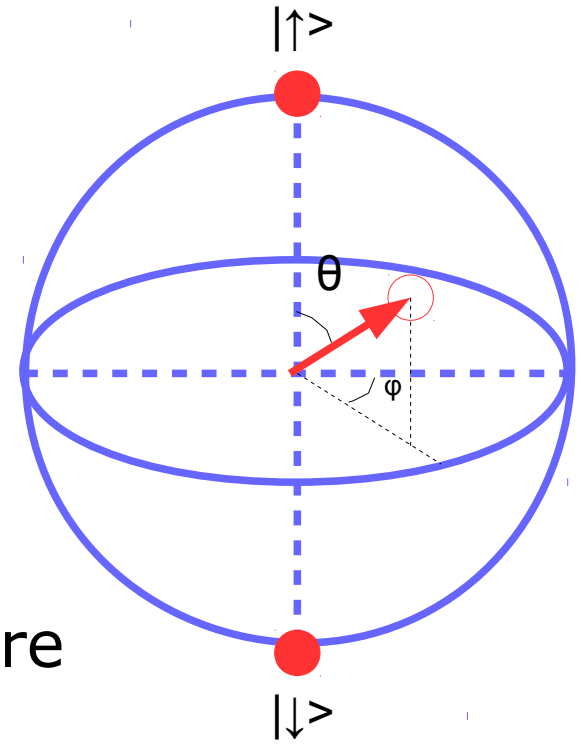

$\omega_L \sim B_{dc}$ sets the qubit frequency, operation temperature

When $\omega_{mmw} = \omega_L$ we have electric spin resonance (ESR)

[J.P.G van Dijk, NPJ 2018]

Mm-wave spin manipulation circuit specification

➢ The Hamiltonian in the rotating frame ($\omega_{frame} = \omega_{mw}$) with rotating wave approximation:

$$H = (\omega_{mw} - \omega_0)\frac{\sigma_z}{2} + \omega_R\left[\cos(\varphi)\frac{\sigma_x}{2} - \sin(\varphi)\frac{\sigma_y}{2}\right]$$

Selects the qubit (frequency)

Sets the rotation speed (Amplitude)

Sets the rotation axis (X/Y) (Phase)

$$U = e^{-i\cdot H\cdot t}$$

Sets the rotation time

$$\omega_0 = \omega_L$$

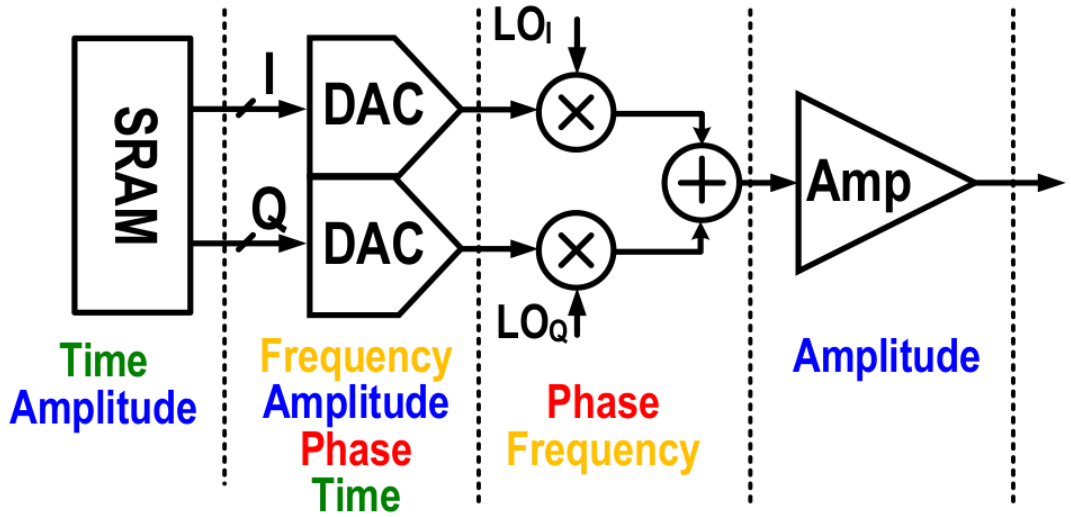

[M. Mabaie, EuMW-2018 Short Course]

[J.P.G van Dijk, NPJ 2018]

ESR spin manipulation

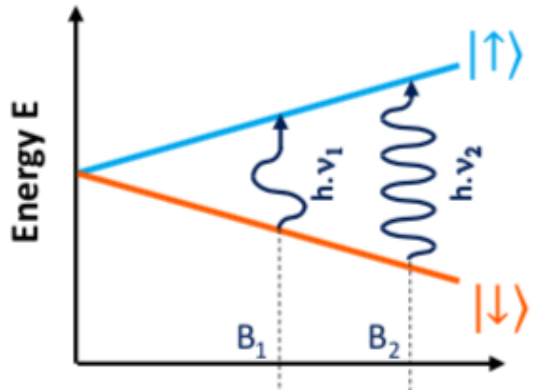

$$\Delta E_Z = g\mu_B B$$

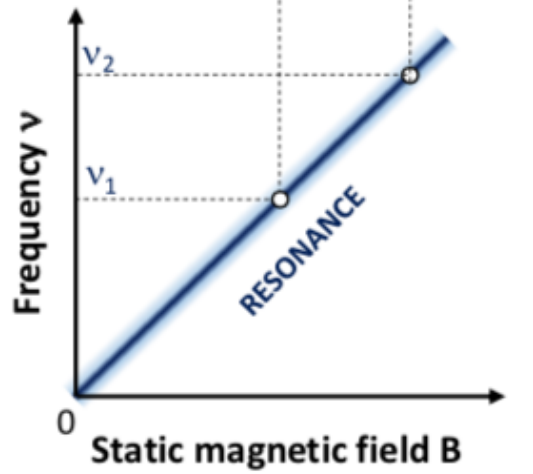

$$\nu = g\mu_B B/h$$

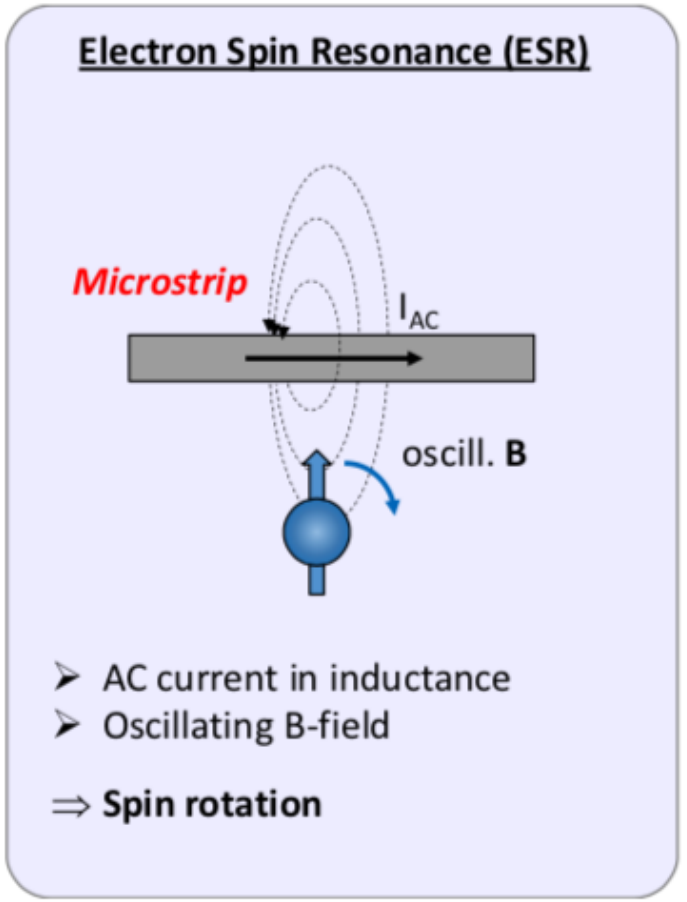

$$\omega_R \propto B_{ac} = \alpha I_{ac}$$

α determined from measurements

[L. Hutin, ESSDERC 2018]

- ESR is the most straightforward way, but difficult to apply locally.

Electrical-only spin manipulation

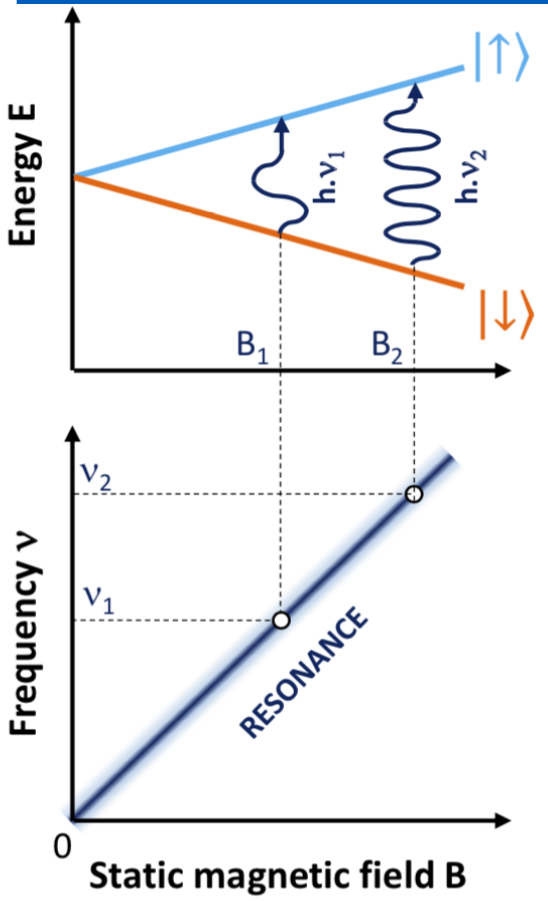

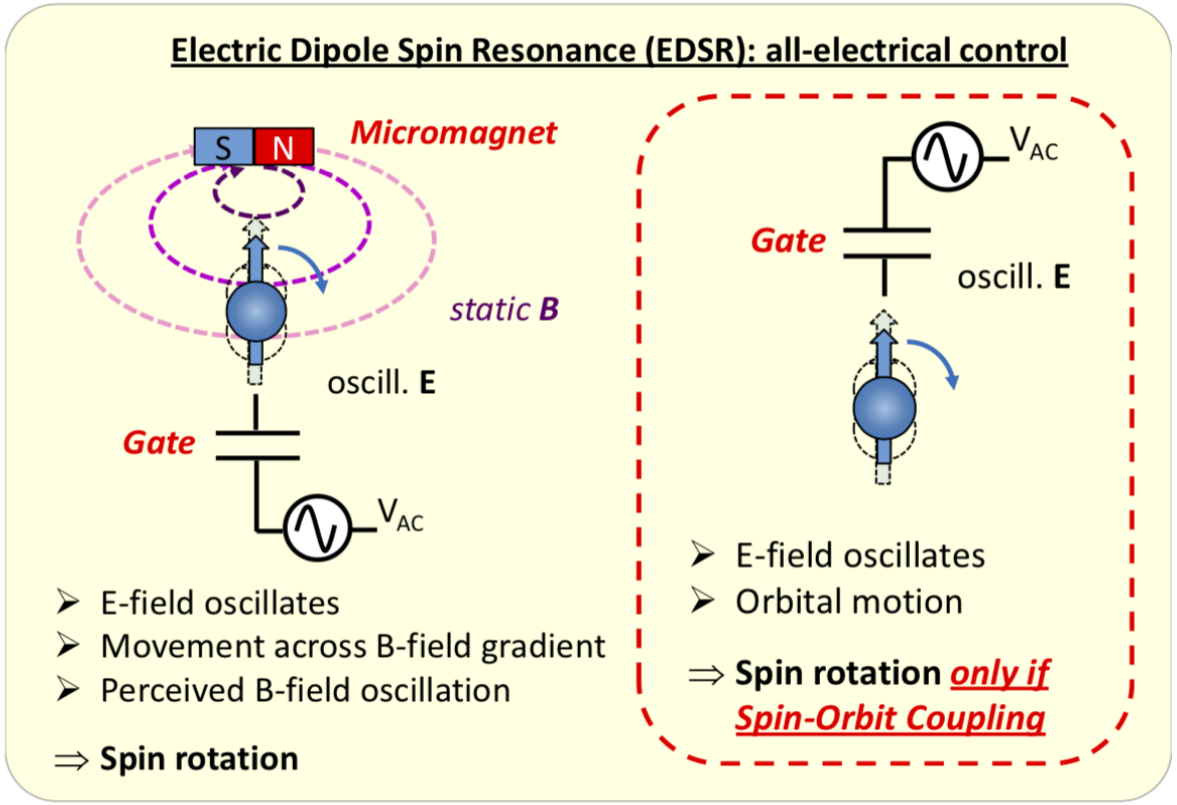

$$\omega_R = \beta V_{ac}$$

β determined from measurements

[L. Hutin, ESSDERC 2018]

For **holes in Si**, SOC is strong enough to **use only V_{AC} on Gates**!

Electrical-only spin manipulation: Rabi frequency

R. Maurand et al., Nature Comm., 7 (2016)

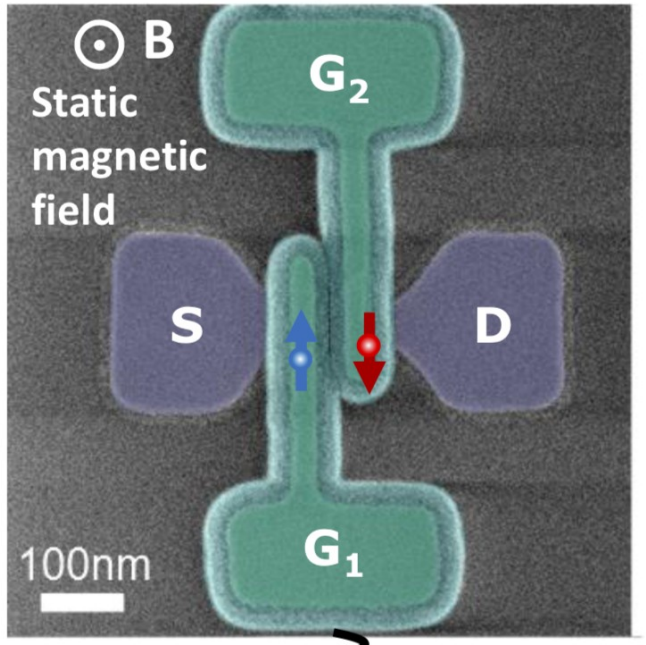

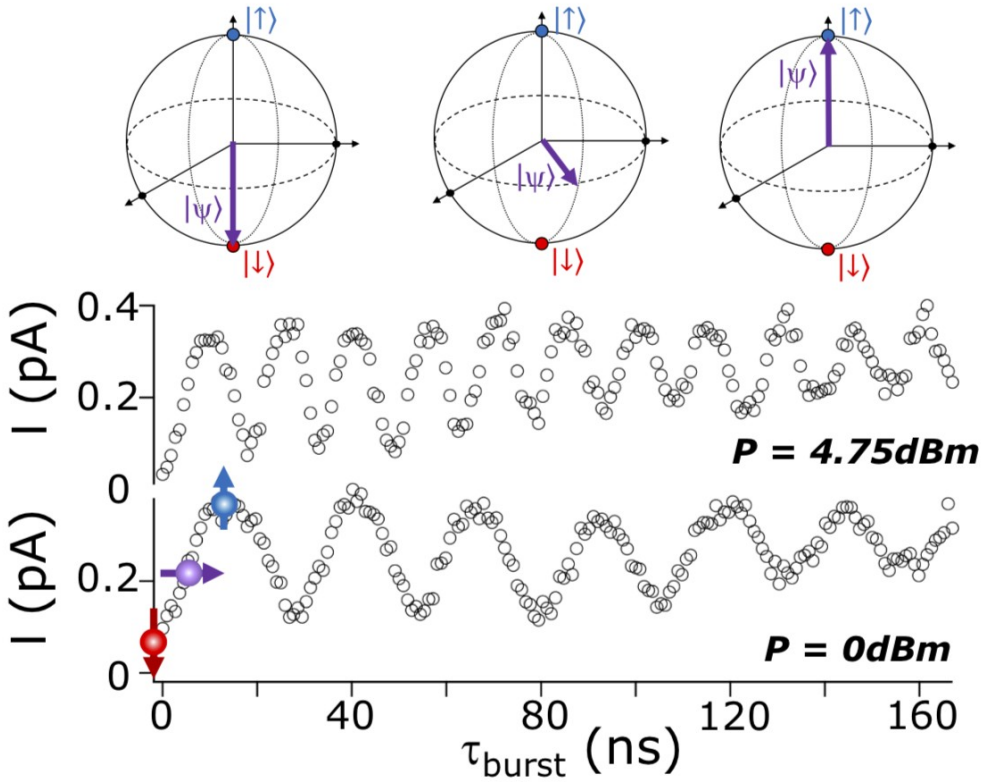

[L. Hutin, ESSDERC 2018]

Rotation speed depends on $P_{MW}^{1/2}$

Pauli spin blockade readout

- The current is rectified under **Pauli Spin Blockade** conditions.
- Lifting it requires the ability to **induce a spin transition** in QD1.
- Send a **resonant excitation on G1** to manipulate the spin, read current across the NW.

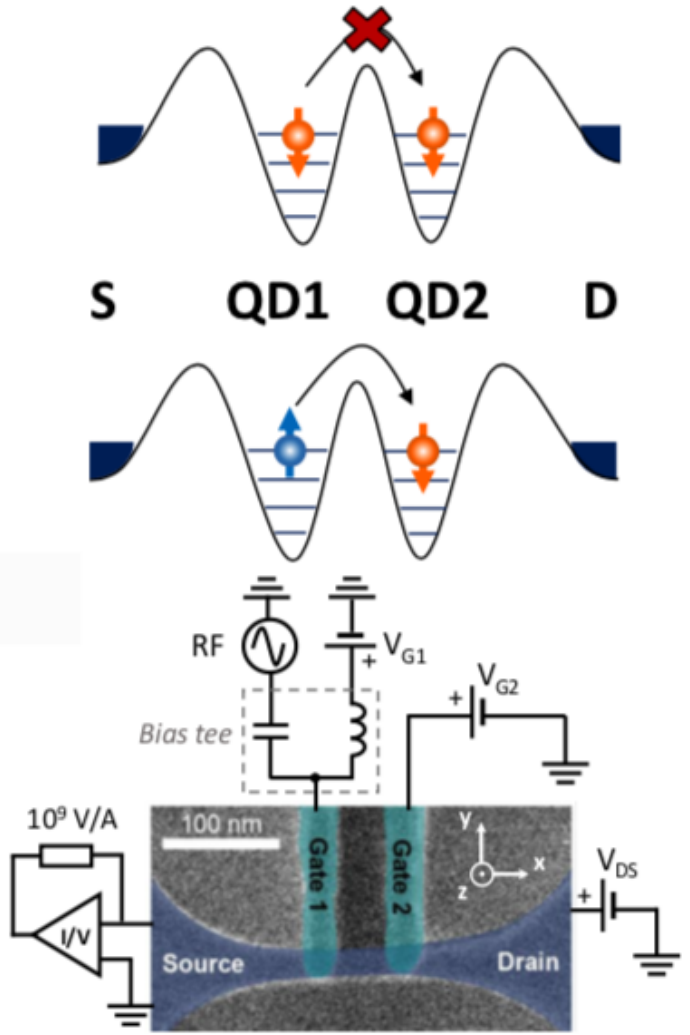

[L. Hutin, ESSDERC 2018]

Quantum computing: current vision is hybrid

Integrated electronics
1% accuracy in all parameters

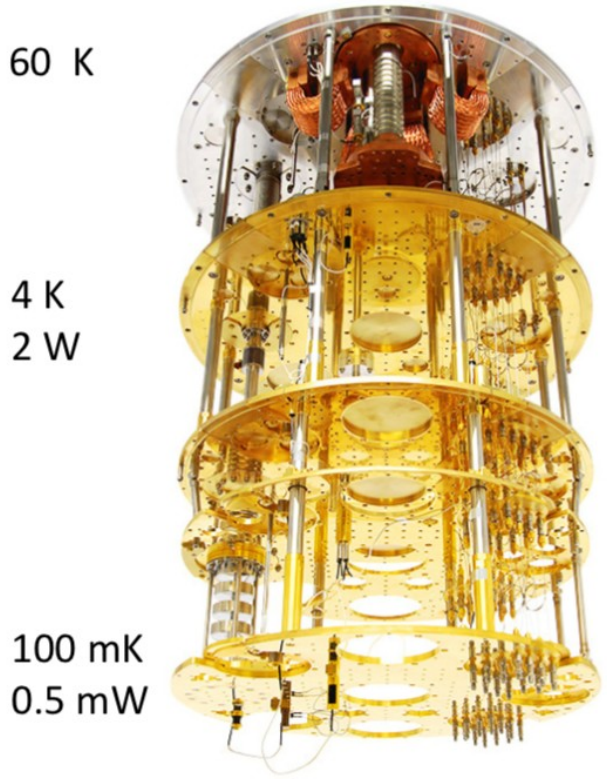

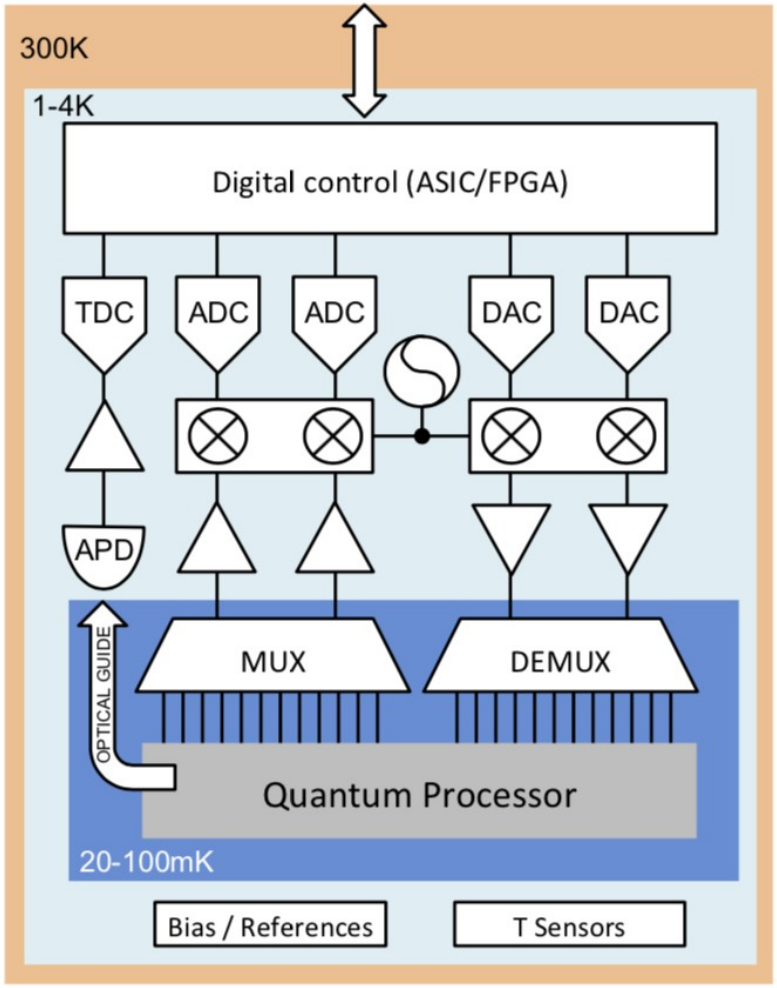

P_{dc} & qubit technology

prevent integration

E. Charbon et al., "Cryo-CMOS for Quantum Computing," IEDM 2016.

Quantum computing for electronics engineers

- Fully coupled N-qubit register => 2^N complex amplitudes **available simultaneously**
- qubits act as gates and as temporary memory cells for intermediate results
- “Logic gate operations” are sequentially executed in time by...
  - applying mm-wave analog-mixed signals (I/Q pulse modulation) to qubit gates
  - ...we perform deterministic phase modulation in 2D
- System time-evolution described by Schrodinger's time-dependent equation
- Readout is probabilistic, based on spin selective tunneling or dispersive
- **Ultra low phase noise, cryogenic mm-wave radar-like circuits needed**

Quantum computing challenges today

- Thermal noise ~kT
- ΔE <0.1 meV => T< 1 K
- Spin relaxation and coherence times ~ μs

  => gate operations must be ~ 10 ps in duration
- Cannot dissipate >10mW power at 0.1 K
- Interface with outside world too big a load for qubit
- Atomic-scale fabrication precision needed with high yield

The original vision

The dimensionless parameters used here would, for example, correspond to the following actual physical parameters: If an exchange constant $J_0 = 80\ \mu\text{eV} \approx 1\ \text{K}$ were achievable, then pulse durations of $\tau_s \approx 25\ \text{ps}$ and decoherence times of $\Gamma^{-1} \approx 1.4\ \text{ns}$ would be needed; such parameters, and perhaps much better, are apparently achievable in solid-state spin systems [19].

[Loss and DiVincenzo, Phys Rev A, 1998]

Si-based qubits typically function at cryogenic temperatures (<300 mK). However, if these devices were able to operate at higher temperatures (>4 K), the interfaces between quantum computer circuits and classical CMOSs could become less complicated and higher density integration would be possible. Smaller QDs are known to have higher charging energies and greater resistance to thermal noise. We

[S. Oda IEDM 2016]

Our approach and goals

- ***Foundry FDSOI*** CMOS-based QD qubits
  - Si n-MOSFET for electron spin qubit
  - SiGe p-MOSFET for hole spin qubit
- ***mm-wave AMS circuits*** for spin manipulation and readout ***on the same die with the qubits***
- > **4 *K*** operation now, ***(maybe) 77 K*** in 15 years

Outline

- Quantum computing fundamentals
- **Quantum computing ICs in 22-nm FDSOI at 2 K**
- Scaling for high temperature quantum computing
- Conclusions

Electron- and hole-spin QD concept in FDSOI

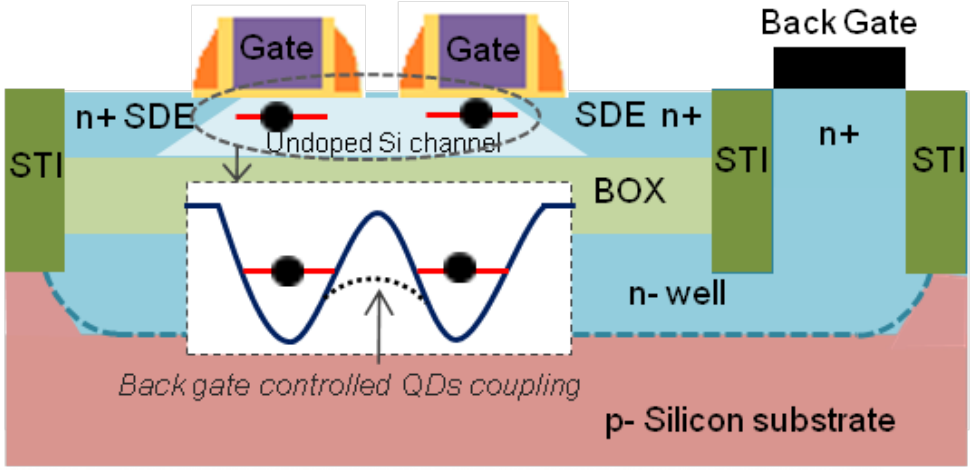

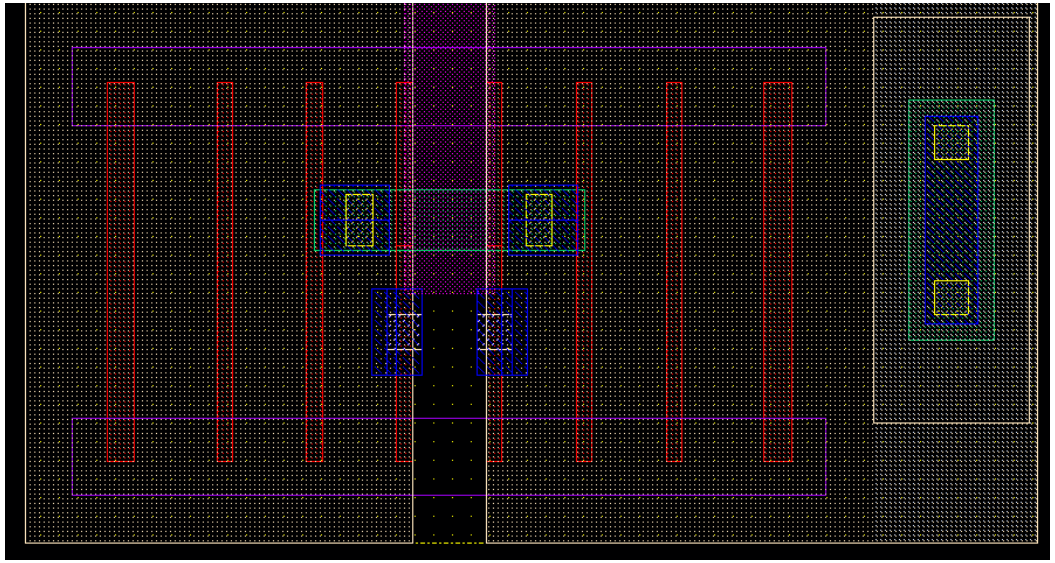

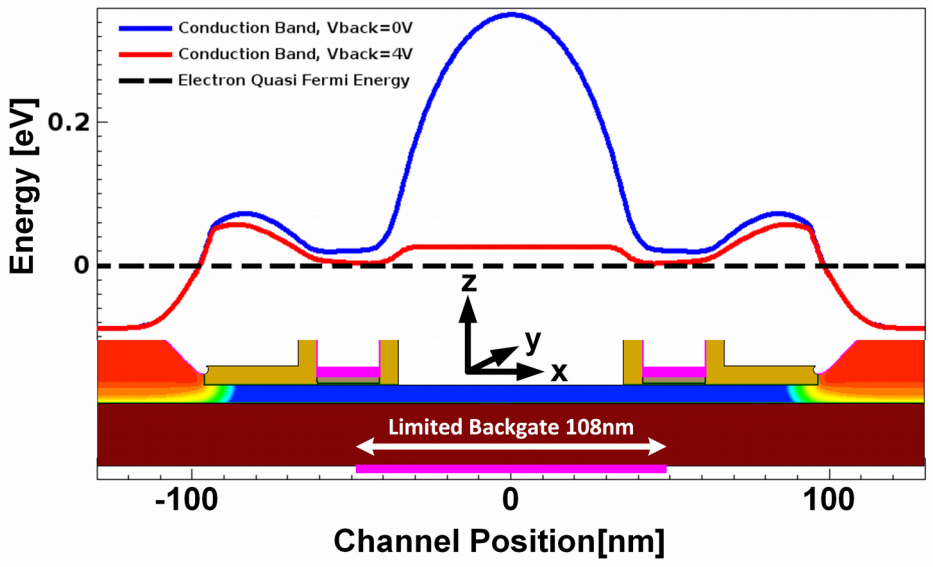

- Double-dot qubit (C-NOT) = 2-gate MOSFET cascode
- Quantum dot (QD) under each top gate
- Individual gate control of each QD
- Potential barrier between dots
- Back gate for entanglement control
- mm-wave E-field applied on gate and *z*-axis dc magnetic field

Low power monolithic quantum processor

- External low phase noise mm-wave signal
- Broadband mm-wave clock distribution
  - dc-100 GHz for 4-6 K operation
  - 140-220 GHz for 8-12 K operation
- n-MOS switch pulse modulators
- Broadband low-noise TIA readout < 3.5 mW per qubit
- SRAM to store the pulse sequences

Example:

- 200 qubits with individual readout: 700 mW
- Mm-wave clock distribution with minimum size inverters + clock amplifier: 200 mW
- Switches do not consume power

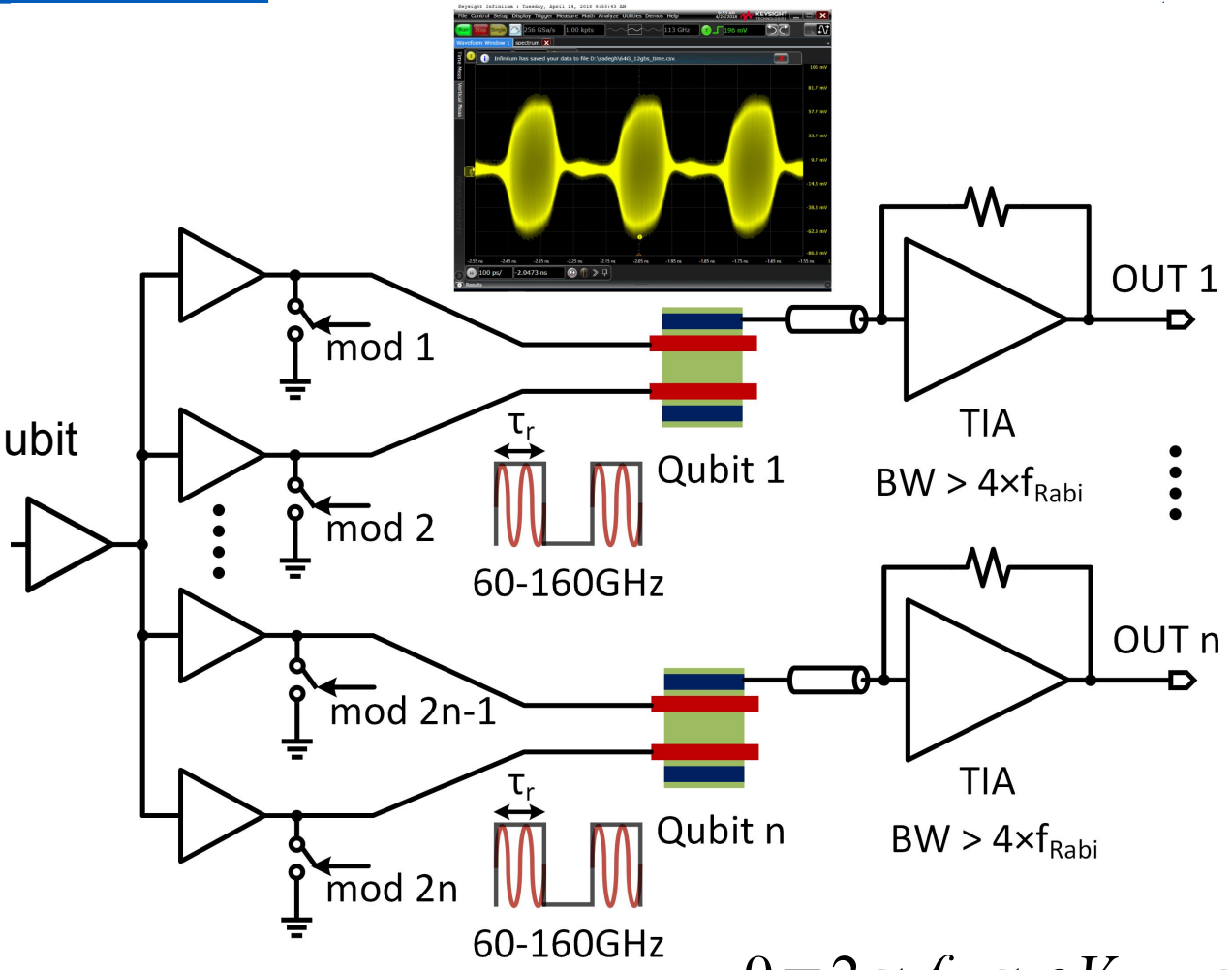

[S.Bonen et al. EDL 2018]

$$\theta = 2\pi f_R \tau \propto V_{mmw} \tau$$

3 and 5 coupled QD hole-spin qubits

3 series QDs

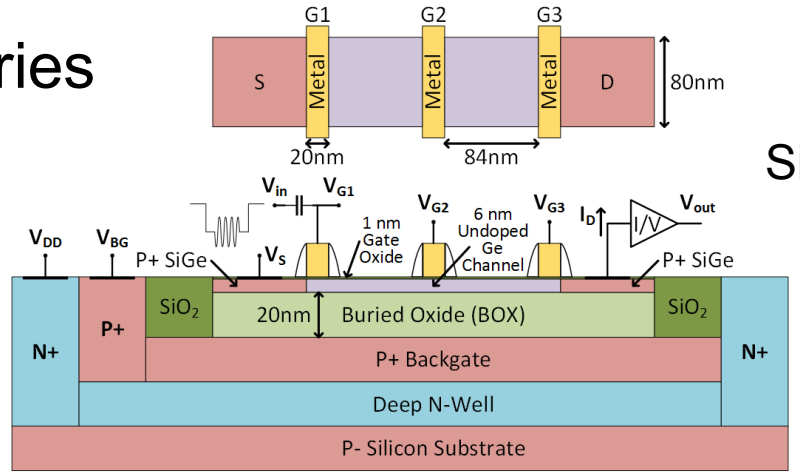

$Si_{0.5}Ge_{0.5}/Si_{0.75}Ge_{0.25}$

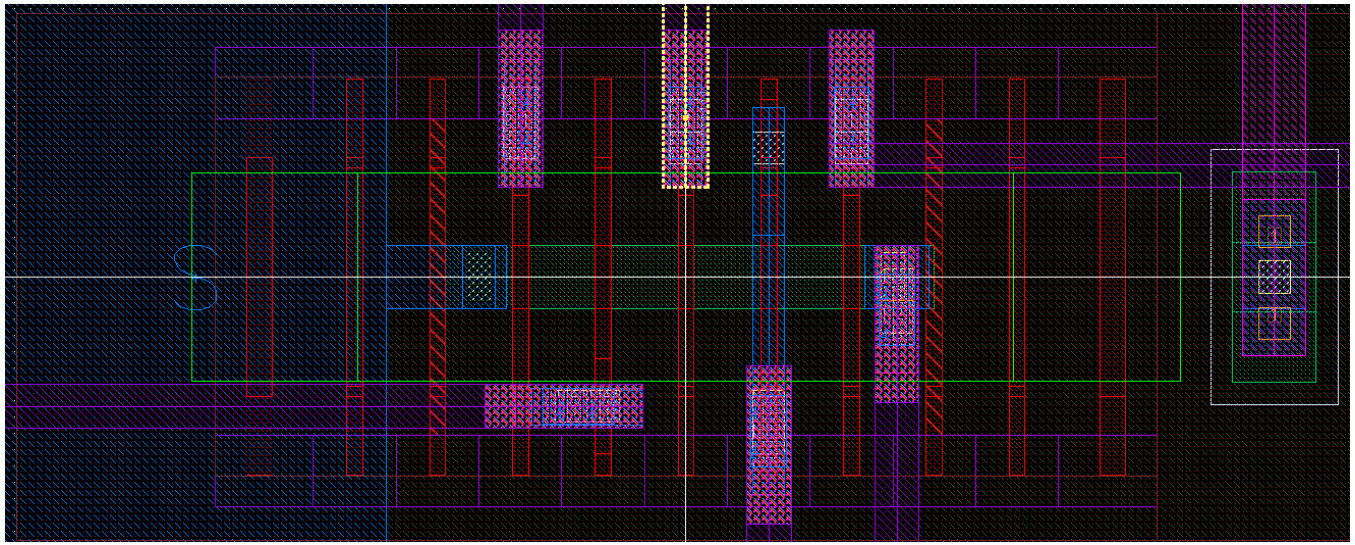

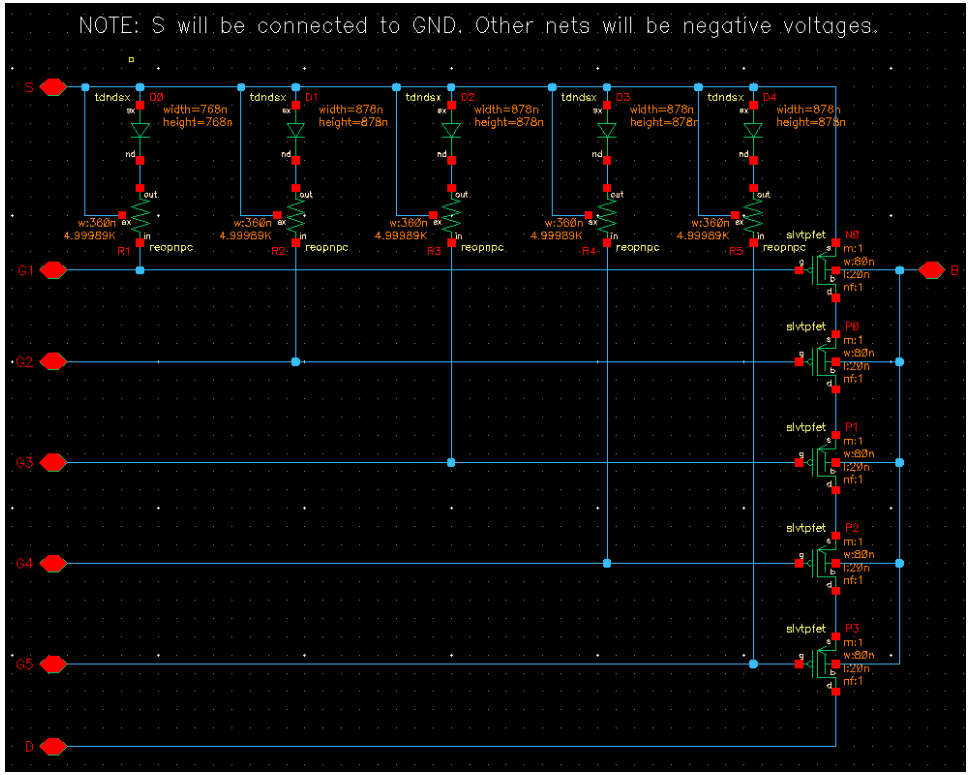

5 gates = 5 serially coupled qubits
Analogy with charge coupled devices and series stacked cascodes

Measurement set-up at 2 K

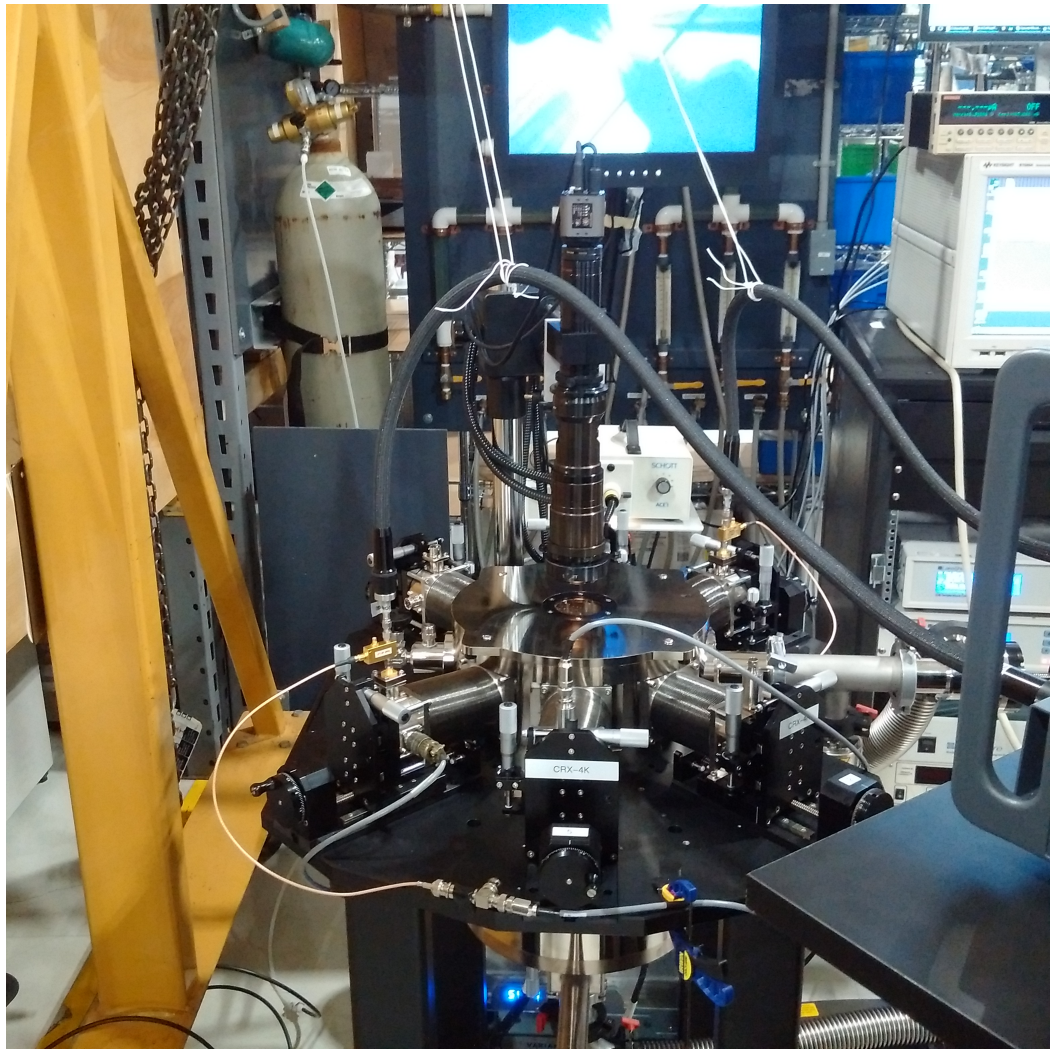

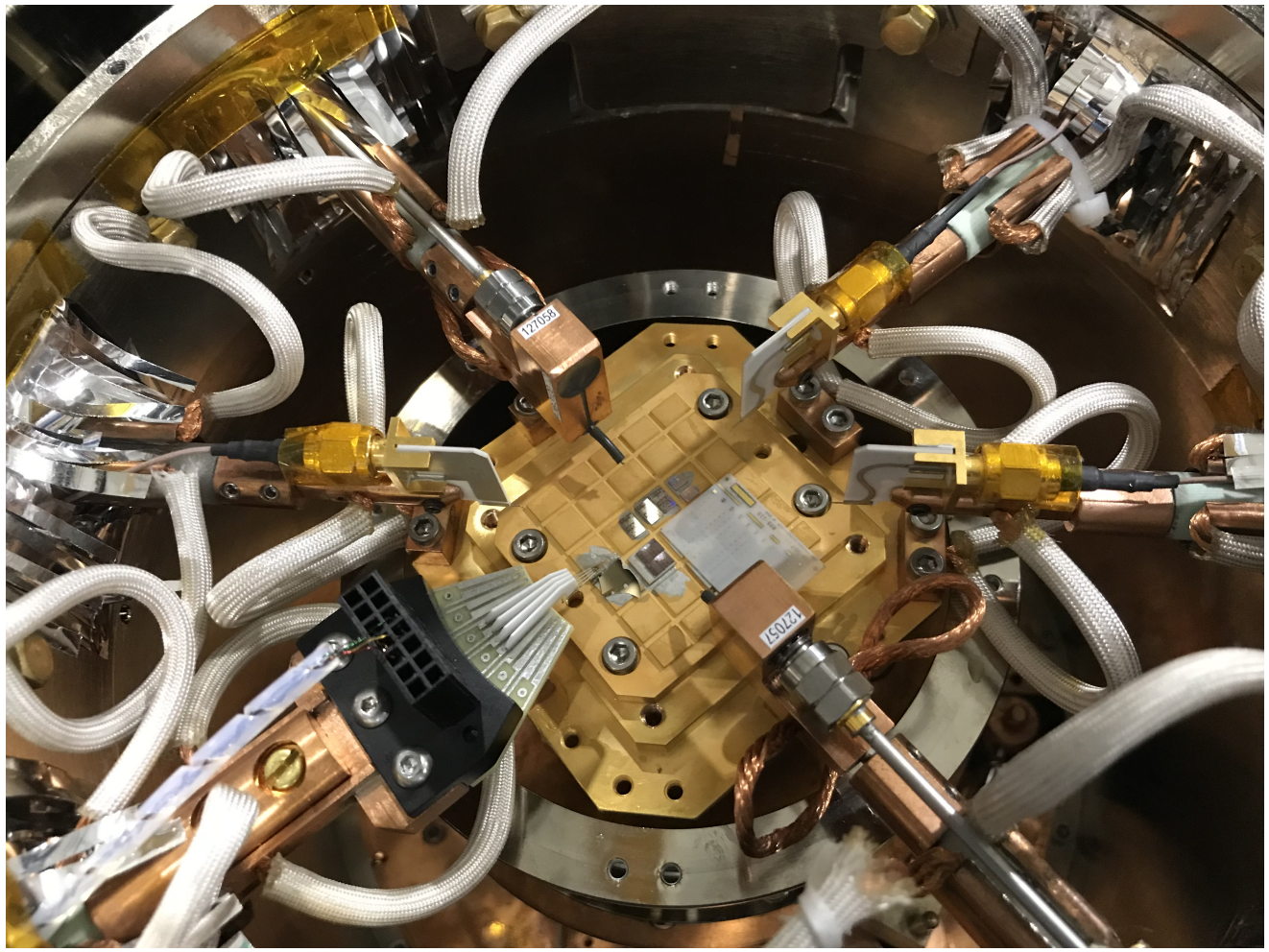

Minimum-size MOSFET characteristics over temp.

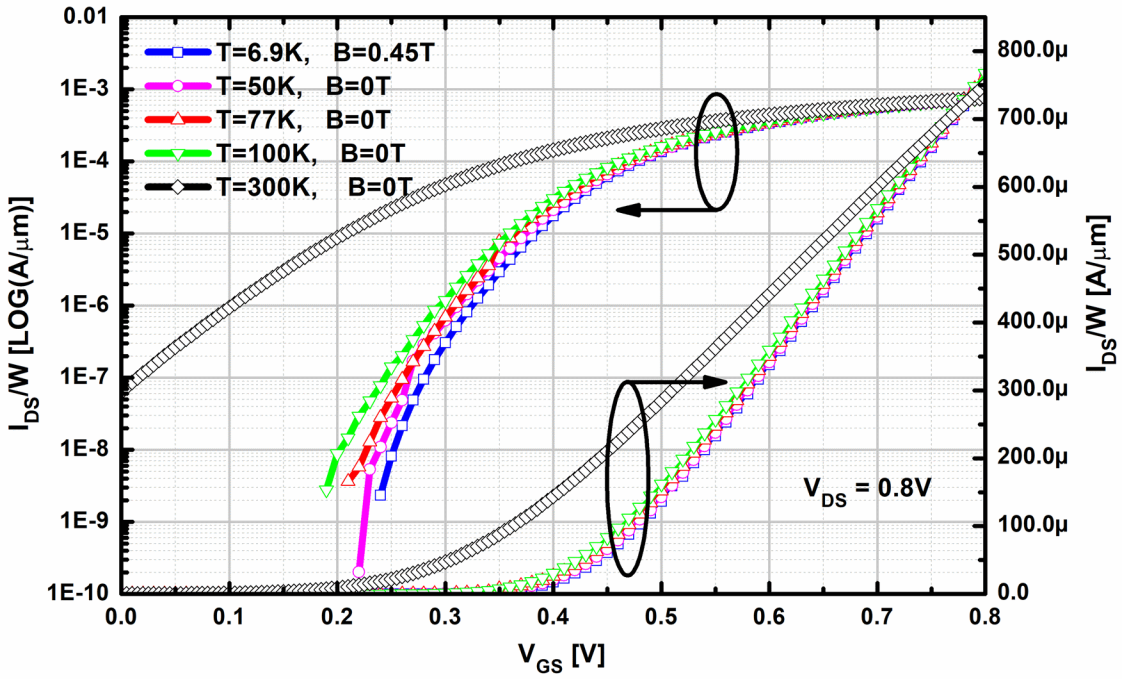

November 2017

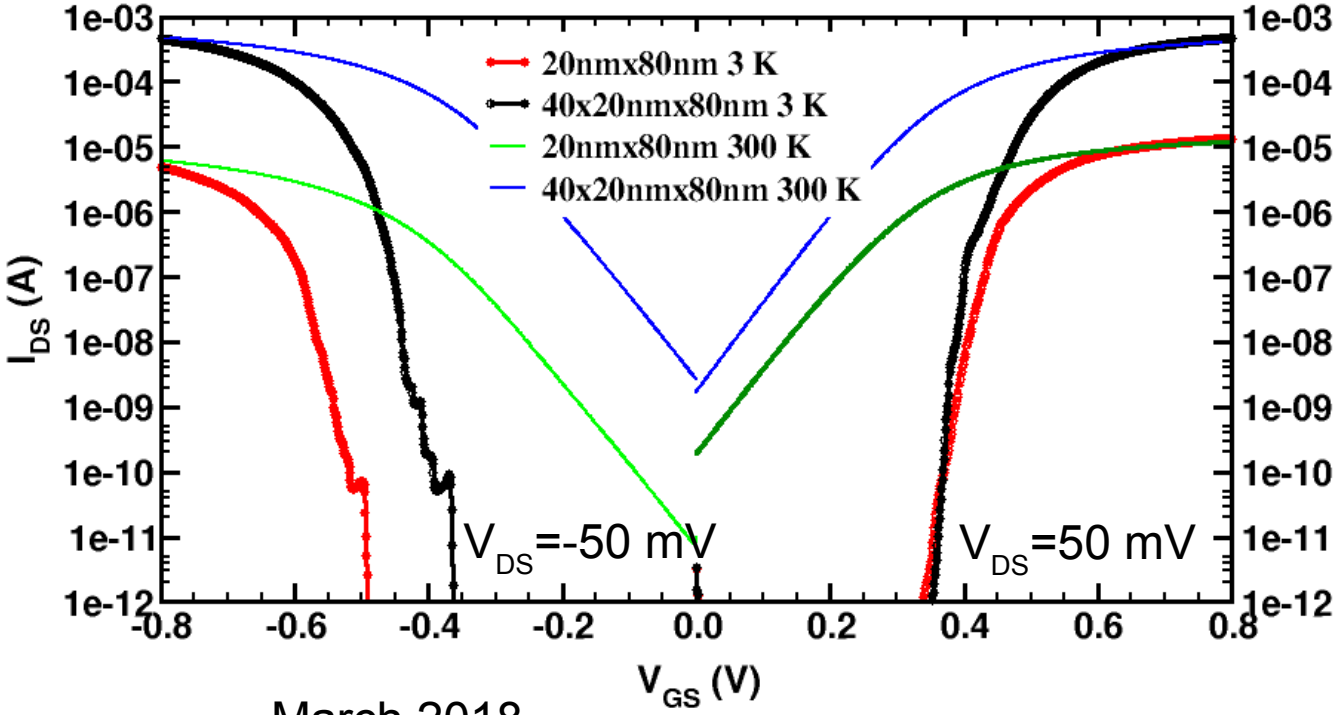

March 2018

Difficult to spot quantum effects unless you look in subthreshold at low V_{DS} (< 50 mV)

Quantum effects in 22-nm FDSOI n-MOSFET at 2 K

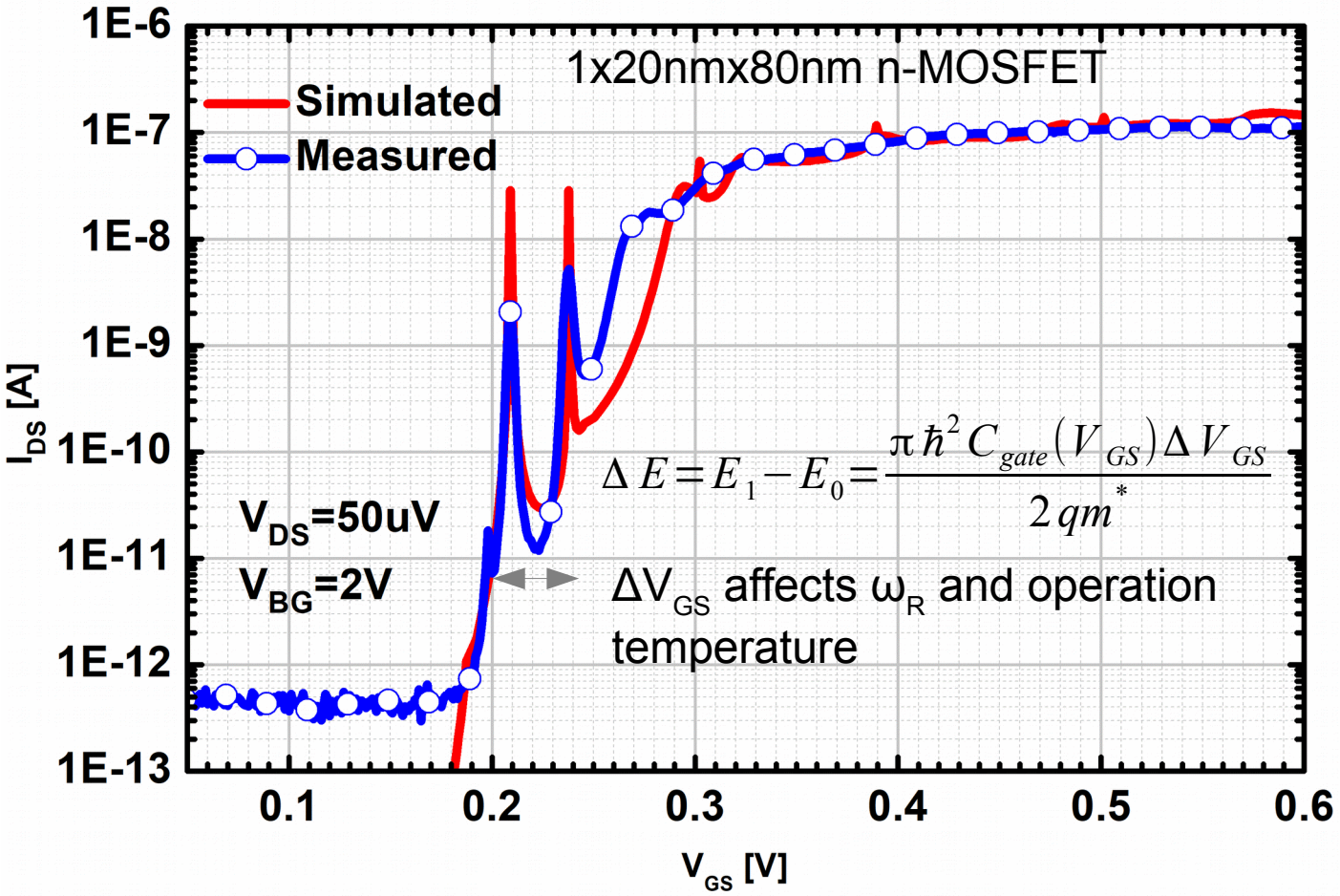

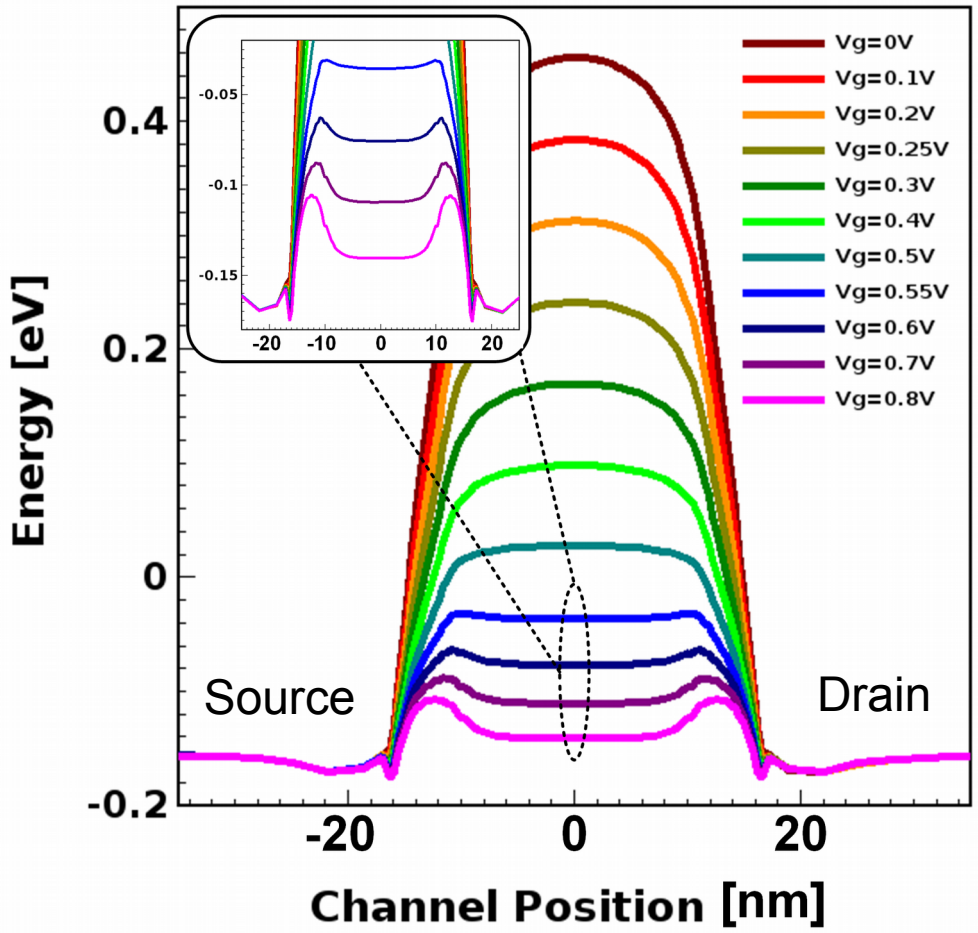

NEGF modelling code by Prof. Peter Asbeck

[S.Bonen et al. EDL 2018]

Quantum effects stronger in p-MOSFET

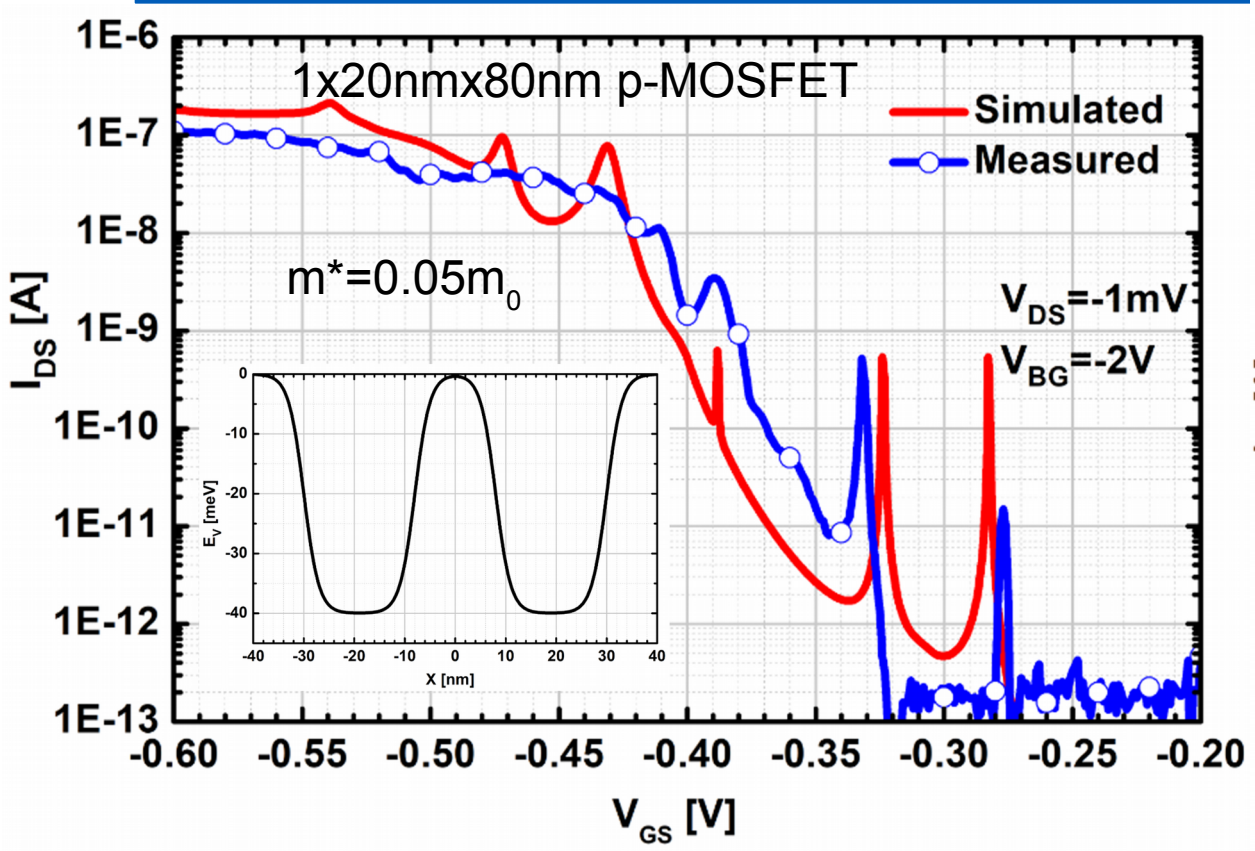

[S.Bonen et al. EDL 2018]

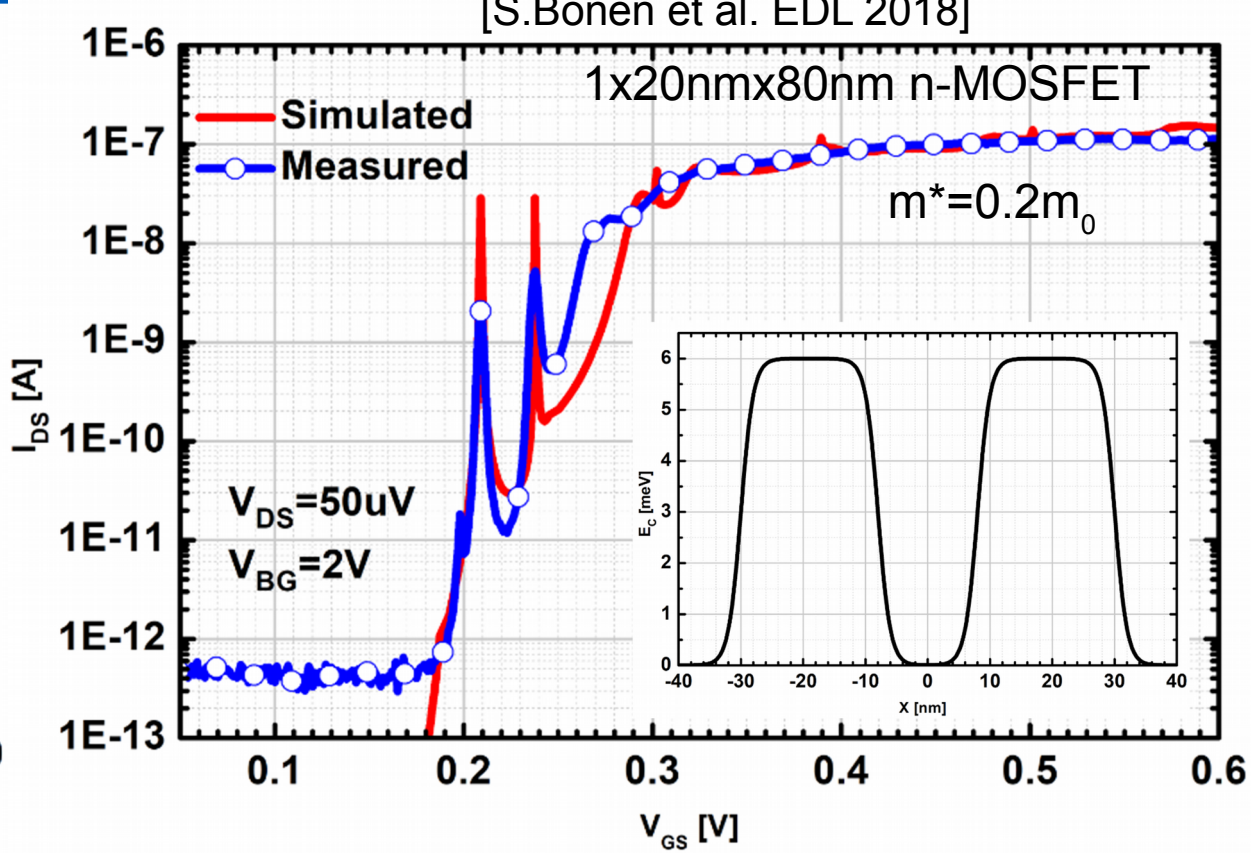

$Si_{0.5}Ge_{0.5}/Si_{0.75}Ge_{0.25}$ S/D-channel heterojunction provides better confinement barrier

ΔV_{GS}, (hence ω_R) doubles in p-MOSFET compared to n-MOSFET

Energy level spacing tuneable from backgate

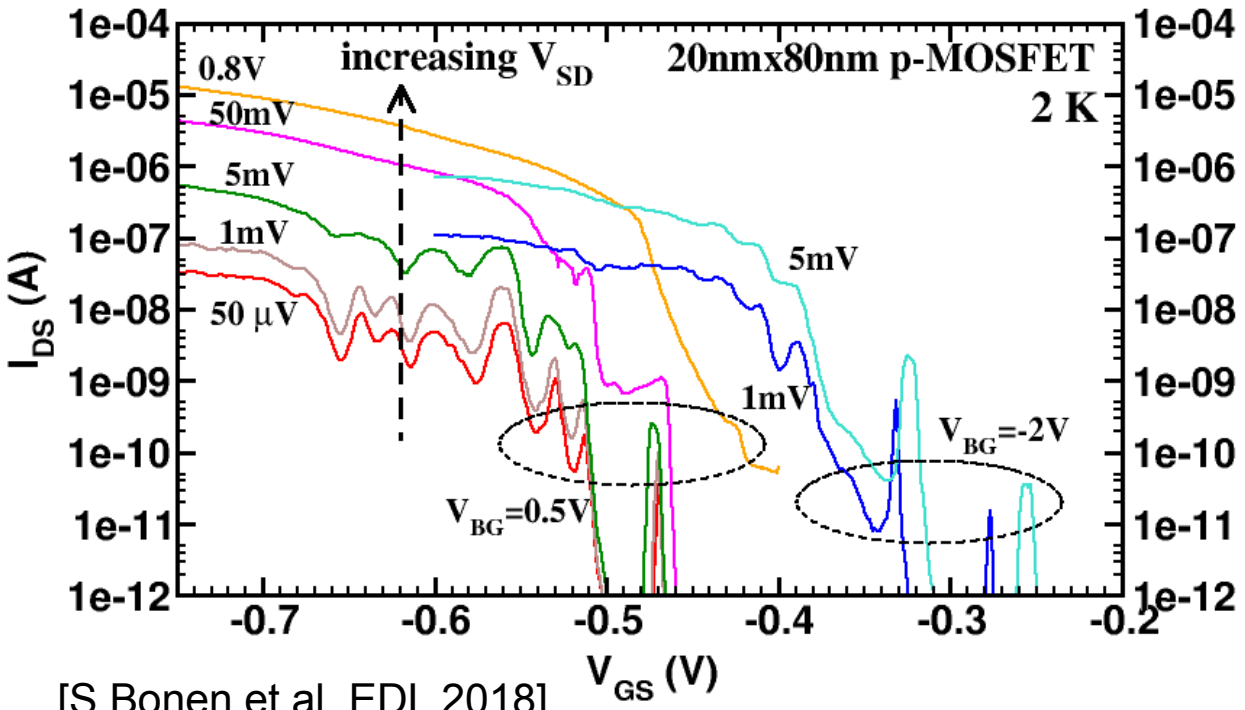

[S.Bonen et al. EDL 2018]

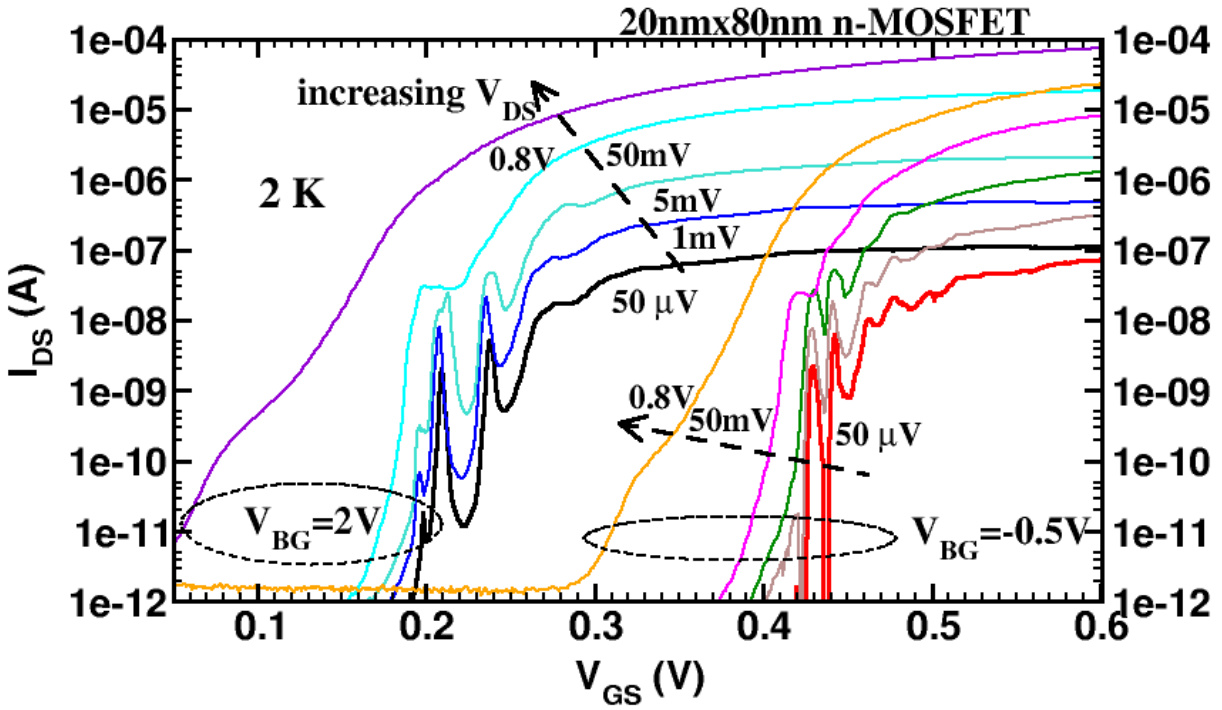

ΔV_{GS} increases (doubles) at +/-2V back gate voltage as C_{gs} decreases

Resonant tunnelling through 2-dot qubit (cascode)

[S.Bonen et al. EDL 2018]

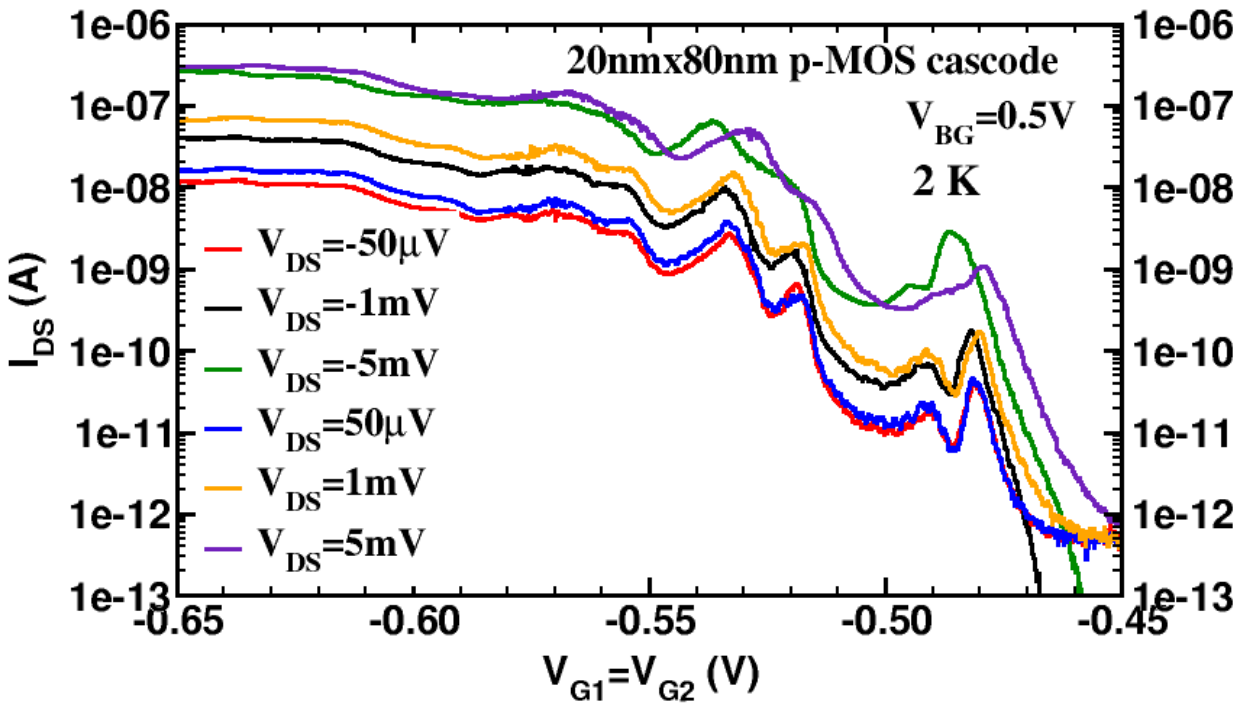

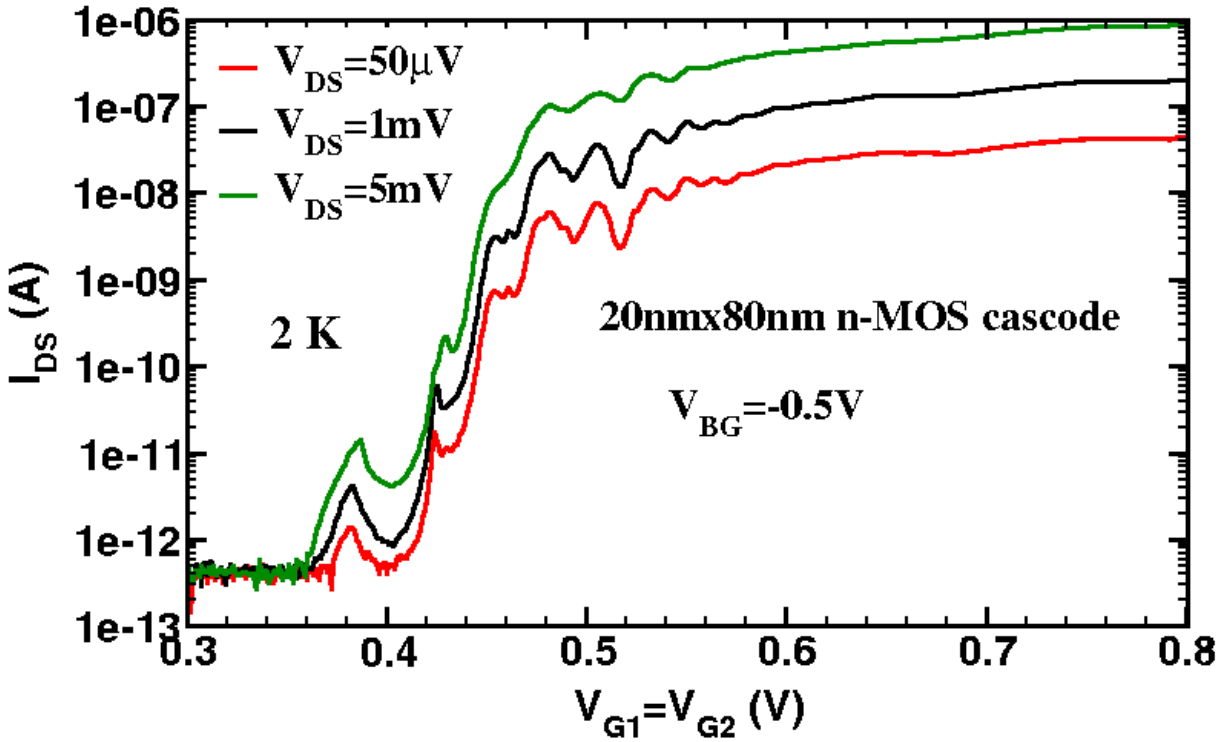

ΔV_{DS} =+/-5 mV , V_{G1}=V_{G2} swept in sync => proves matching between adjacent qubits

“Classical” MOSFET behaviour in saturation

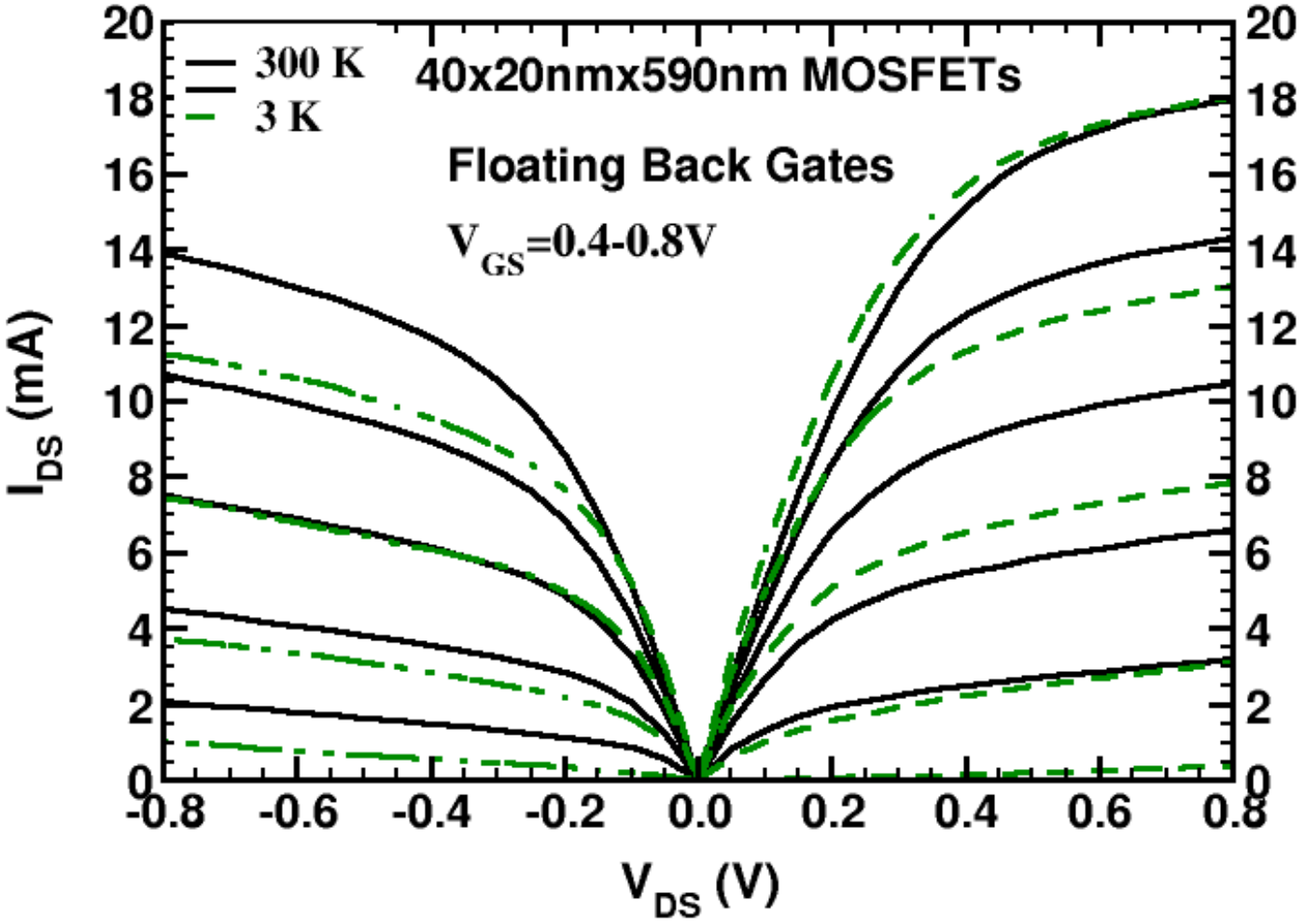

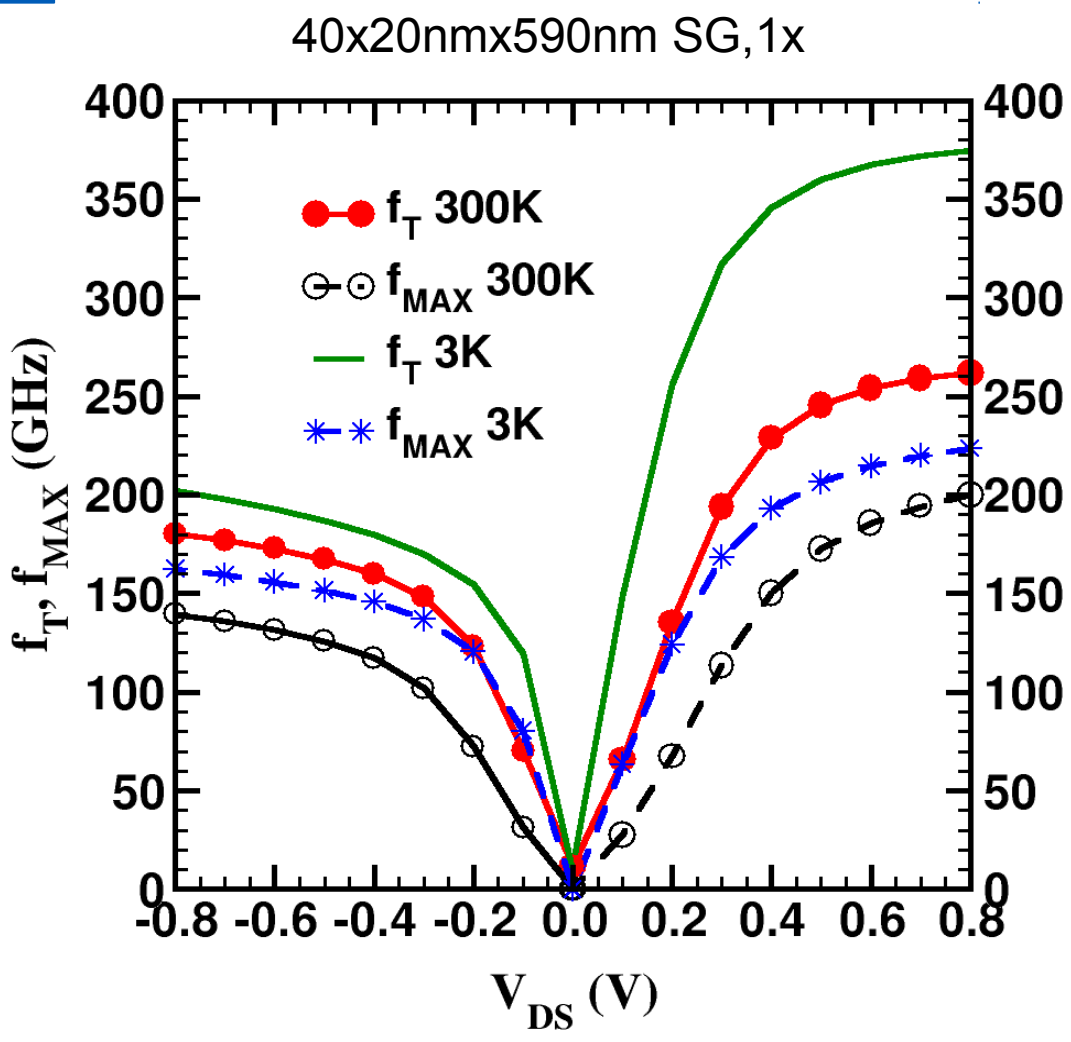

Peak f_T, f_{MAX} current densities invariant with temp.

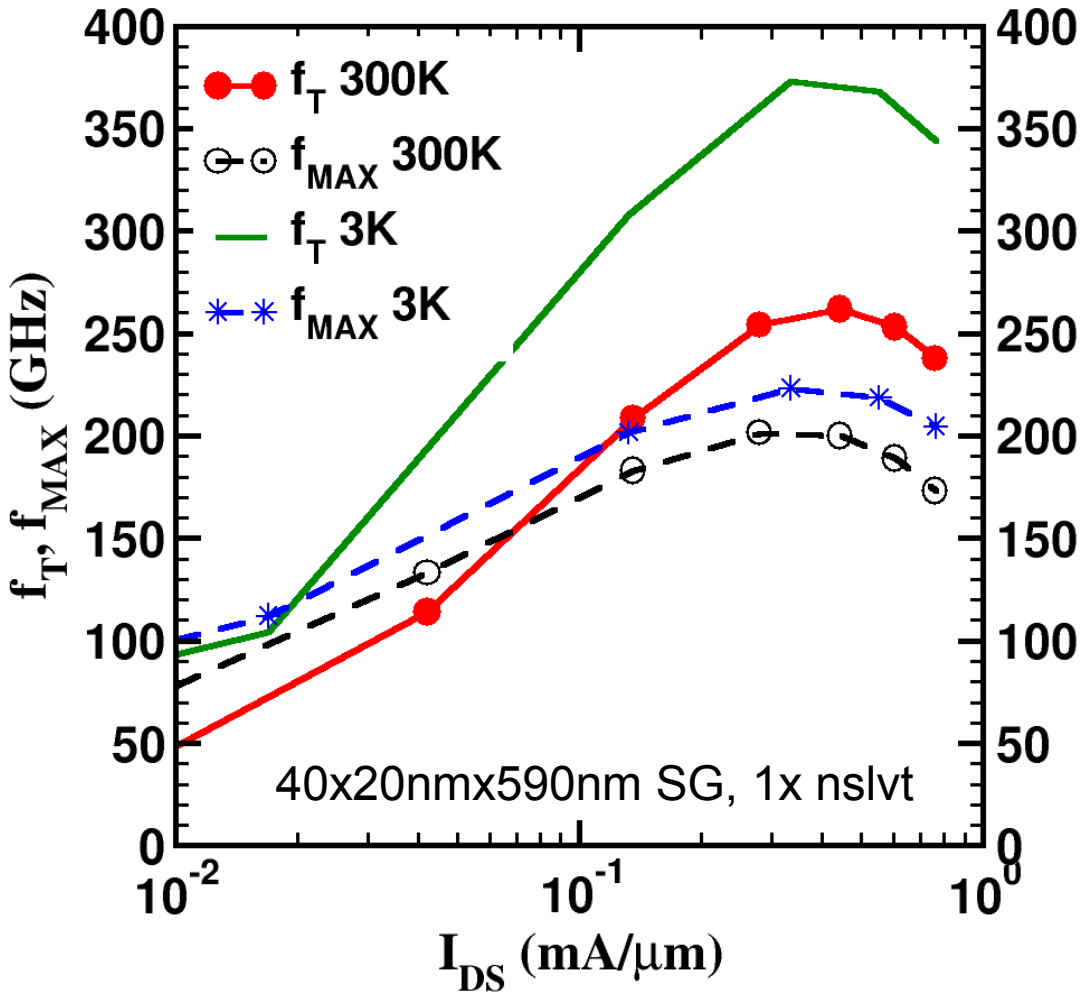

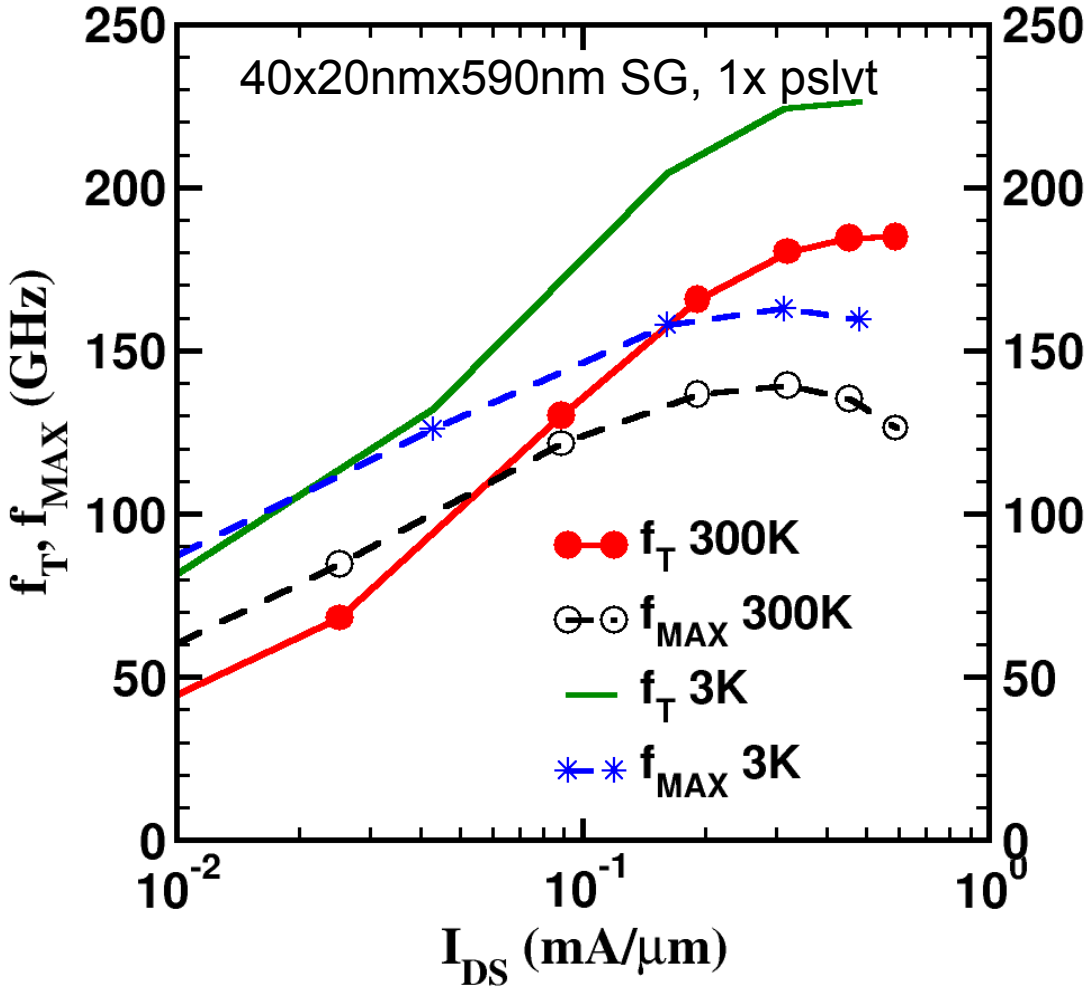

MOM capacitor and poly resistor vs. temperature

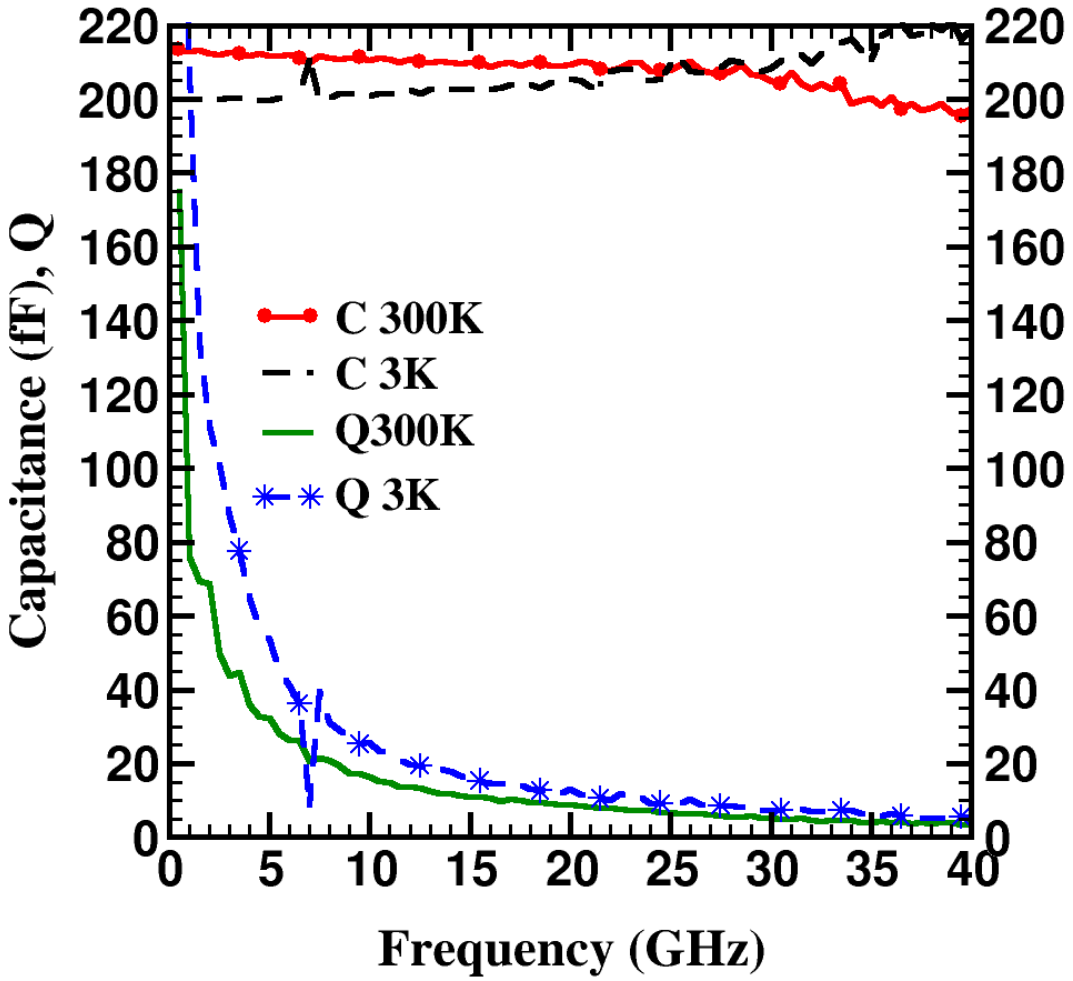

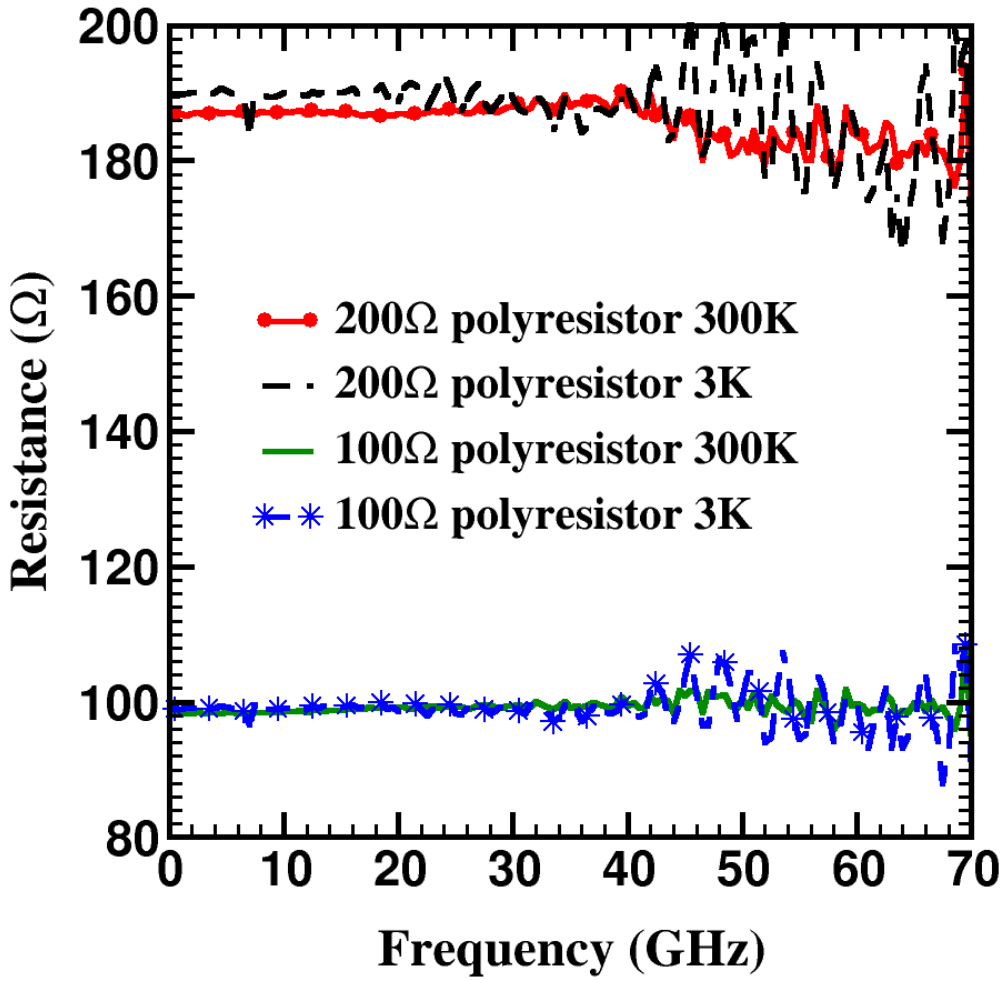

Monolithic integration of qubits and readout TIA

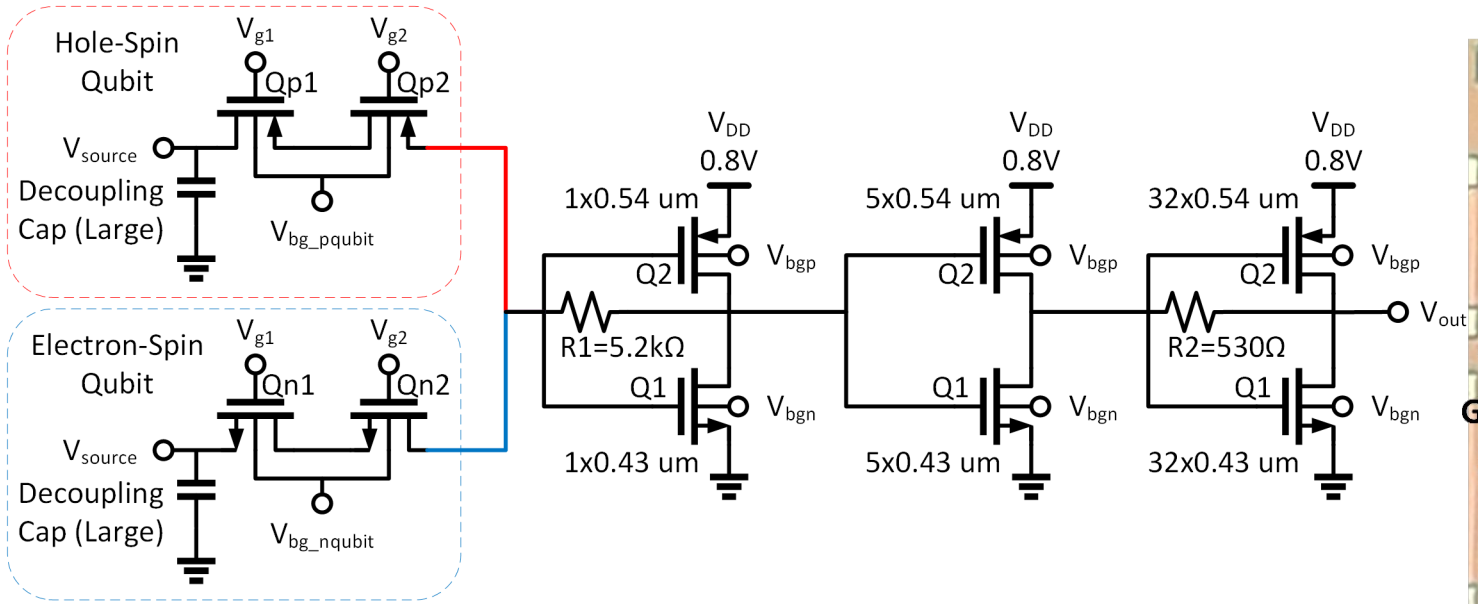

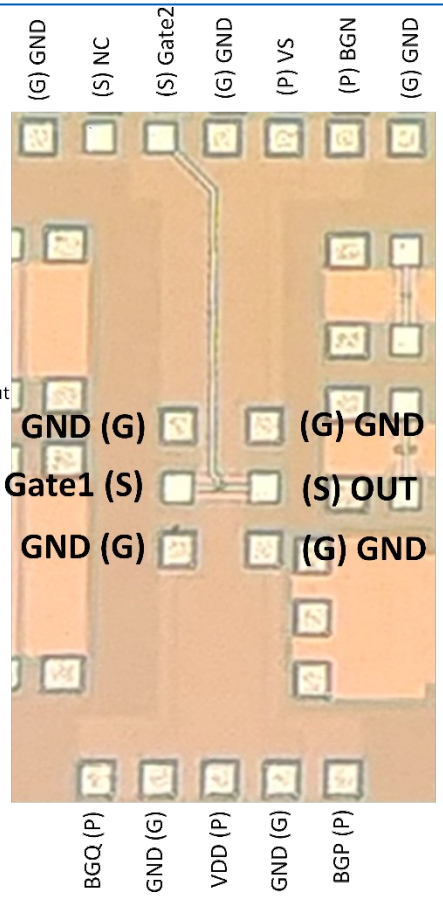

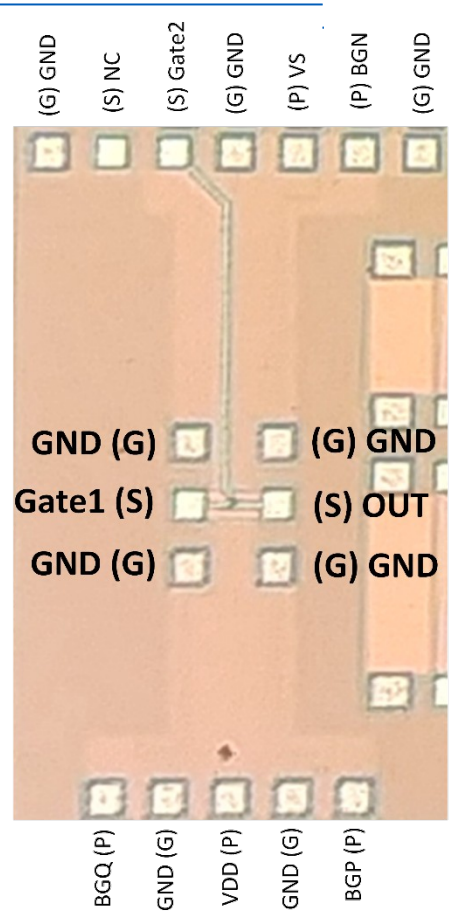

Challenges:

- Large gain > 140 dBΩ
- Bandwidth, noise
- Drive 50 Ohm off chip with minimum size 1x20nmx80nm MOSFET

TIA and n-qubit+readout circuit vs. temperature

[S.Bonen et al. EDL 2018]

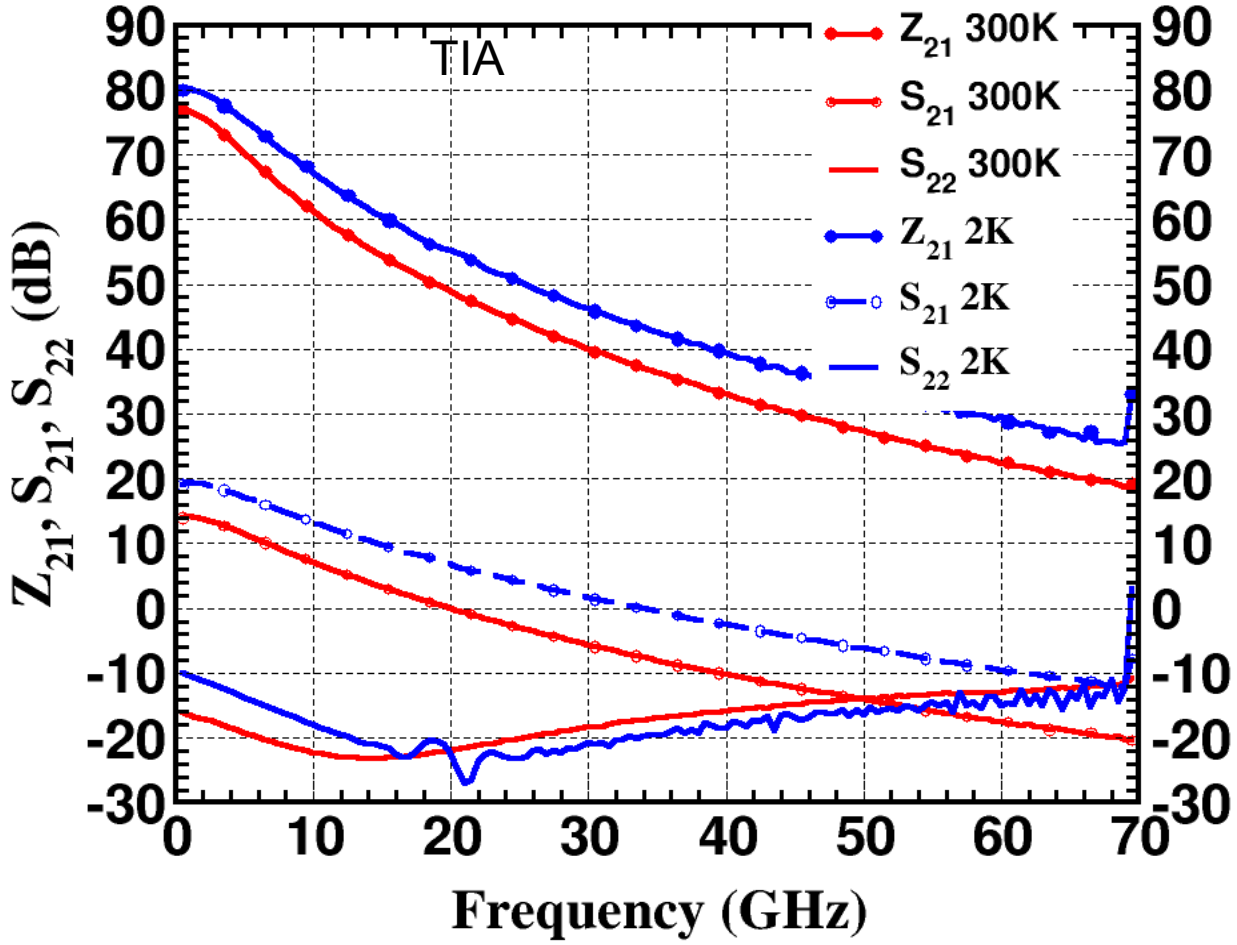

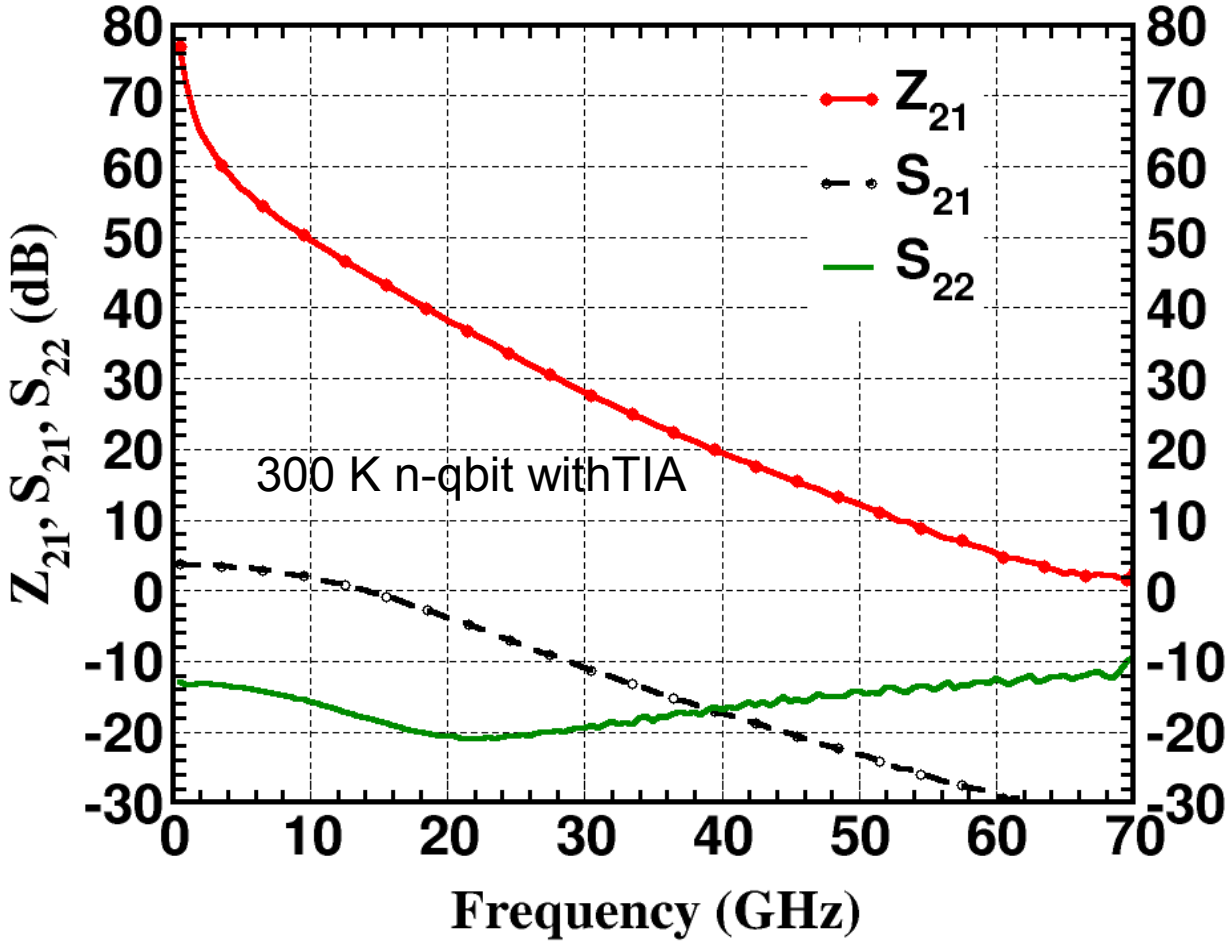

10 coupled double QD qubits in parallel

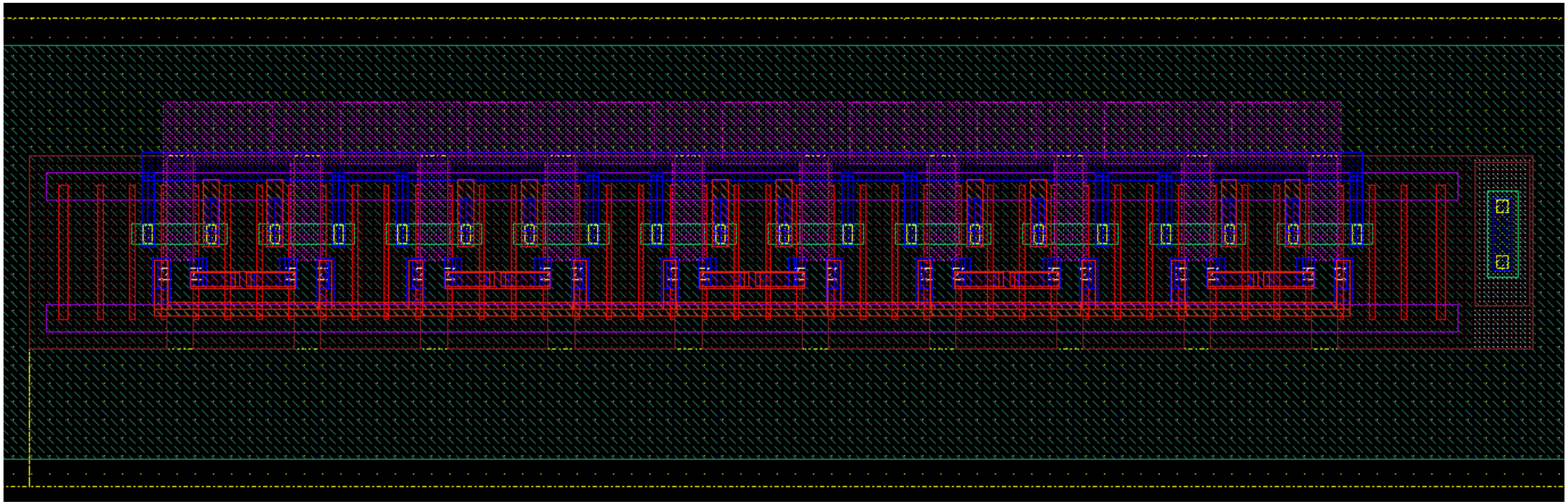

Improves matching

Qubits spins manipulated in parallel => 10 electron/hole spins majority gate

Equivalent to redundant qubits for error correction?

10xnqubit+5-stage TIA

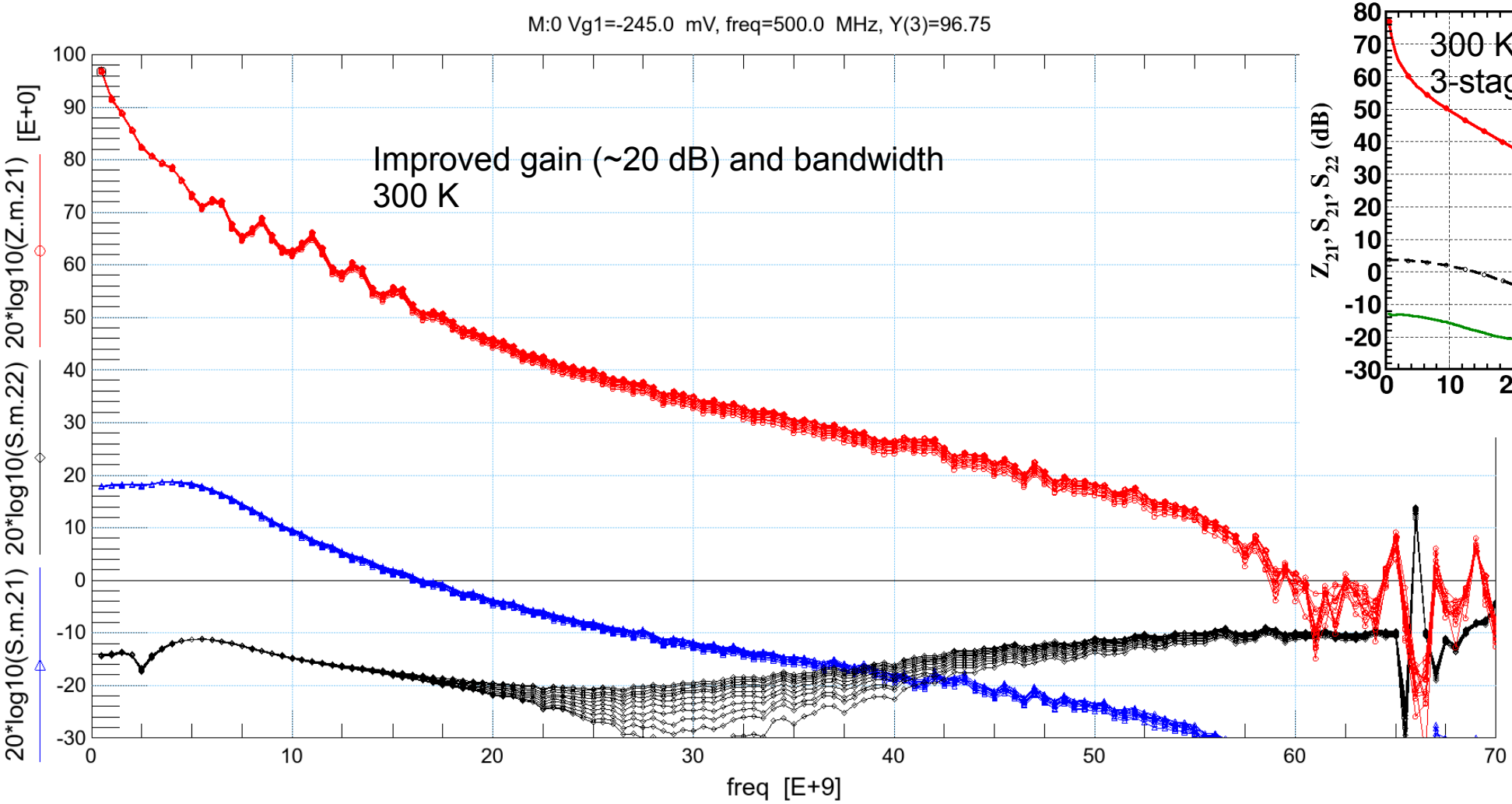

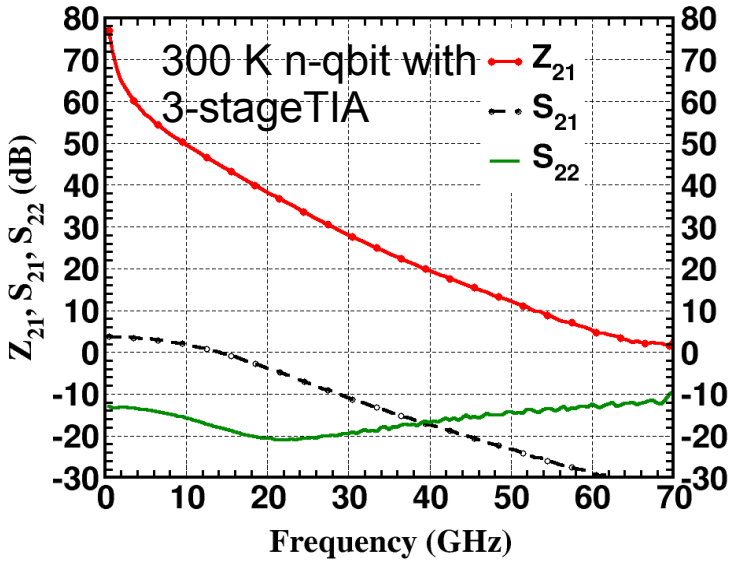

Broadband amplifiers/switches in 22nm FDSOI

[A. Zandieh et al. BCICTS 2018]

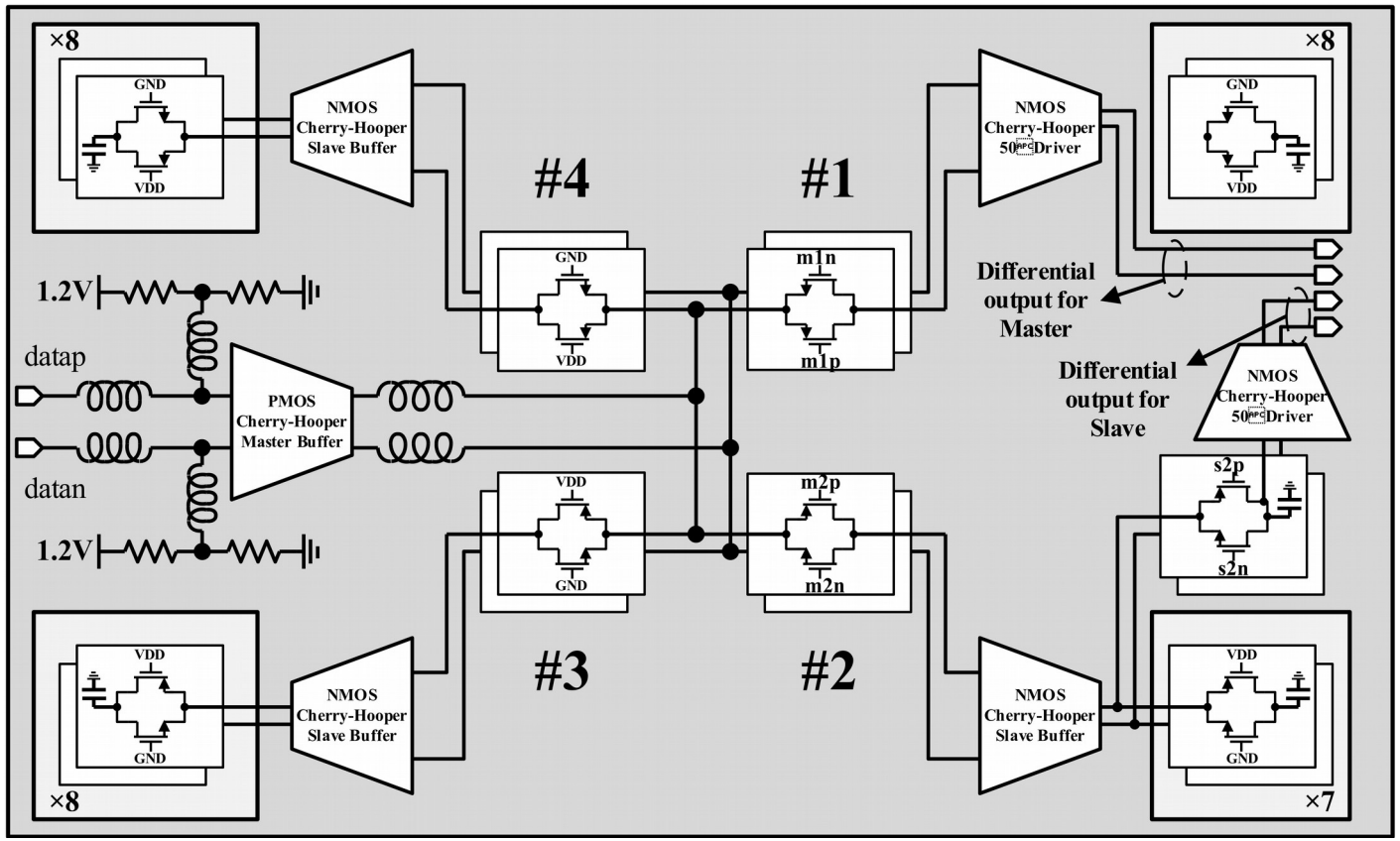

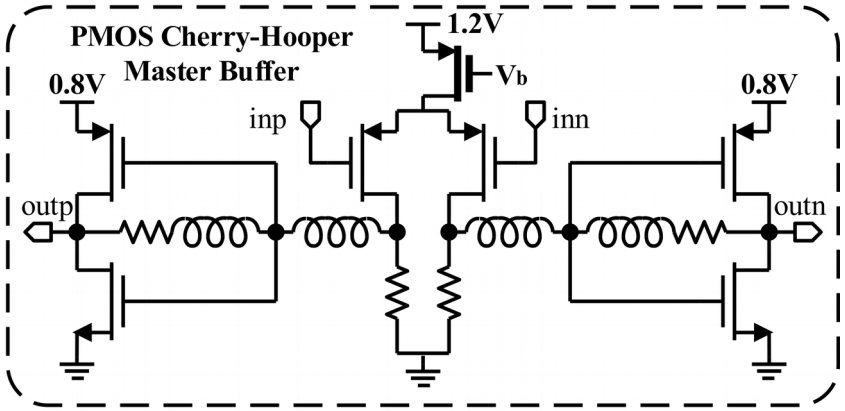

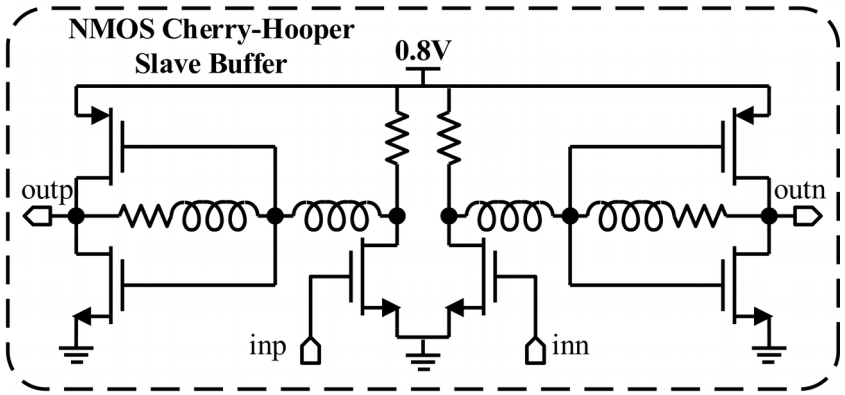

Sampling switch insertion loss & isolation

[A. Zandieh et al. BCICTS 2018]

- S_{21} input to master switch output
- ~30dB isolation at low frequency
- ~27dB isolation at 56 GHz
- 2x relaxed pitch CMOS switch

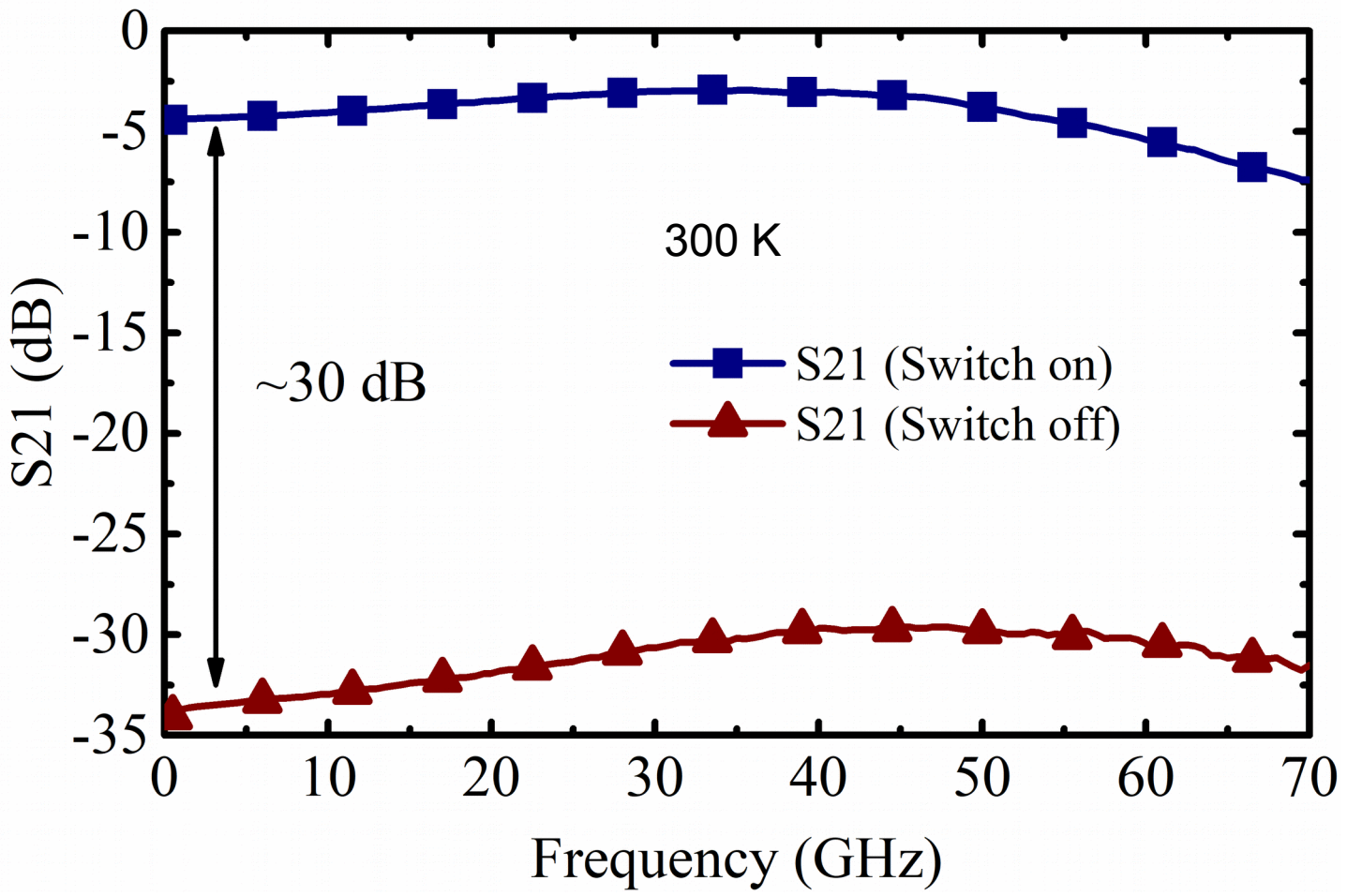

Single-ended-to-diff ESR signal amplifier

[A. Zandieh et al. BCICTS 2018]

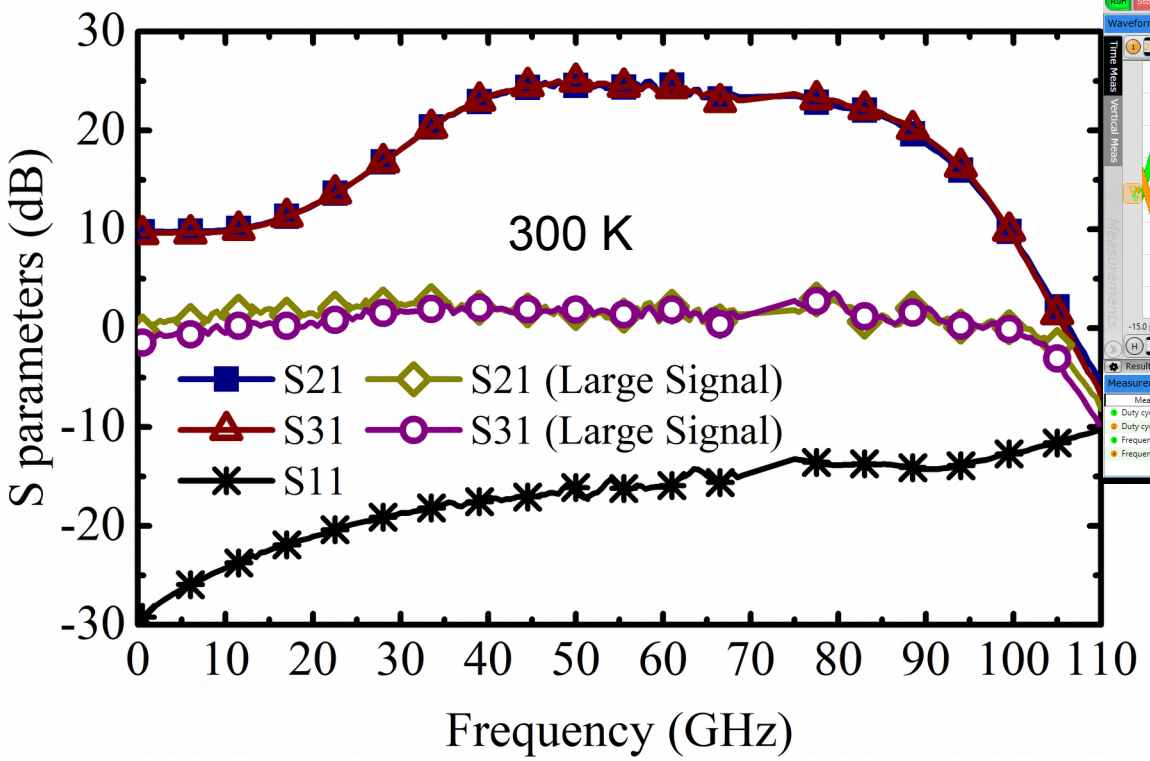

100 GHz

4 GHz

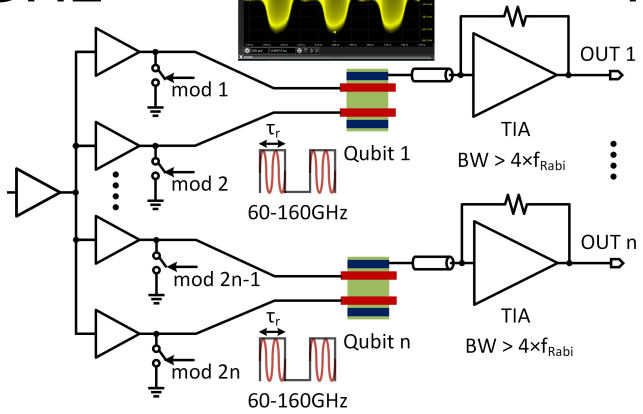

Common-Mode Rejection up to 100 GHz

Impact of process variation

- ΔW, ΔL, $\Delta t_{Si(Ge)}$=> E_1-E_0, f_R
- Gate oxide spacer and source/drain-to-channel potential barrier => E_1-E_0
- Surface roughness => E_1-E_0
- DC external magnetic field value (feedback loop) =>E_m, f_{Larmor}
- Δt_{OX}, ΔW, ΔL, $\Delta t_{Si(Ge)}$ => V_T, f_R variation
- g?, f_{Larmor}, f_R

Some of them may be adjustable/corrected from back gate

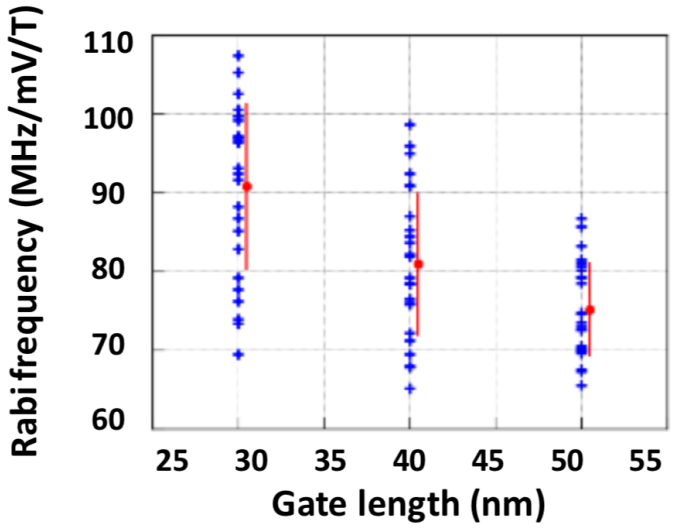

FDSOI hole-spin qubit]

Fig. 3: Rabi frequency in rough hole qubit as a function of gate length. Each cross is a different realization of a Gaussian surface roughness profile with rms = 0.4 nm. The red dot and bar are mean and standard deviation.

[M. Vinet et al., IEDM 2018]

Impact of process variation: 22nm FDSOI

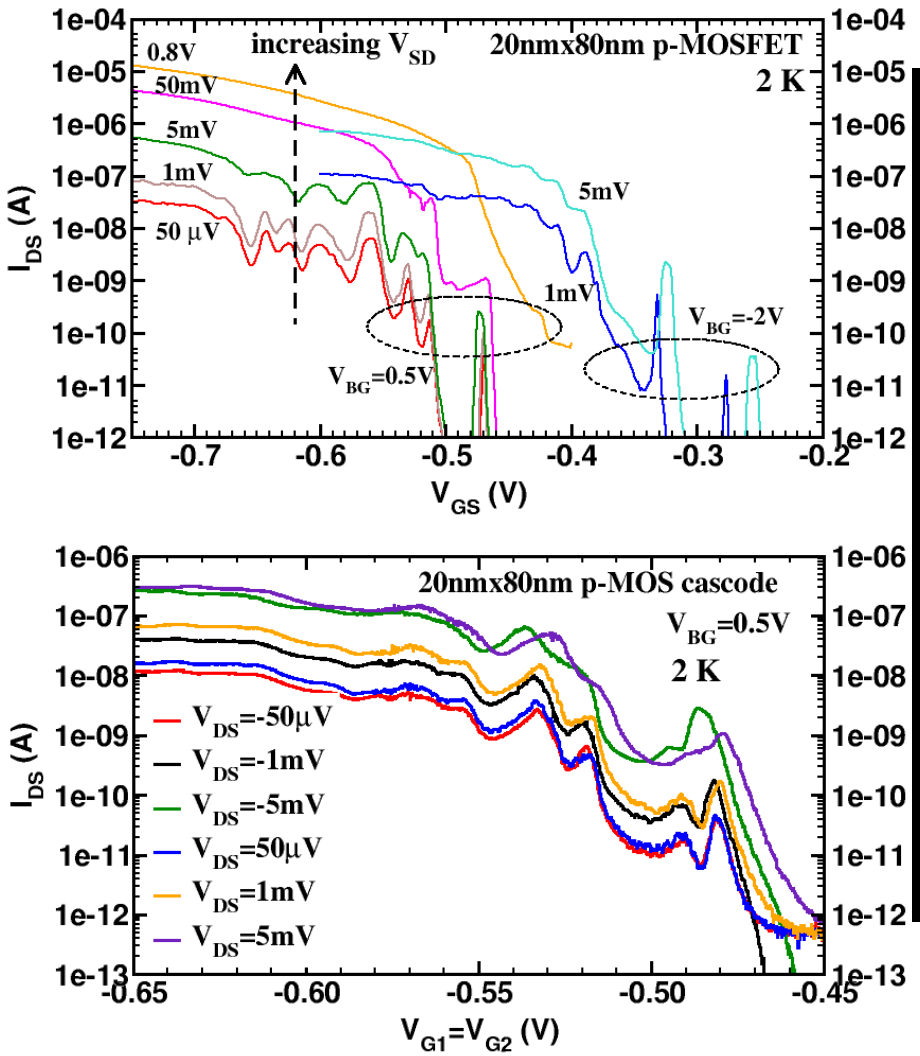

p-MOSFET V_{ds}= -1 mV zoom

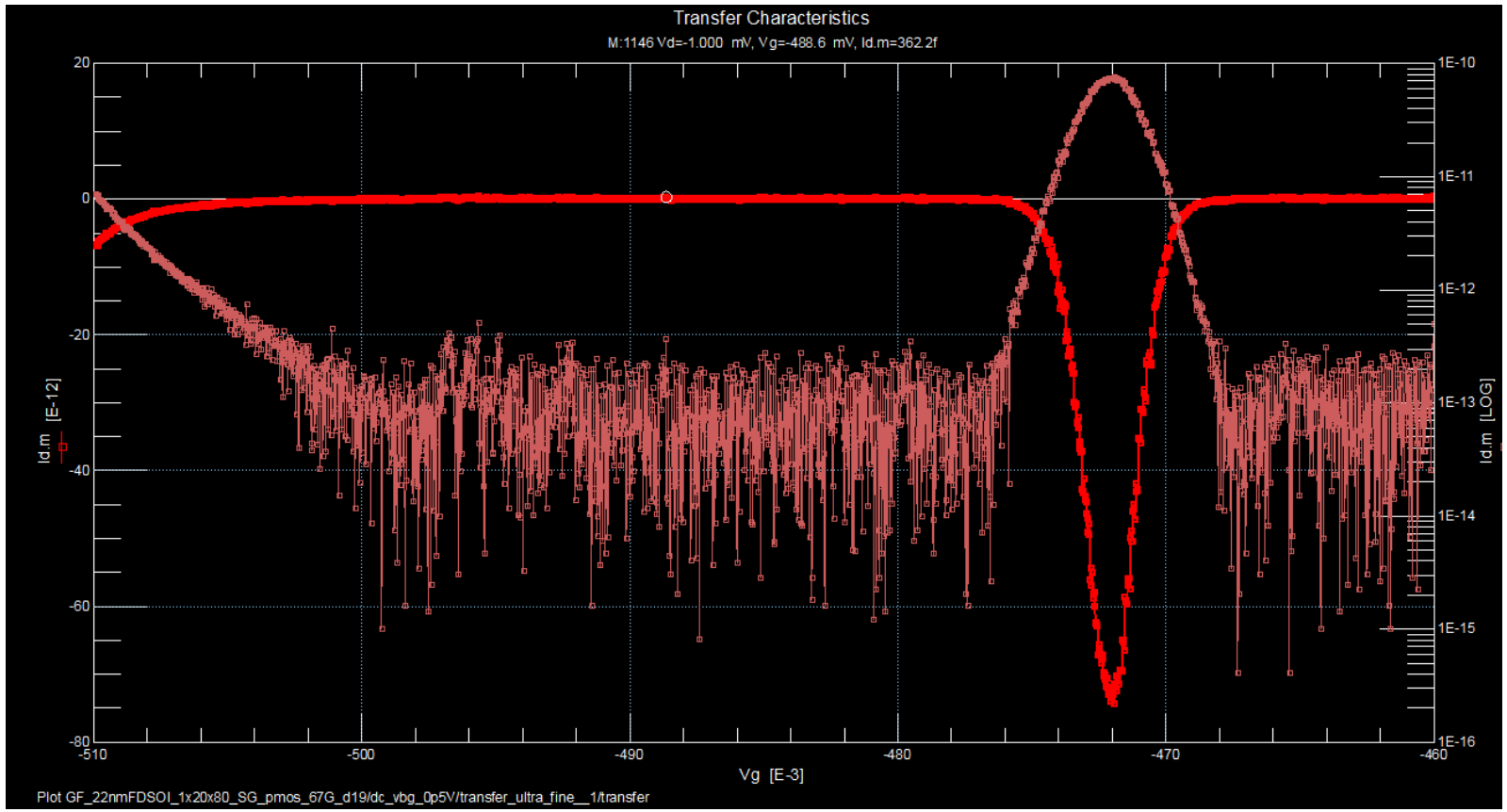

Impact of process variation: die to die

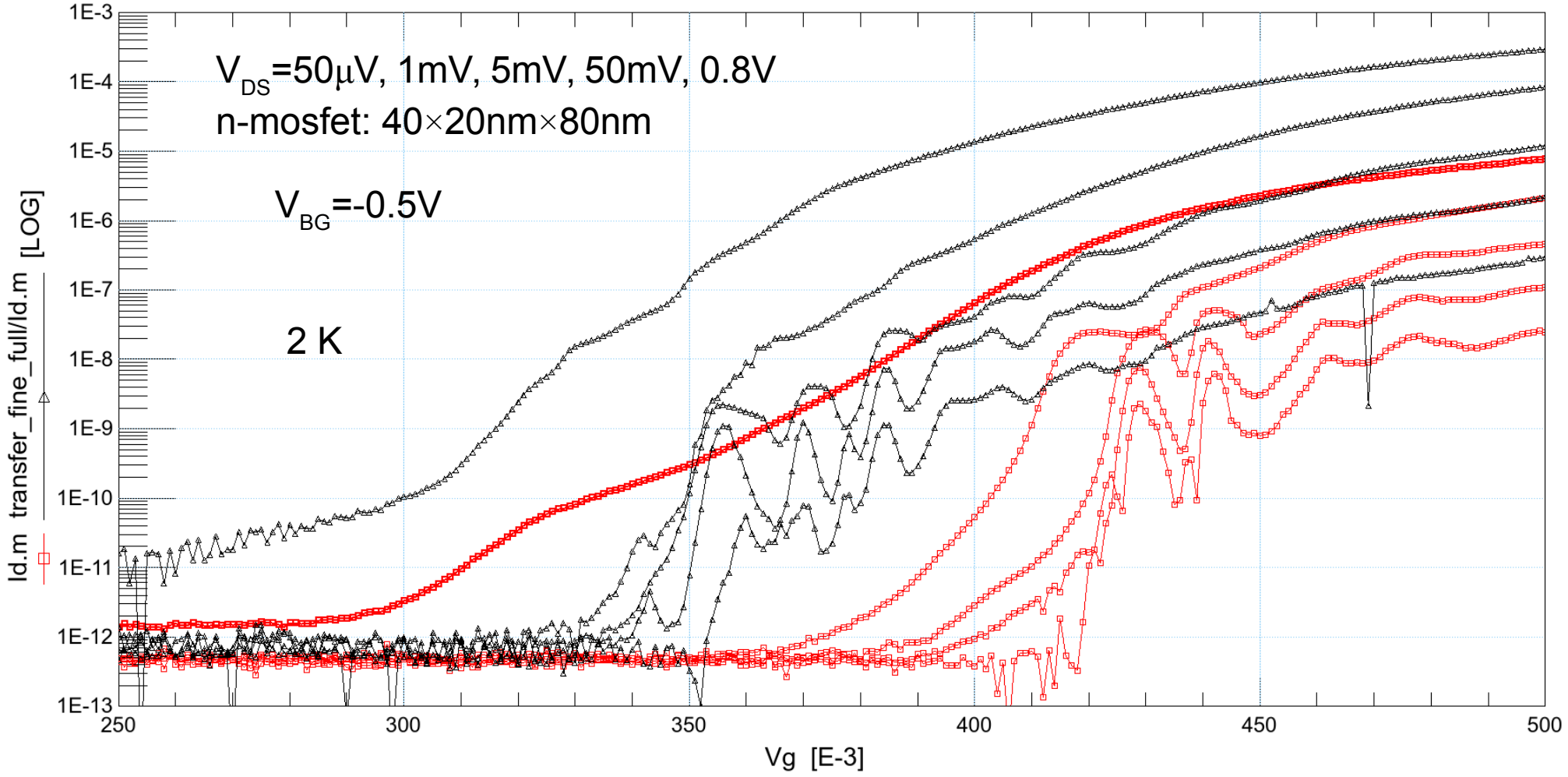

Plot GF_22nmFDSOI_40x20x80_SG_nmos_67G_TS_d19/dc_vbg_n0p5V/transfer_fine_full_die20/transfer

Impact of process variation: L_G=20nm vs. 28nm

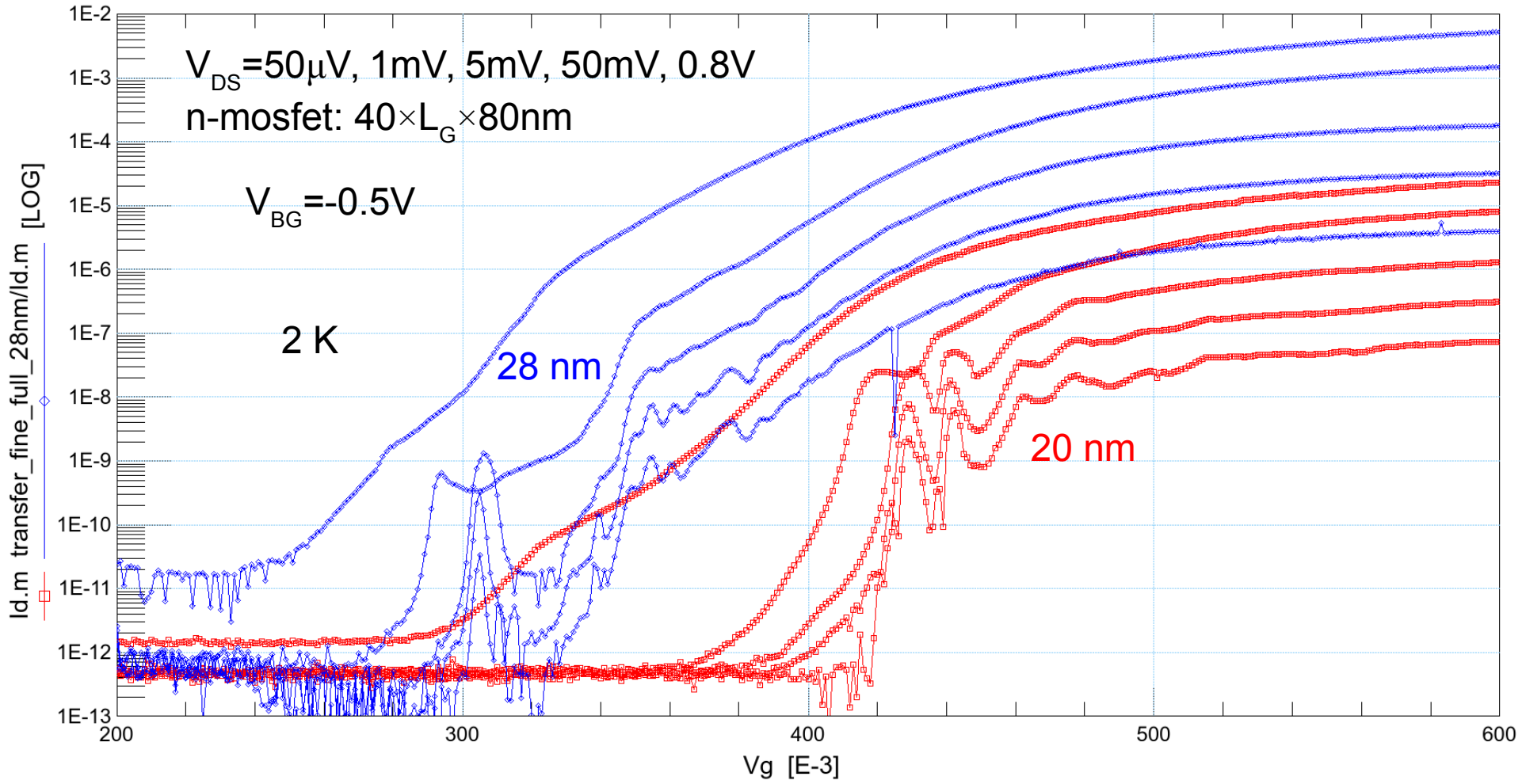

Plot GF_22nmFDSOI_40x20x80_SG_nmos_67G_TS_d19/dc_vbg_n0p5V/transfer_fine_full_die20/transfer

Mm-wave spin manipulation circuit specification

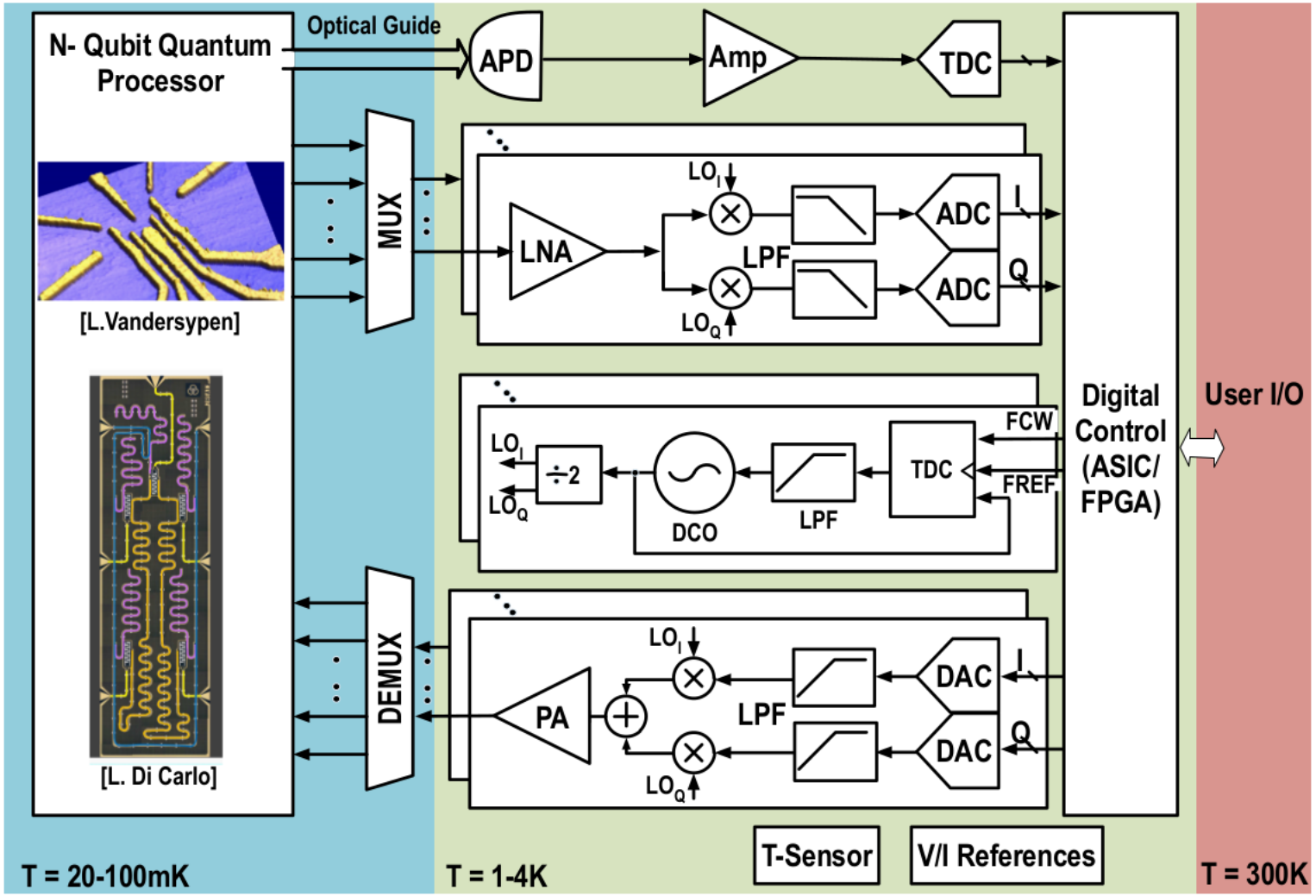

[M. Mabaie, EuMW-2018 Short Course]

[J.P.G van Dijk, NPJ 2018]

Carrier and circuit design specification

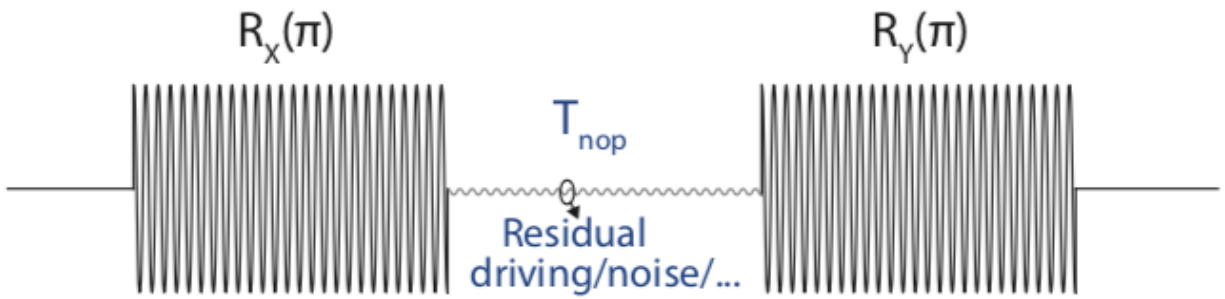

FIG. 11. The state of a qubit is affected during idle times between operations due to e.g. residual driving on the ESR-line.

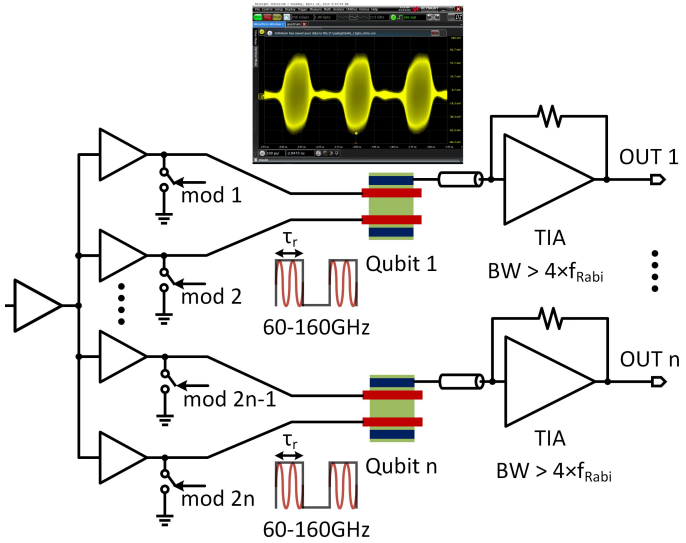

- Carrier frequency accuracy, phase noise, amplitude accuracy
- Switch isolation
- DAC precision
- Frequency spacing in case of FDM
- TIA gain, noise, bandwidth

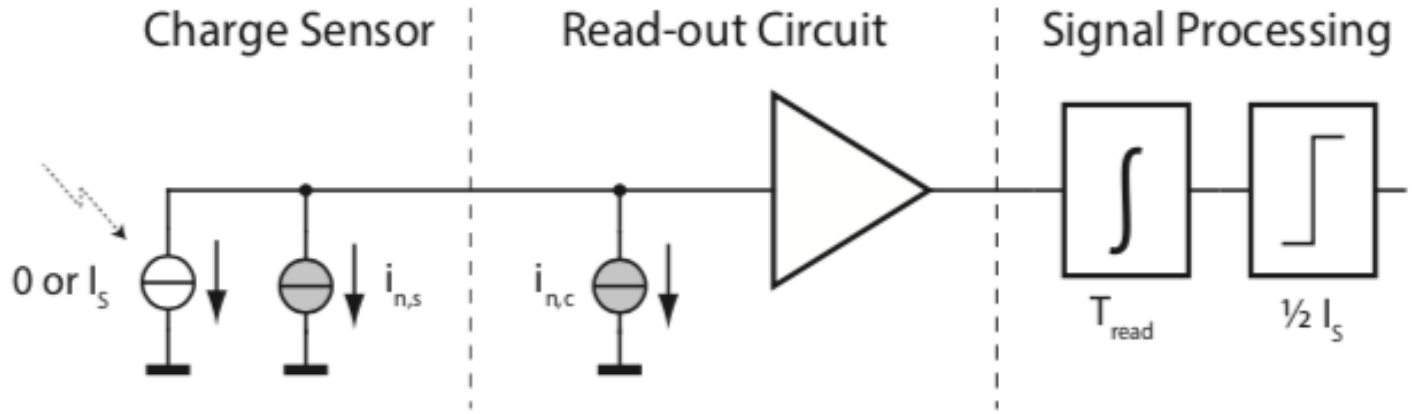

[J.P.G van Dijk, NPJ 2018]

Specification for qubit fidelity due to inaccuracy

➢ For 99.999% fidelity:

$$\frac{\Delta\omega_R}{\omega_R} \ll 0.002$$

$$\frac{\Delta t}{T_{pulse}} \ll 0.002$$

$$\frac{\Delta\omega_{mw}}{\omega_R} \ll 0.003$$

$$\Delta\varphi < 0.2 \text{ degree}$$

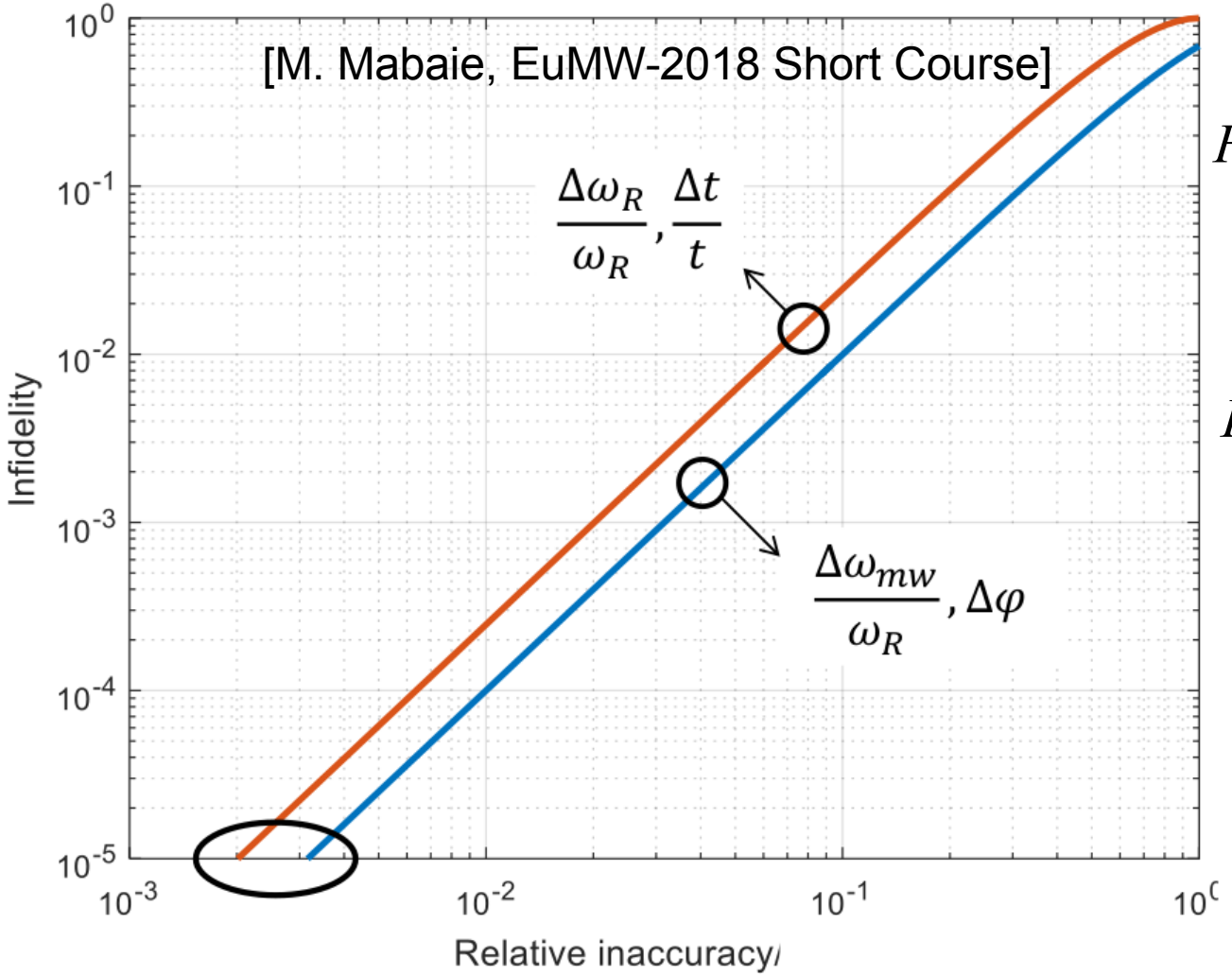

$$F_{X,Y} = 1 - \frac{1}{4}\left(\frac{\Delta f_R}{f_R}\right)^2 \theta^2$$

$$F_{X,Y} = 1 - \frac{1}{4}\left(\frac{\Delta \tau}{\tau}\right)^2 \theta^2$$

[J.P.G van Dijk, NPJ 2018]

Impact mm-wave signal inaccuracy on qubit fidelity

- For $\omega_1 = 2\pi \cdot 2$ MHz: f_R=400 MHz
  - Assuming equal contributions

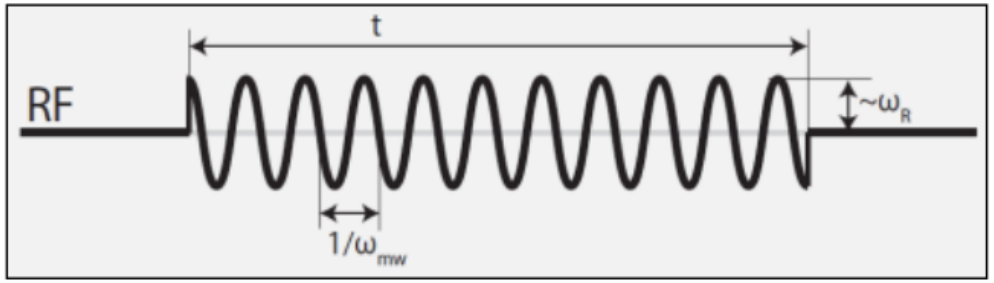

[M. Mabaie, EuMW-2018 Short Course]

Error Source	*Type*	*Value*	*Contribution*	
Nuclear spin 800 ppm ^{29}Si	noise	1.91 kHz_{rms}	1-F = 0.036 ppm	<< 10^{-8}
Microwave frequency	inaccuracy	2.6 kHz 0.52 MHz	1-F = 1.66 ppm	
(nominally 10 GHz) 100 GHz	noise	2.6 kHz_{rms} 0.52 MHz_{rms}	1-F = 1.66 ppm	
Microwave amplitude*	inaccuracy	2.89 µV 8.4 µV	1-F = 1.66 ppm	
(nominally 3.4 mV) 10 mV	noise	2.89 μV_{rms} 8.4 μV_{rms}	1-F = 1.66 ppm	
Microwave duration π	inaccuracy	41.0 ps 1.06 ps	1-F = 1.66 ppm	
(nominally 50 ns) 1.25 ns	noise	41.0 ps_{rms} 1.06 ps_{rms}	1-F = 1.66 ppm	+

[J.P.G van Dijk, NPJ 2018] *F = 99.999%*

Outline

- Quantum computing fundamentals
- Quantum computing ICs in 22-nm FDSOI at 2 K
- **Scaling for high temperature quantum computing**
- Conclusions

QD coupling energy splitting, *T* with scaling

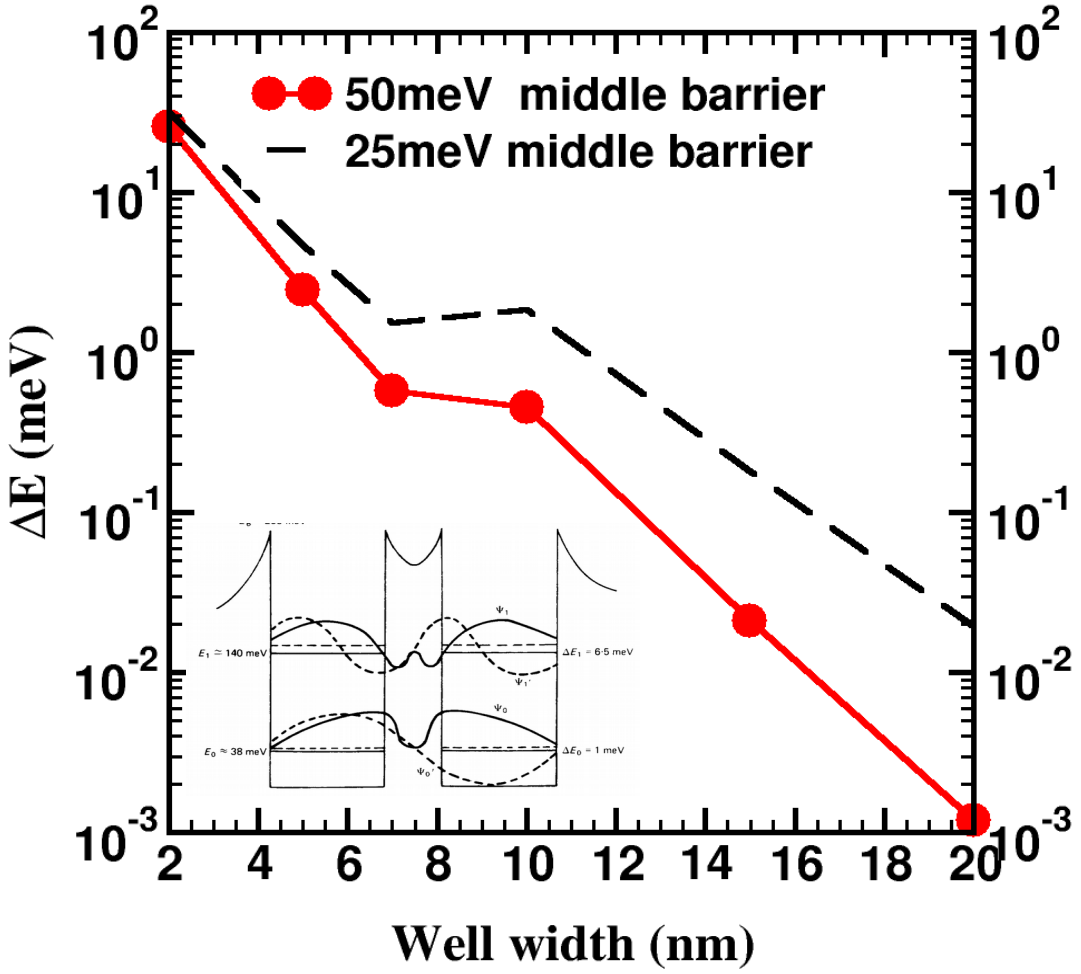

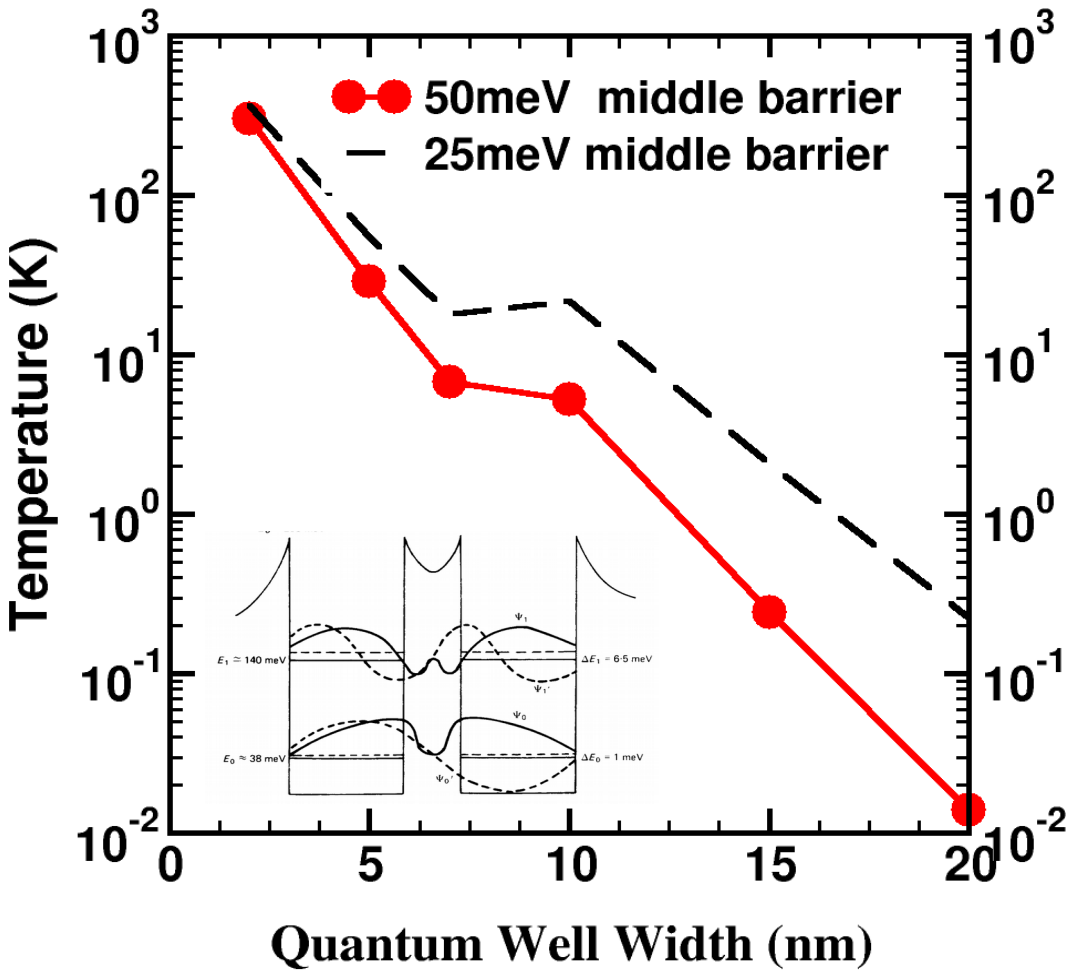

f_T, f_{MAX} smaller in 7nm FinFET node

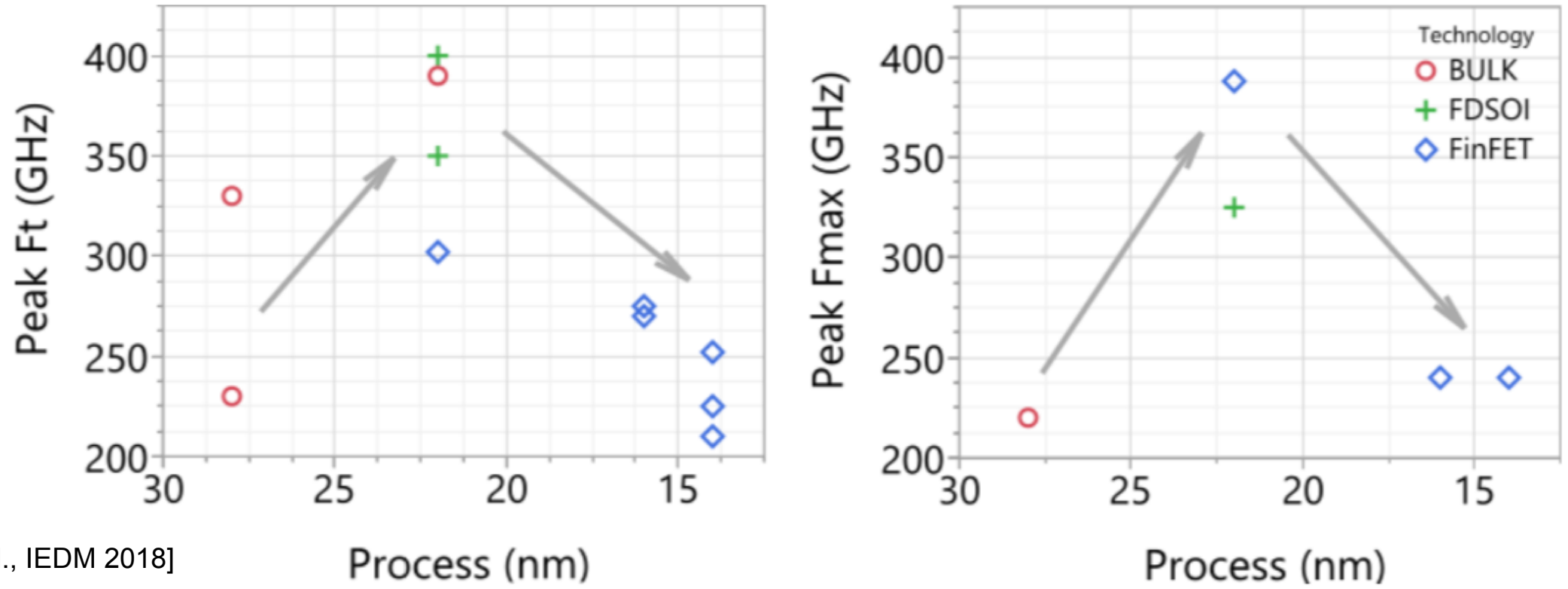

[H.-J. Lee et al., IEDM 2018]

Figure 5: f_t and f_{max} trends by process node: both ft and fmax reach the peak performance around 20 ~ 25nm due to the excessive parasitic capacitance by high density interconnect

Only SiGe cascodes have gain above 200 GHz

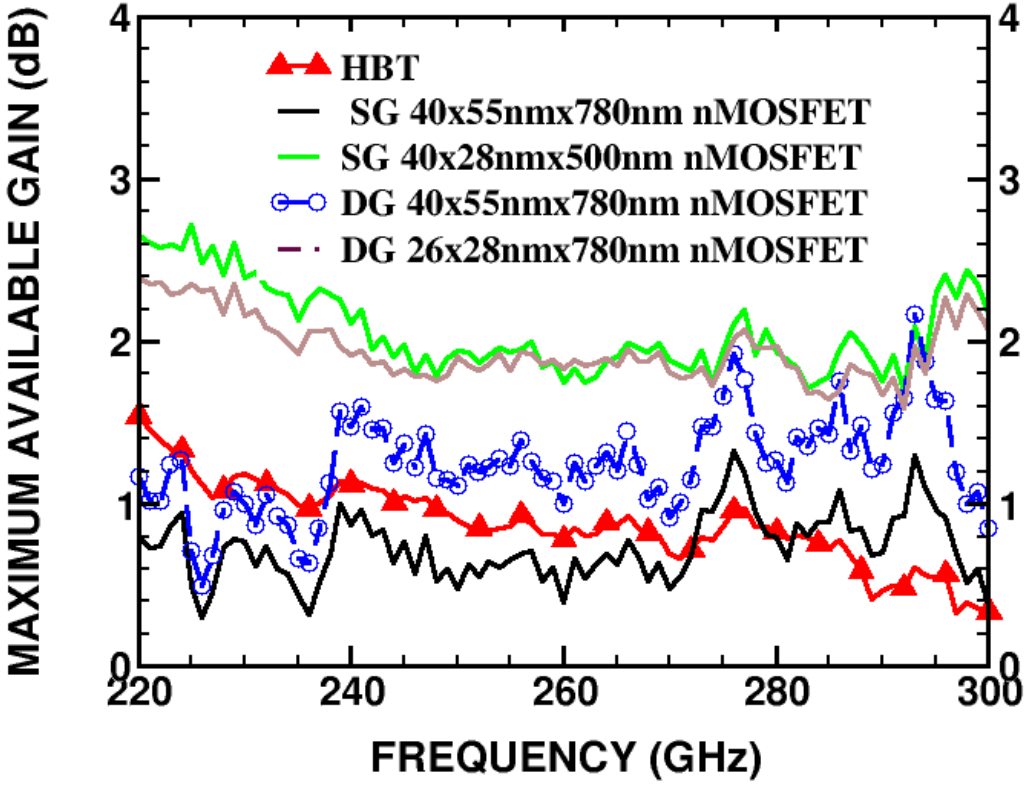

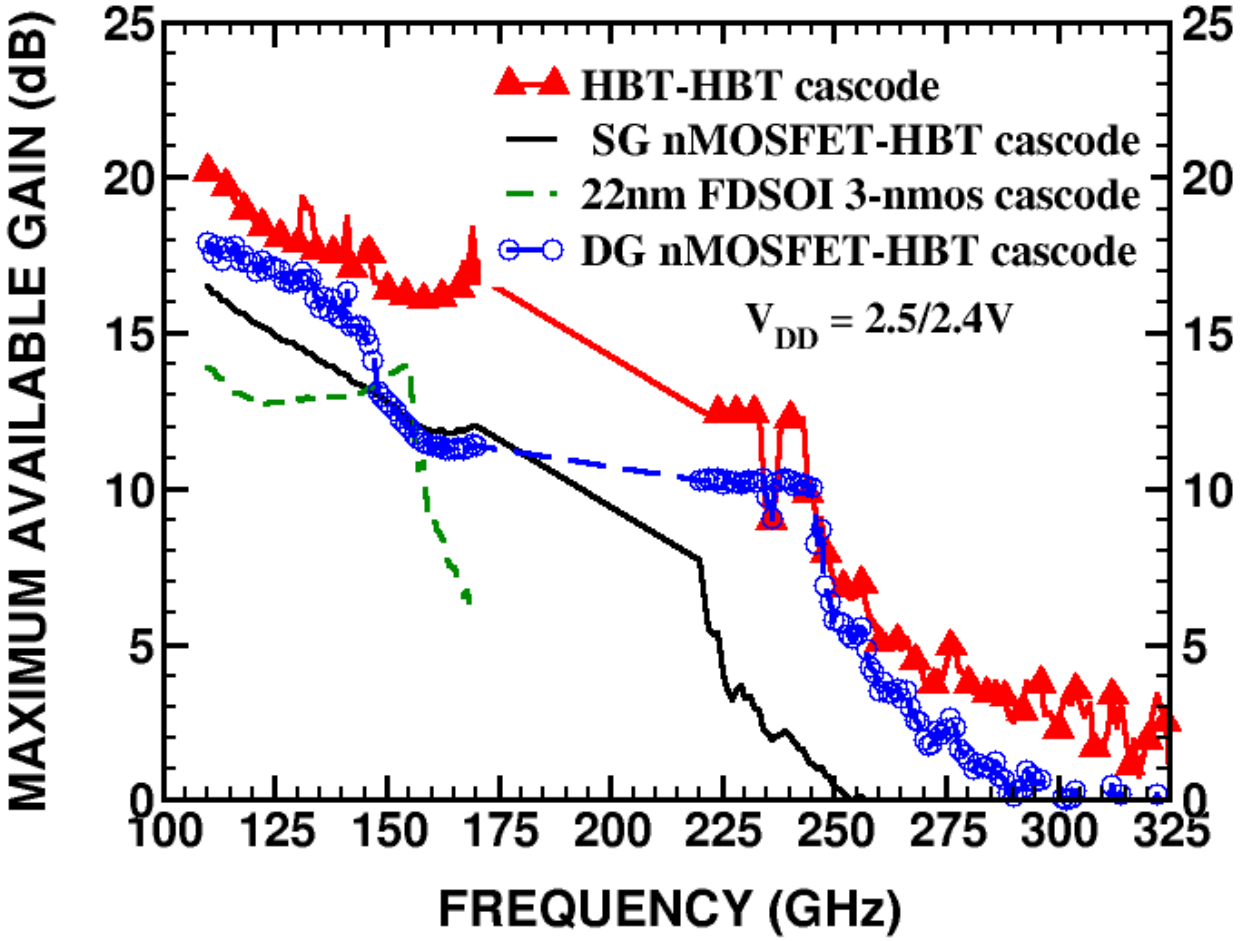

S.P. Voinigescu et al., IEEE Proc. June 2017

f_T scaling: SiGe HBT vs. FinFET

[S. Voinigescu et al, IEEE Proc. 2017]

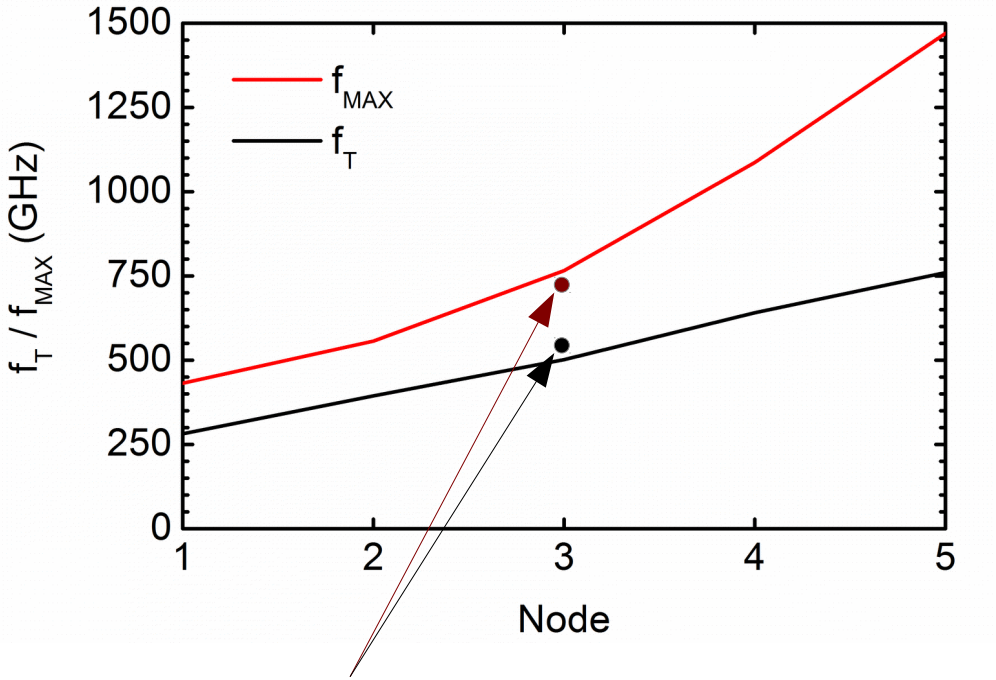

f_T/f_{MAX}= 500/700 GHz
[IHP IEDM 2016]

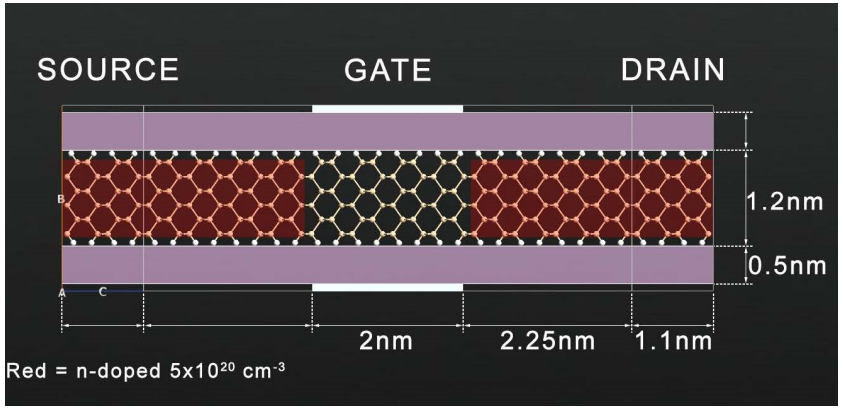

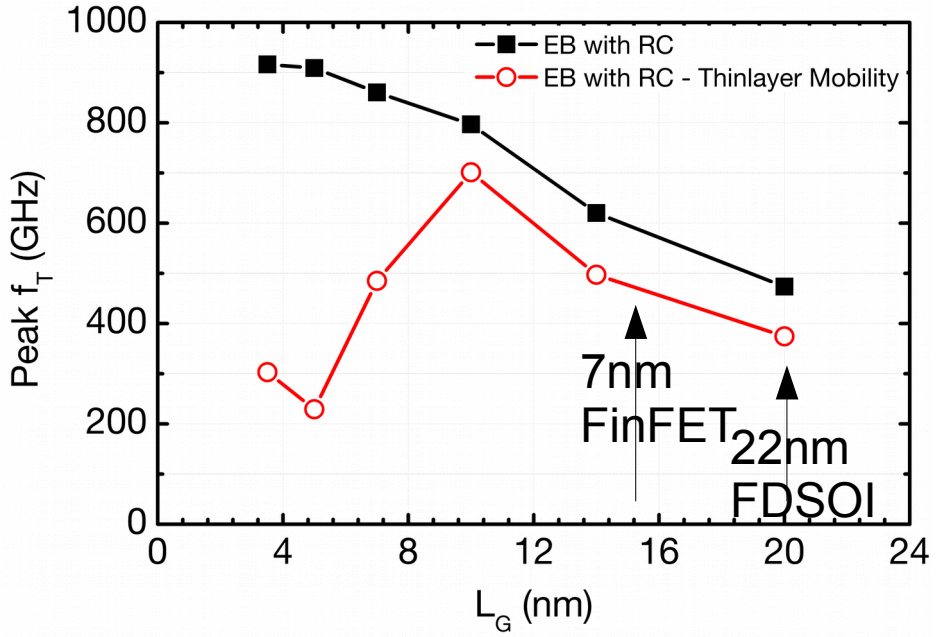

[M. Schroter et al, IEEE Proc. 2017]

Qubit operation temperature scaling

- f_L, T increase ~ L^{-2}, W^{-2} (very favourable scaling law!)
- f_L, T increase linearly with dc magnetic field B_{dc}
  - B_{dc}=2.9T => ΔE_m=0.33meV, f_L=80.4 GHz, T=4 K, 22-nm FDSOI
  - B_{dc}=8.6T => ΔE_m=1meV, f_L=241.2 GHz, T=12 K, 12-nm FDSOI
  - B_{dc}=17.3T => ΔE_m=2meV, f_L=582.4 GHz, T=24 K, 7-nm FDSOI SiGe BiCMOS?
- Magnetic field and double-dot coupling energy limit T, f_L

Challenges

- Qubit fidelity << transistor fidelity => error correction
  - We are currently in vacuum tube era (1905)
  - We are still waiting for the transistor to be discovered (1947)
- Spin readout
- Entanglement across multiple (all N) qubits
- (Minor) process/mask changes still needed
- Power removal level of integration: e.g. 1000-qubit processor at 4 K

Conclusions

- MOSFETs theoretically scalable to 2-3 nm gate length
- f_{MAX} saturated but g_m, f_T, *MAG* <170 GHz all improve
- **Monolithic integration** of CMOS spin control/readout circuits and qubits
- > 60GHz spin-manipulation/readout low-noise, AMS circuits needed
- At 2-4 K, minimum-size 22nm FDSOI MOSFET can be used as qubit in the subthreshold and as "classical" transistor in saturation
- 100-qubit processor < 2 W, probable now at 4 K in 22-nm FDSOI
- Future scaling to 5-nm source-drain spacing => >77 K operation

Acknowledgments

- Students: S. Bonen, U. Alakusu, S.M. Dadash, M. Gong, Y. Duan, A. Zandieh
- Prof. P. Asbeck, Dr. Daughton, Prof. G. Adam, Dr. M. Iordanescu, N. Messaoudi Prof. R. Mansour, Dr. D. Harame, Dr. A. Muller,
- NSERC for funding
- GlobalFoundries and STMicroelectronics for technology access and chip donations
- Lakeshore, Keysight, U Waterloo, IMT Bucharest for cryo measurements
- Dr. P. Chevalier, Dr. A. Cathelin for SiGe BiCMOS technology access
- Integrand for EMX software
- CMC and Jaro Pristupa for CAD tools and support

Superconducting qubits: most common today

- **Linear resonant circuit**
  - Low loss: Q >> 1
  - Low temperature: $kT << hn_0$
  - Linear elements: harmonic

Linear Resonant Circuit

$$\nu_0 = \frac{1}{2\pi\sqrt{LC}}$$

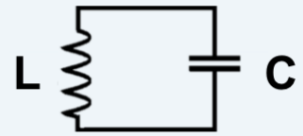

Energy Spectra of Quantum LC Circuit

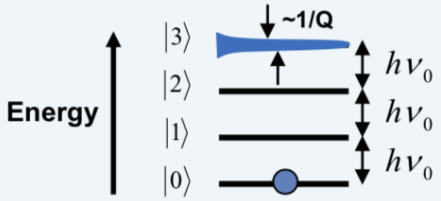

- **Nonlinear resonant circuit**
  - Josephson tunnel junction
  - Anharmonic
  - Solid-state artificial atom

Josephson Junction: Nonlinear Inductor

$$I = I_C \sin\varphi \qquad V = \frac{\Phi_0}{2\pi}\frac{d\varphi}{dt}$$

$$L_J = \frac{\Phi_0}{2\pi I_C \cos\varphi}$$

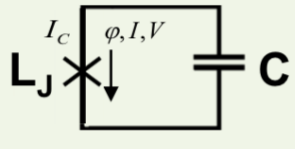

Energy Spectra of Quantum LC Circuit

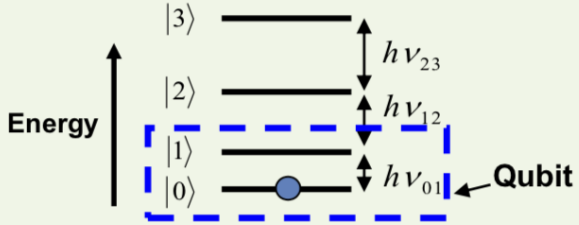

Leo Esaki | Ivar Giaever | Brian David Josephson

The Nobel Prize in Physics 1973 was divided, one half jointly to Leo Esaki and Ivar Giaever *"for their experimental discoveries regarding tunneling phenomena in semiconductors and superconductors, respectively"* and the other half to Brian David Josephson *"for his theoretical predictions of the properties of a supercurrent through a tunnel barrier, in particular those phenomena which are generally known as the Josephson effects"*.

SEM of Al shadow-evaporated Josephson junction

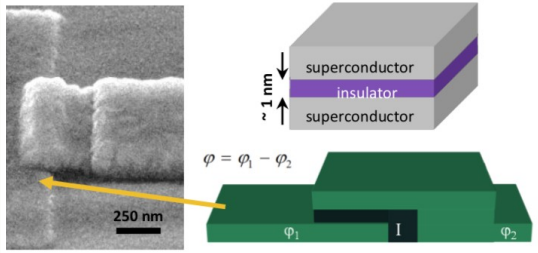

SIS (Josephson) Junction

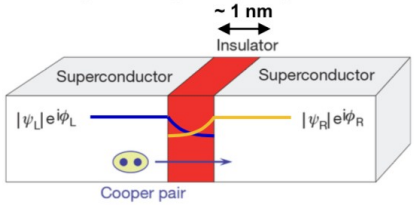

$$\varphi = \varphi_L - \varphi_R$$

Current:	$I = I_c \sin\varphi$
Voltage:	$V = \frac{\Phi_0}{2\pi}\frac{d\varphi}{dt}$
Inductance:	$V = L_J \frac{dI}{dt}$

I_c is the critical current, which depends on superconductor material and insulator thickness

$\Phi_0 = h/2e$ is the superconducting flux quantum and has value 2.07×10^{-15} Wb = 2.07 mA · pH = 2.07 mV · ps

[W. Oliver, EuMW 2018 short course]

Coupled QD spin manipulation and readout

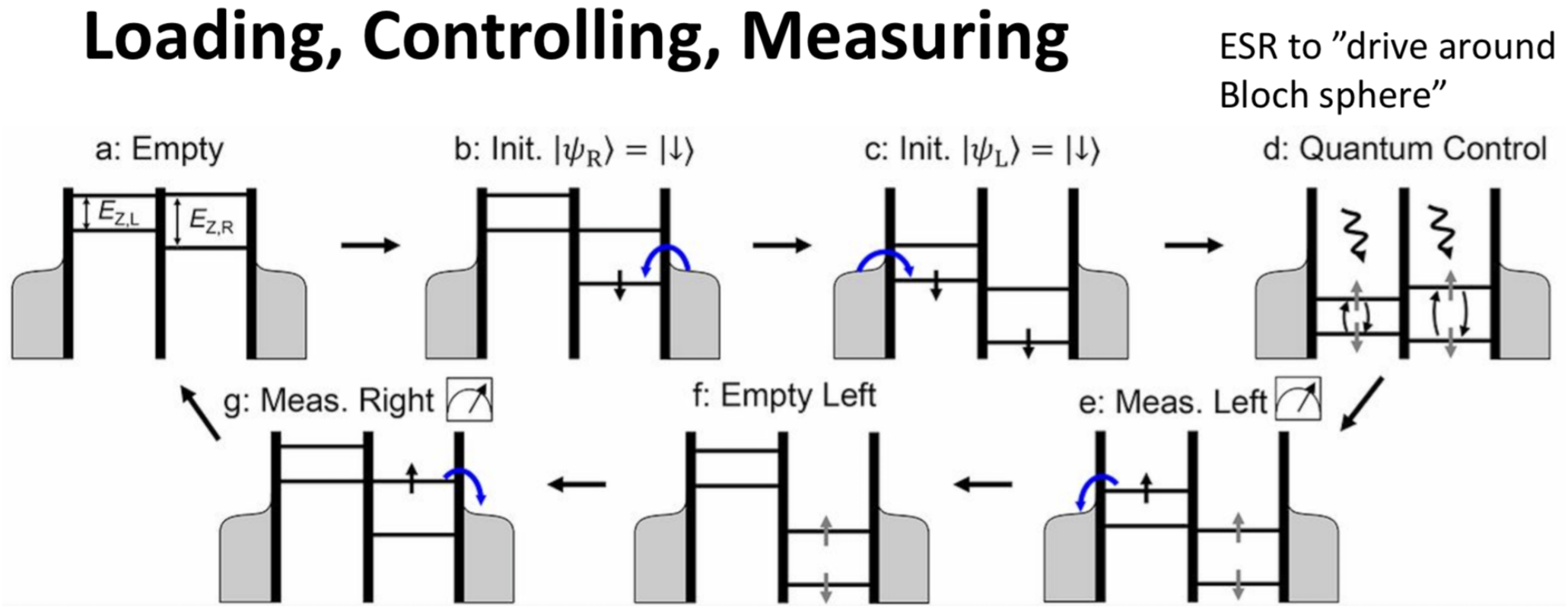

Resonantly driven CNOT gate for electron spins
By D. M. Zajac, A. J. Sigillito, M. Russ, F. Borjans, J. M. Taylor, G. Burkard, J. R. Petta
Published Online07 Dec 2017
DOI: 10.1126/science.aao5965

[M.B. Ritter, IEDM 2018 short course]

Entanglement in coupled QD CNOT gate

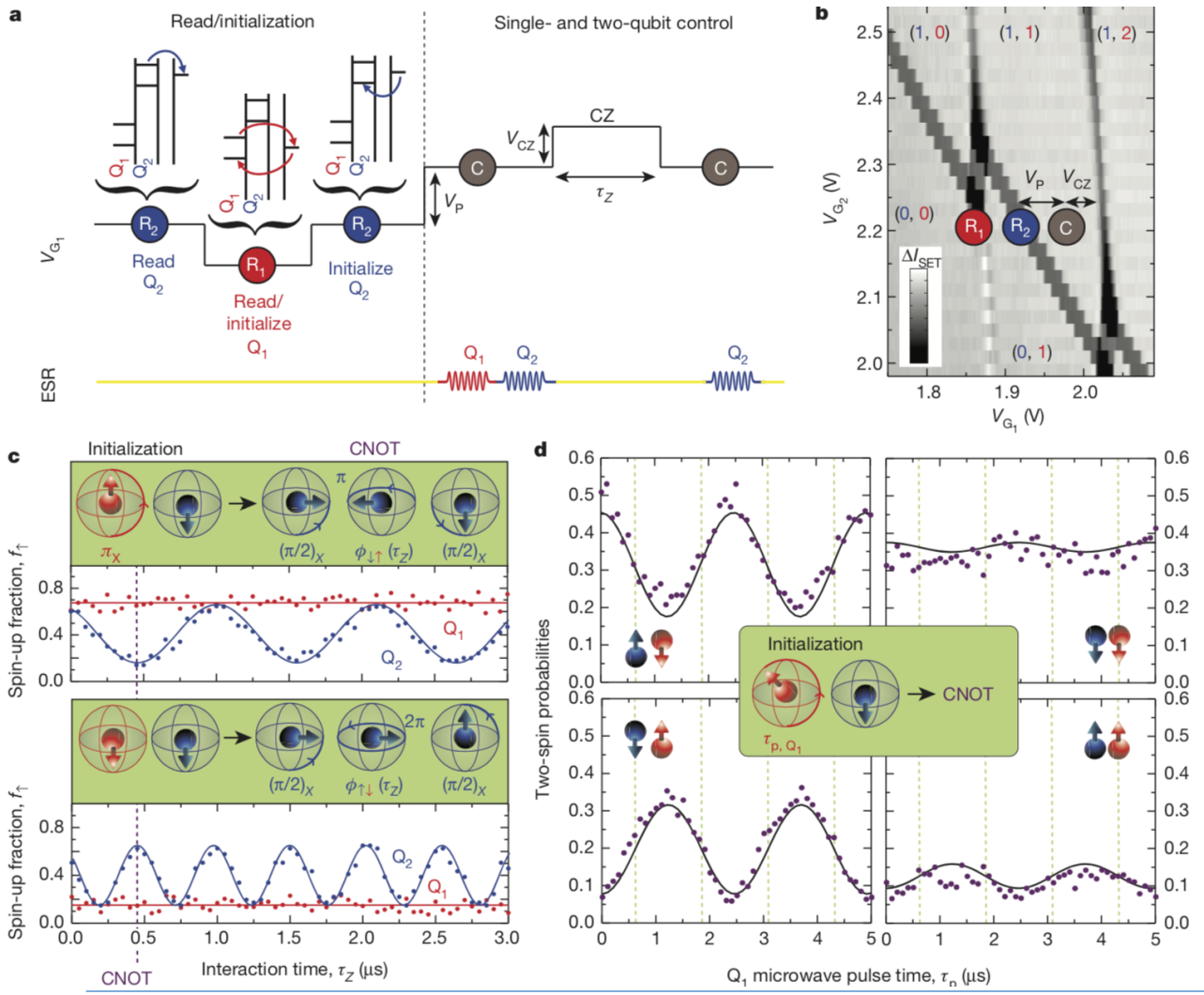

Figure 4 | Two-spin correlations for a two-qubit logic gate. **a**, Pulsing protocol for two-qubit read-out and single- and two-qubit operations. After read-out of Q_2 (R_2) and Q_1 (R_1), we pulse back to (R_2) to ensure proper initialization. Individual qubit operations are performed with high ϵ, whereas the CZ operation occurs in the presence of interaction. **b**, Stability diagram showing the operation regime. **c**, Spin-up fraction of both qubits after initializing Q_1 spin up (top) and spin down (bottom) using a microwave pulse and applying a controlled rotation using Q_2 as the target qubit. A CNOT gate is achieved in 480 ns, as indicated by the dotted purple line (see inset for the corresponding Bloch sphere animation). **d**, Two-spin probabilities as functions of the microwave pulse length on Q_1 after applying a CNOT gate (see inset for the corresponding Bloch sphere animation), showing clear anticorrelations between the two qubit spin states. The different plots correspond to different spin states of $Q_{1,2}$, as indicated. The black lines correspond to fits based on a CNOT gate, and include the experimental read-out errors (see Supplementary Information section 9). The green dotted lines correspond to the intended maximally entangled states.

[Velshorst, et al. Nature 2015]

SC qubits: FDM spin manipulation

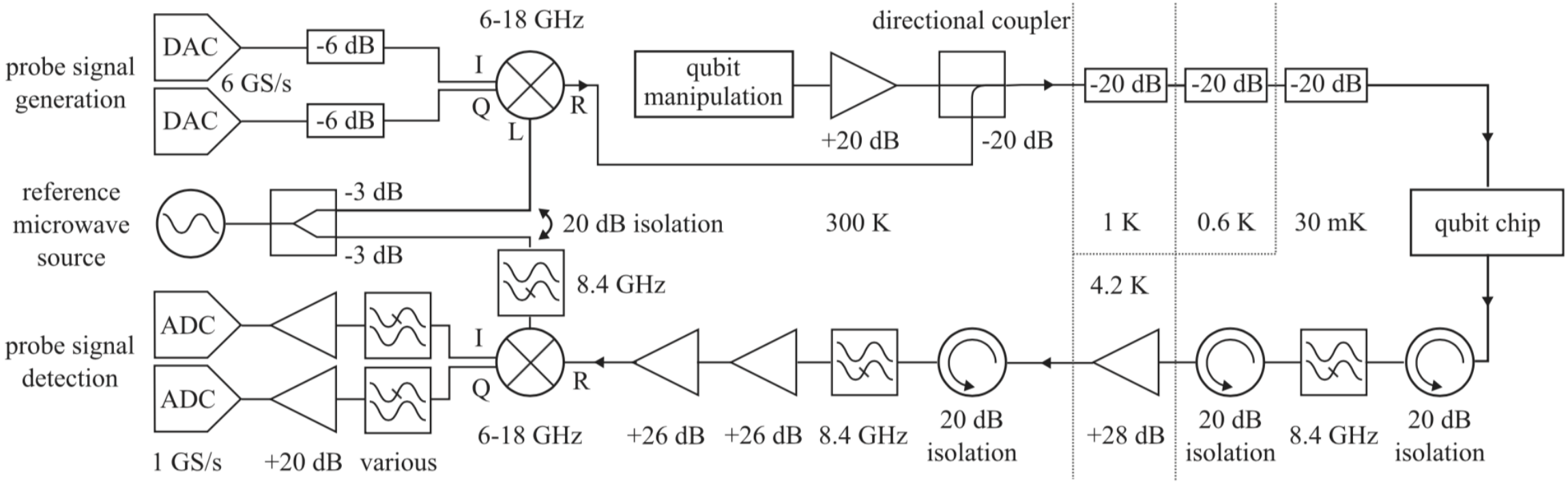

[M.Jerger et al., Appl. Phys. Lett. 101, 2012]

SC qubits: FDM spin manipulation

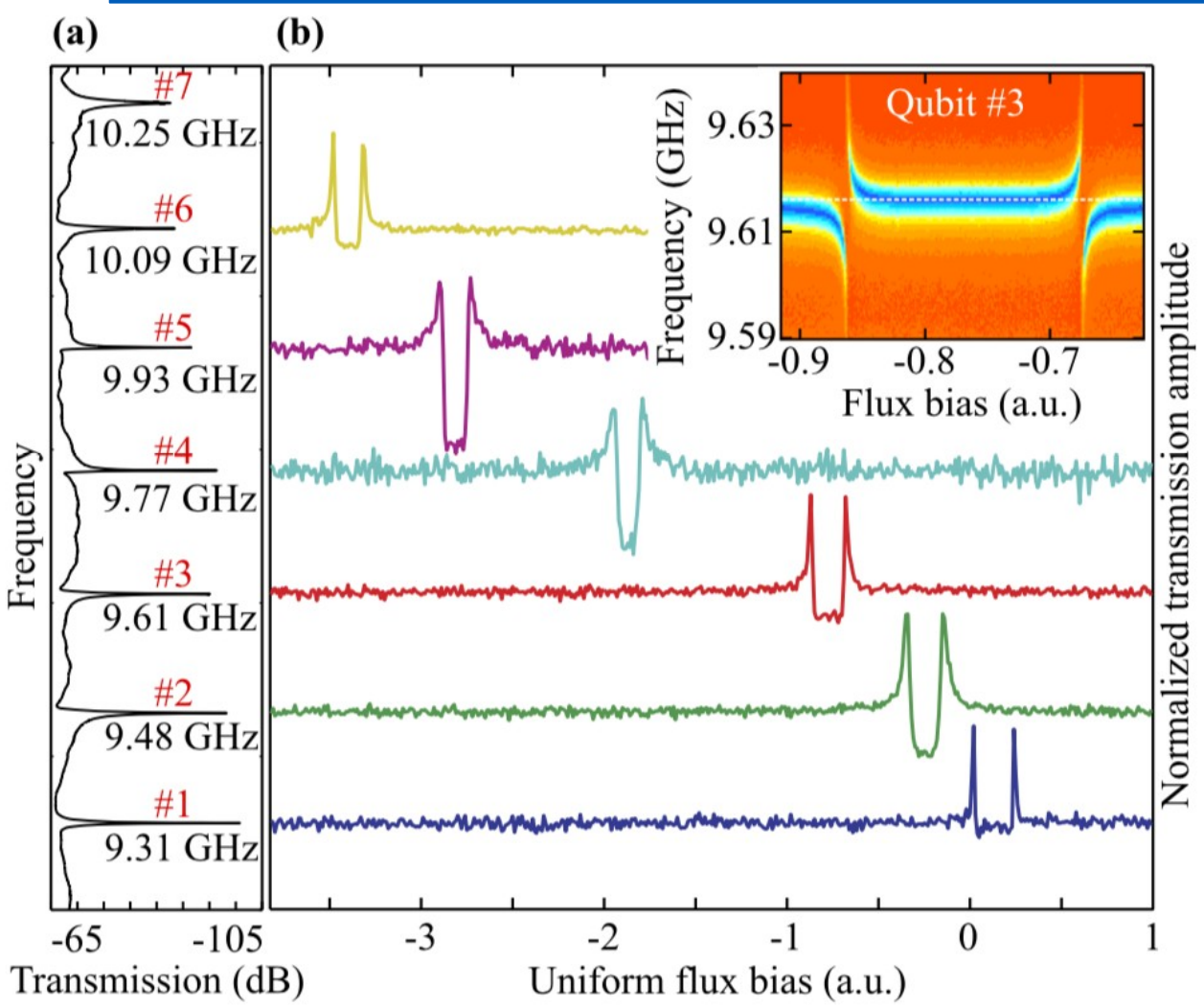

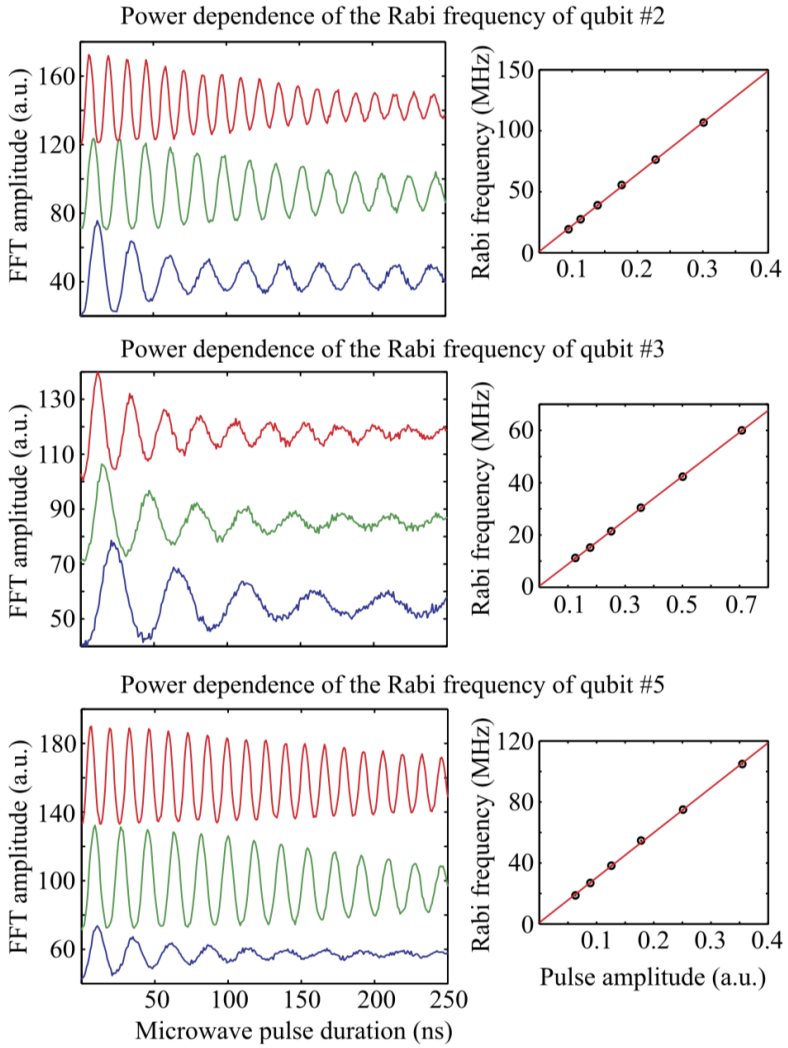

[M.Jerger et al., Appl. Phys. Lett. 101, 2012]

2-dot qubit (cascode)simulated E_C profiles

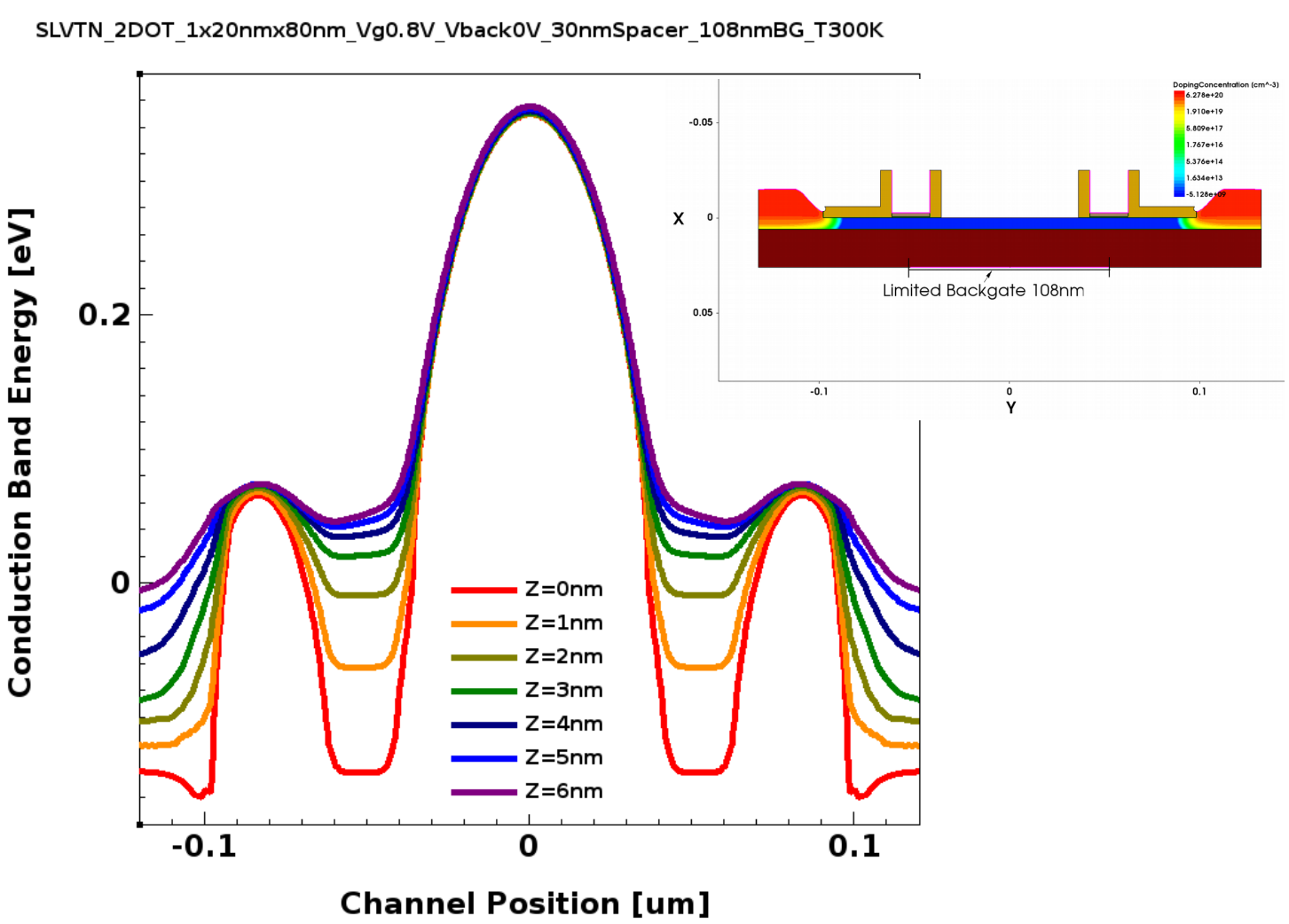

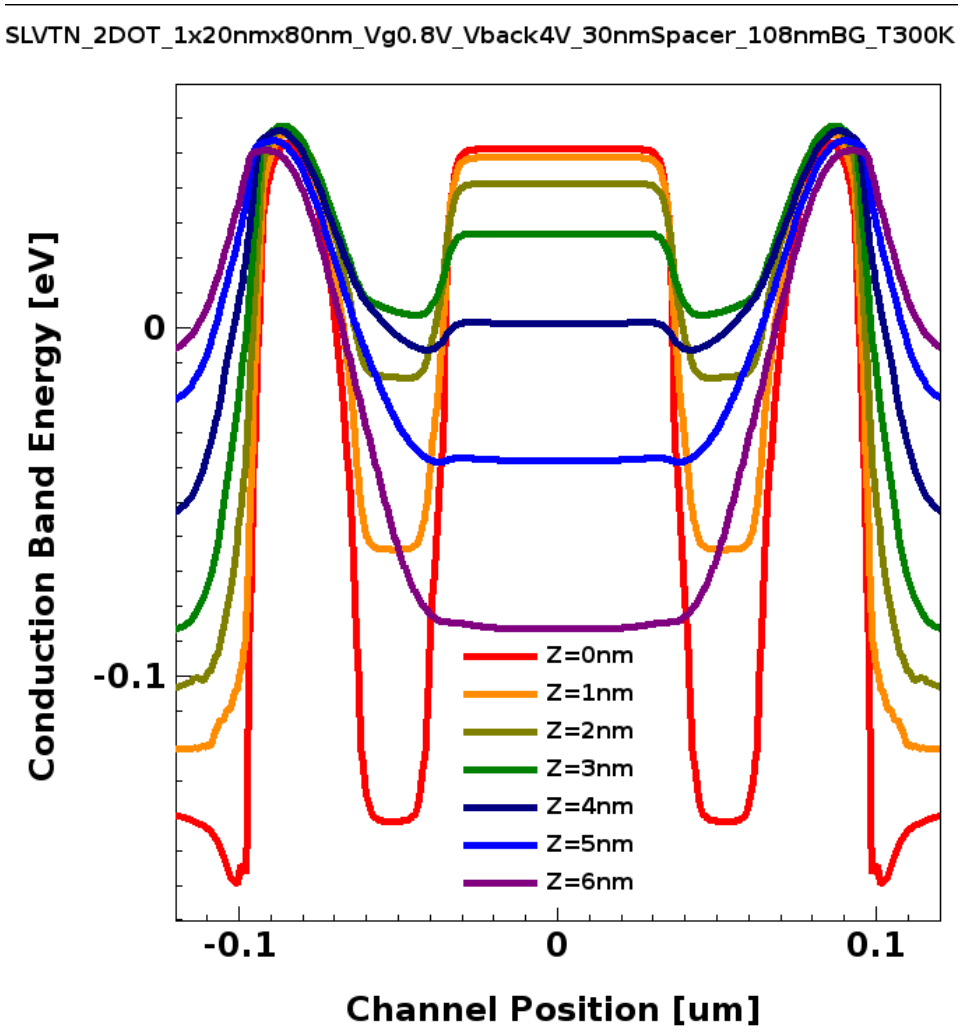

22-nm FDSOI mm-wave qubit test structures

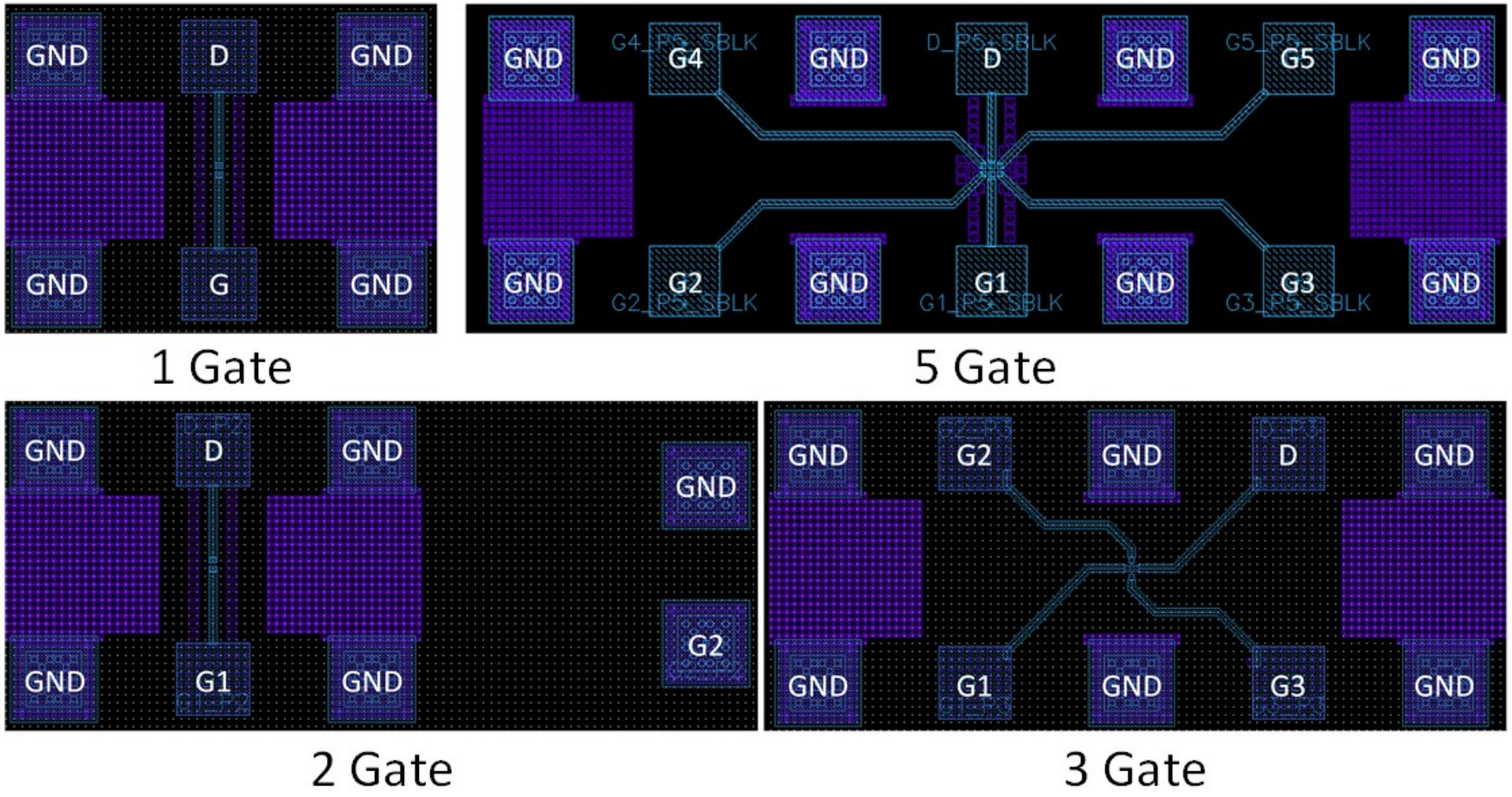

5 coupled QD electron-spin qubits

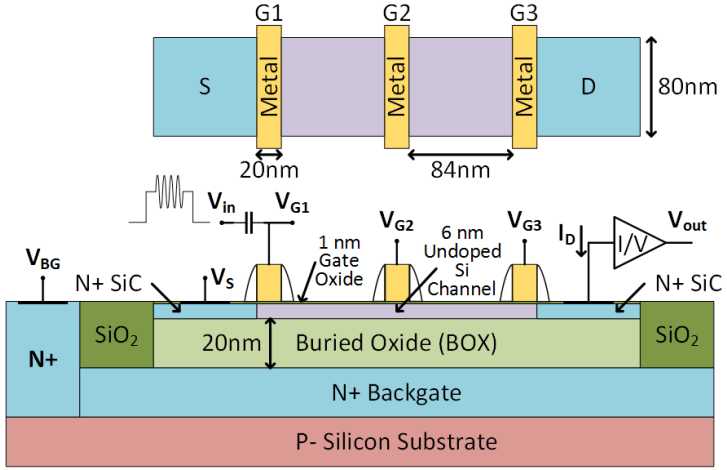

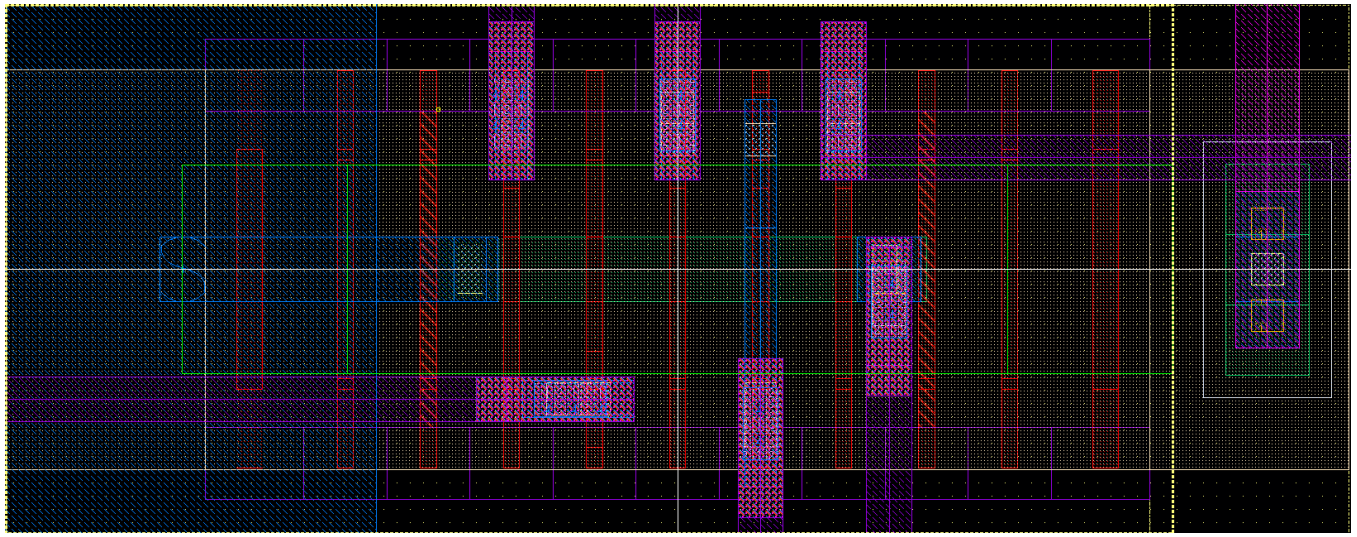

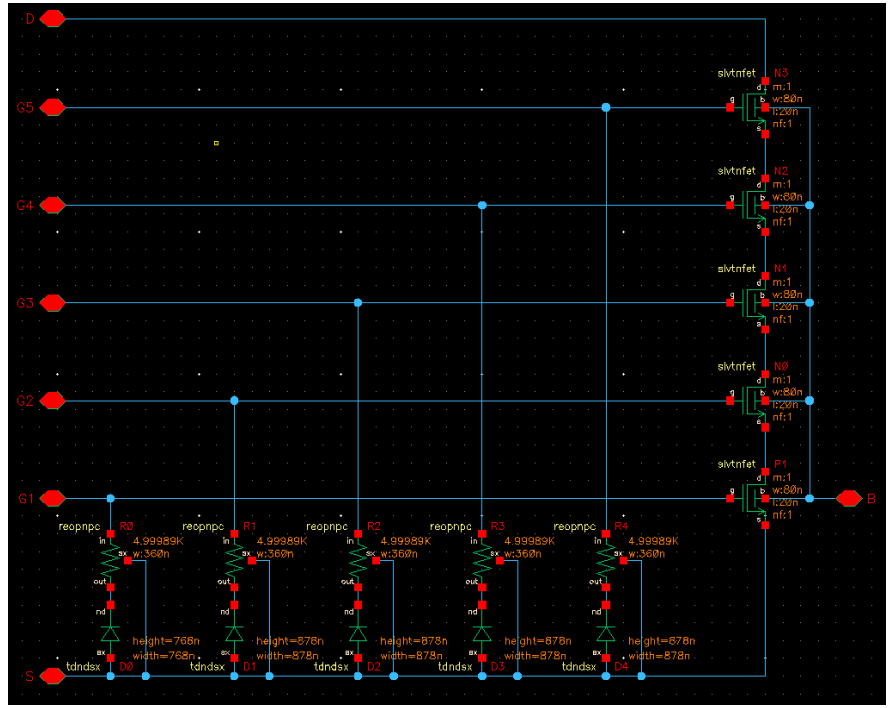

1nm MoS_2 SWCNT FET

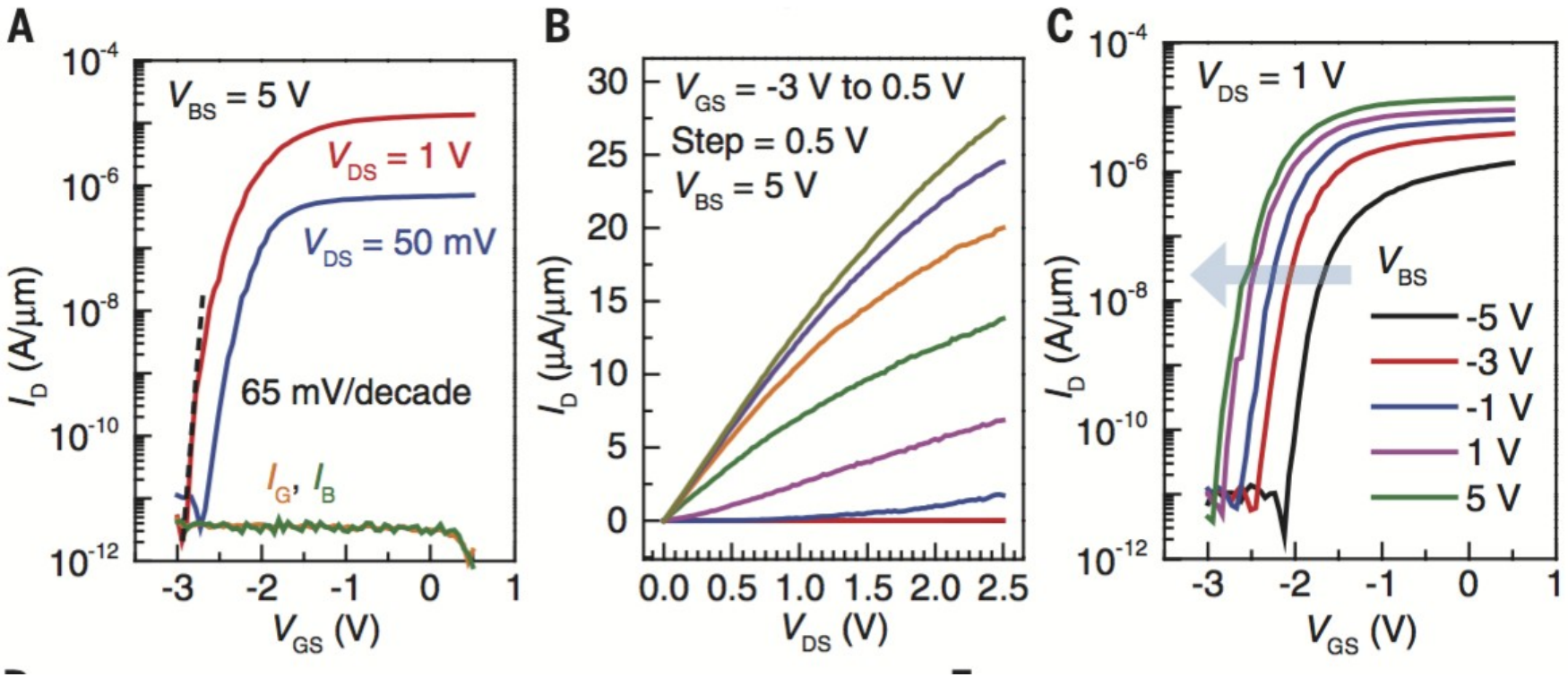

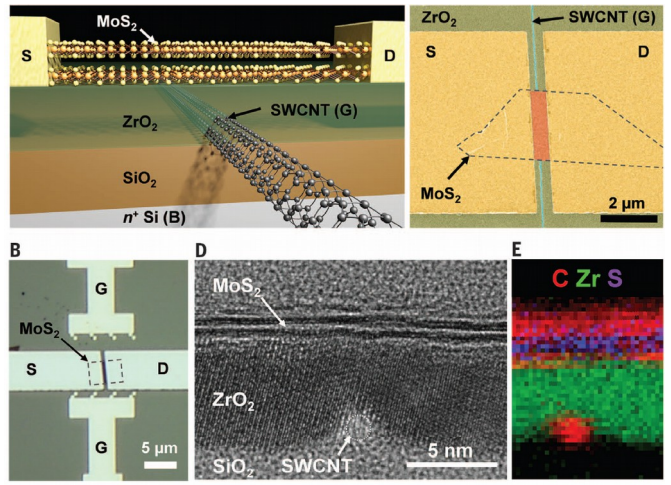

Fig. 2. 1D2D-FET device structure and characterization. (A) Schematic of 1D2D-FET with a MoS_2 channel and SWCNT gate. (B) Optical image of a representative device shows the MoS_2 flake, gate (G),

[Desai et al., Science Oct. 2016]

Design specification: mm-wave carrier

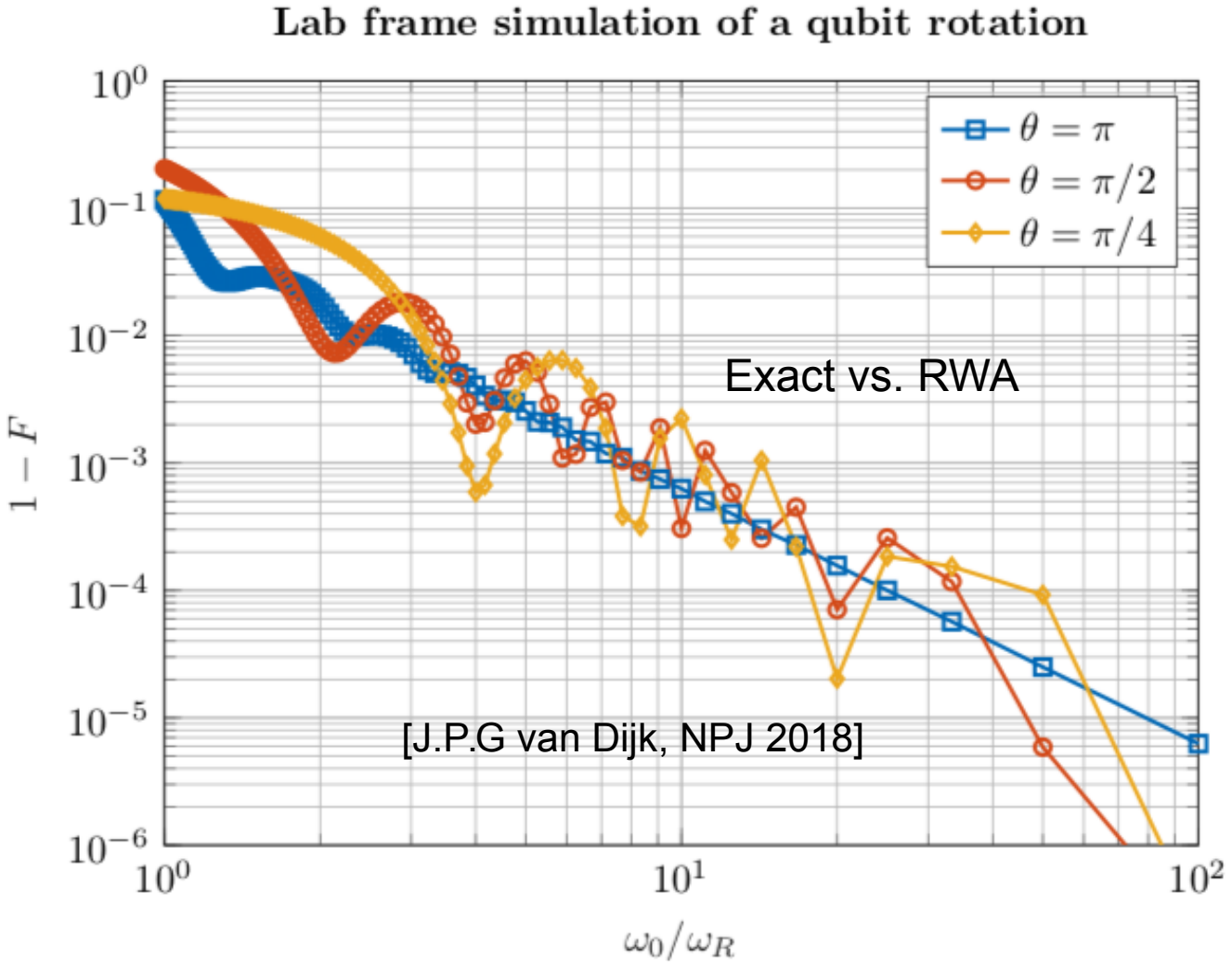

$$H = (\omega_{mmw} - \omega_L)\frac{\sigma_z}{2} + \omega_R\left[\cos(\phi)\frac{\sigma_x}{2} - \sin(\phi)\frac{\sigma_y}{2}\right]$$

$$F_{X,Y} = 1 - \frac{1}{2}\left(\frac{\Delta f_{mmw}}{f_R}\right)^2\left[1 - \cos(\theta)\right]$$

$$F_{X,Y} = 1 - \frac{1}{2}\Delta\phi^2\left[1 - \cos(\theta)\right]$$

- 1-F = single-spin qubit gate fidelity
- Rotation by θ
- For 1-F = 10^{-4}, the rotating wave approx. (RWA) requires $f_R < f_L/25$
- f_L= 240(60) GHz => f_R<= 9.6(2.4) GHz

Design specification: mm-wave envelope, PN

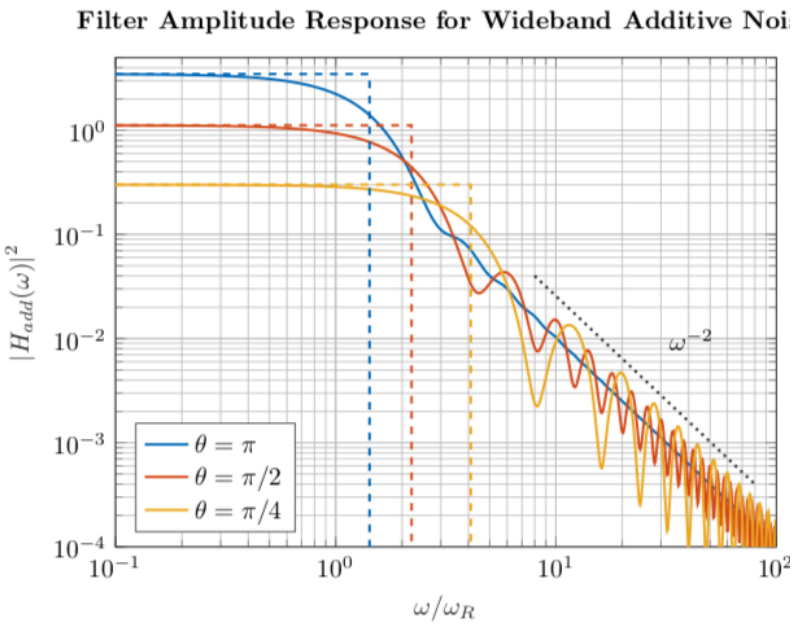

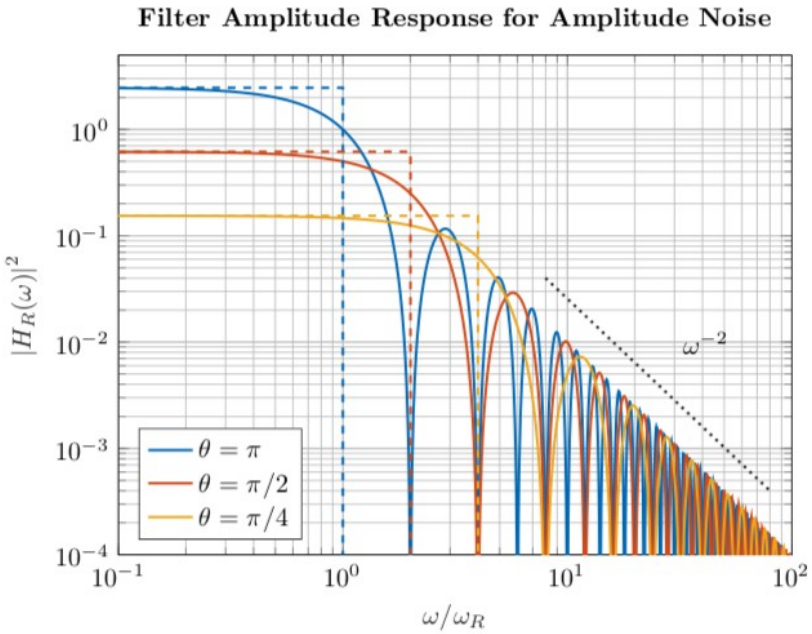

$$F_{X,Y} = 1 - \frac{1}{\pi}\int_{\omega_{min}}^{\infty} \frac{S_r(\omega)}{\omega_R^{\,2}} \left|H_R(\omega)\right|^2 d\,\omega$$

$$\sigma_\tau = \frac{\tau}{\pi}\sqrt{\int_{f_{min}}^{\infty} S_\phi(f)\sin^2(2\pi f\,\tau)\,df}$$

- Mm-wave amplitude (~ f_R) and duration, τ, determine rotation angle $\theta = \omega_R \tau$
- For 1-F = 10^{-4} requires relative errors <0.63%

$$F_{X,Y} = 1 - \frac{1}{4}\left(\frac{\Delta f_R}{f_R}\right)^2 \theta^2$$

$$F_{X,Y} = 1 - \frac{1}{4}\left(\frac{\Delta \tau}{\tau}\right)^2 \theta^2$$

$$\left|H_R(0)^2\right| = \frac{1}{4}\theta^2 \qquad ENBW_R = \omega_R \frac{\pi}{|\theta|}$$

[J.P.G van Dijk, NPJ 2018]

Design specification example: FDM spacing

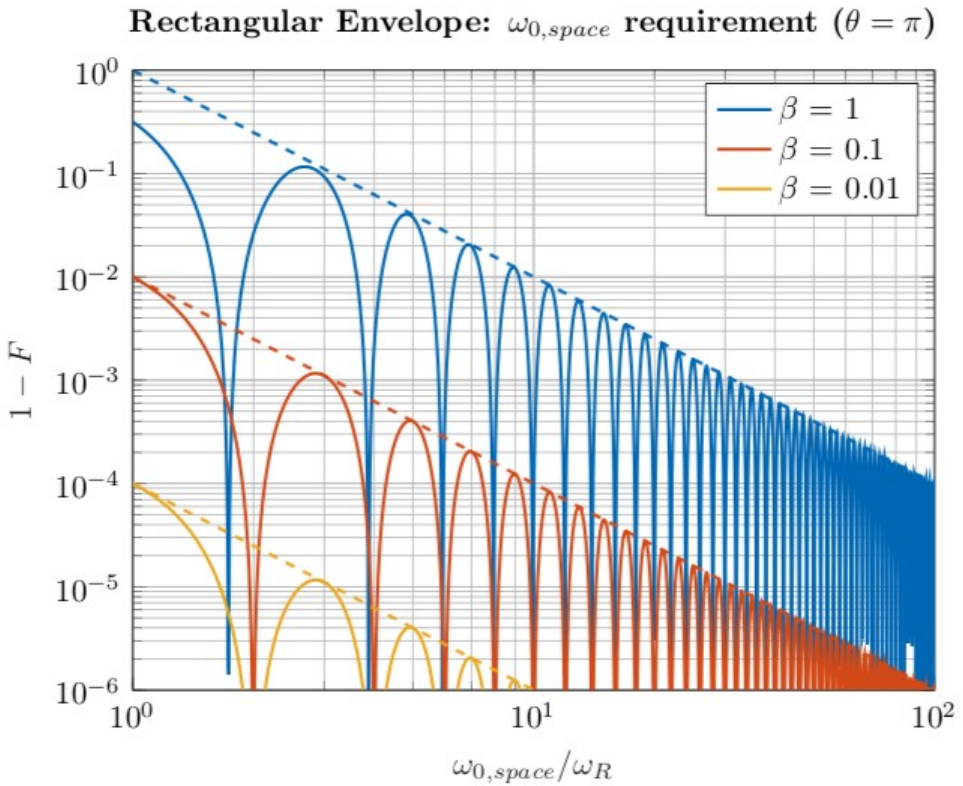

(a) The frequency spacing required to achieve a certain fidelity at given relative signal strength β, for a rectangular envelope. The upper bound is given in Eq. 22.

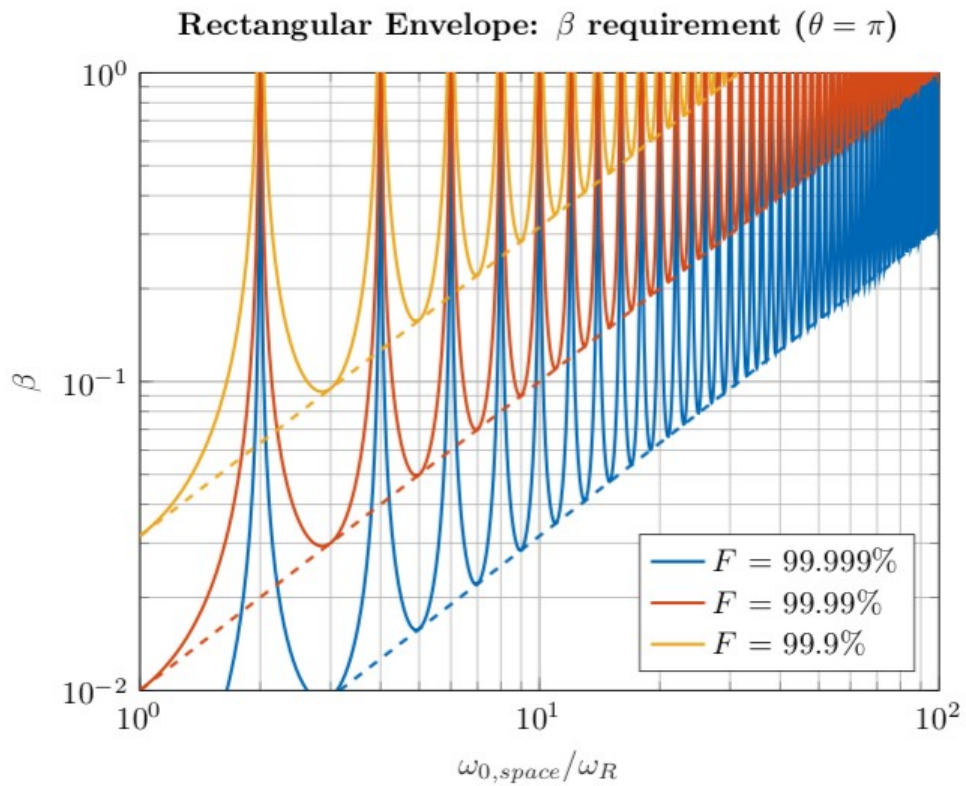

(b) The driving tone attenuation β required at a certain frequency spacing to achieve a given fidelity, for a rectangular envelope. The lower bound is given in Eq. 23.

[J.P.G van Dijk, NPJ 2018]

FIG. 10. Qubit frequency multiplexing: requirements in case of a rectangular envelope.

Design specification example: single-spin π-rotation

TABLE I. Example specifications for the control electronics. The PSD values provided as a comment assume a white spectrum for the amplitude and frequency noise (i.e. -20 dB/dec for the phase noise).

	Value	Infidelity contribution to an operation	Infidelity contribution to idling	Comment
Frequency				
nominal	10 GHz	0.64×10^{-9}		RWA when driving a qubit
spacing	1 GHz		$1{\times}10^{-6}$	FDMA leakage with rectangular envelopes
inaccuracy	11 kHz	$125{\times}10^{-6}$	$308{\times}10^{-6}$	
oscillator noise	11 kHz_{rms}	$125{\times}10^{-6}$	$308{\times}10^{-6}$	ENBW = 2.5 MHz, $\mathcal{L}$(1 MHz) = -106 dBc/Hz
nuclear spin noise	1.9 kHz_{rms}	$3.6{\times}10^{-6}$	$8.9{\times}10^{-6}$	From [33], $T_2^* = 120\,\mu s$
wideband noise	12 μV_{rms}	$125{\times}10^{-6}$		ENBW = 2.9 MHz, $S_{add} = 7.1\,\text{nV}/\sqrt{\text{Hz}}$
Phase				
inaccuracy	0.64 °	$125{\times}10^{-6}$	$31{\times}10^{-6}$	FDMA Z-corrections limit the no operation
Amplitude				
nominal	2 mV			Full-scale: 4 mV, RMS: 1.4 mV_{rms}
inaccuracy	14 μV	$125{\times}10^{-6}$		
noise	14 μV_{rms}	$125{\times}10^{-6}$		ENBW = 1.0 MHz, PSD = $14\,\text{nV}/\sqrt{\text{Hz}}$, SNR = -40 dB
off-spur	19 μV		$217{\times}10^{-6}$	-41 dBc
off-noise	10 μV_{rms}		$125{\times}10^{-6}$	ENBW = 2.0 MHz, PSD = $7.1\,\text{nV}/\sqrt{\text{Hz}}$
Duration				
nominal	500 ns			
inaccuracy	3.6 ns	$125{\times}10^{-6}$		
noise	3.6 ns_{rms}	$125{\times}10^{-6}$		
		$F_{X,Y}$ = **99.9 %**	F_I = **99.9 %**	

[J.P.G van Dijk, NPJ 2018]